The University of Nottingham

UNITED KINGDOM · CHINA · MALAYSIA

Design, synthesis, and optimisation of highly selective macrocyclic CDK9 inhibitors

Rui Gao, MPharm

Thesis submitted to the University of Nottingham

for the degree of Doctor of Philosophy

March 2018

Abstract

Cyclin dependent kinases (CDKs) belong to a family of serine/threonine protein kinases that play a key role in cell cycle and transcriptional regulation. CDK9, in complex with its regulatory partner cyclin T1, is involved in RNA transcriptional regulation through phosphorylating the RNA polymerase II. Inhibition of CDK9 can target multiple cancer-relevant pathways by downregulating the transcriptionally inducible genes of cancer cells, such as cell cycle regulators and antiapoptotic factors. Although many CDK inhibitors have been in clinical trials, there is only one CDK9-selective compound (BAY1143572) in trials. Therefore, it is still necessary to study other highly selective CDK9 inhibitors.

Through the analysis of the cocrystal structure of lead compound 5-(2-((3-(1,4-diazepan-1-yl)phenyl)amino)-pyrimidin-4-yl)-*N*,4-dimethyl-thiazol-2-amine (**5**) bound to CDK2 and CDK9, compound (**5)** favours the "inward" conformation in CDK9, while it adopts both the "inward" and "outward" conformations in CDK2. Aurora A and aurora B (ARKs) inhibitors are also found to adopt the similar "outward" conformation" in ATP binding site of ARKs. Therefore, an "inward" conformation macrocyclic structure was designed to improve the selectivity against CDK9 over CDK2 and ARKs.

Three series of macrocyclic compounds were designed, synthesised and tested against CDK9, CDK2, and ARKs. The first series macrocyclic compounds with amide linker

shows poor inhibitory activity against CDK9, and the molecular docking study shows these macrocyclic compounds fail to reside in the ATP binding site of CDK9.

Following that, ring closing metathesis (RCM) was exploited as an alternative cyclisation strategy. Although the synthesis work was unsuccessful at the first onset, compound 6-methyl-12-oxa-3,6-diaza-2(4,2)-pyrimidina-1,4(1,3)-dibenzenacyclodo-decaphan-8-ene (**43**) with a similar structure as designed compounds was introduced as the model compound to optimise the RCM reaction. The thiazole group was then demonstrated to be the interfering factor in RCM and compound 11-oxa-3-aza-2(4,2)-pyrimidina-5(1,4)-piperazina-1,4(1,3)-dibenzenacyclo-undecaphan-7-ene (**44**) with a replacing phenyl group was successfully synthesised and showed poor activity against CDK2 and ARKs (>219 nM for these three kinases).

According to the published paper regarding lead compound (**5)**, extensive substituents modification (-CH3, -CN, -F) of compound (**44**) afforded 11-oxa-3-aza-2(4,2)-pyrimidina-5(1,4)-piperazina-1,4(1,3)-dibenzenacyclo-undecaphan-7-ene-1-carbonitrile (**79**) as the most selective CDK9 inhibitor. It shows 60-fold selectivity for CDK9 over CDK2 and 90-fold selectivity for CDK9 over ARKs. A further Diversity Kinase Profile Screening demonstrates the high selectivity of compound (**79**) that only tyrosine-protein kinase Lyn(h) appeared as the off-target.

To improve the inhibitory activity against CDK9, alternative macrocyclic pyrimidine systems were designed, and compound 1-methoxy-4-(4-methylpiperazine-1-carbonyl)-

3,8-diaza-2(4,2)-pyrimidina-1(1,3),4(1,2)-dibenzenacyclononaphan-7-one (**89**) showed an attractive Glide score based on molecular docking studies. Because of the time limit, the synthetic work for compound (**89**) has not been finished.

Acknowledgements

Firstly, I would like to express my deep gratitude to my supervisor, Professor Peter M. Fisher, whose support and guidance helped me a lot to understand and develop my project. With his help, I have gained a deeper understanding of drug design and acquired multidisciplinary skills.

Secondly, I also would like to thank Dr. Hao Shao, Dr. Fadi Soukarieh and Dr. Christophe Fromont, who helped me a lot in the laboratory and gave some good advice in chemistry. Further thanks go to Dr. Jim Wilson for the help in my molecular docking study. I also acknowledge Dr. Tracey Bradshaw and Dr. James Krupa for the invaluable help in my thesis writing. All the colleagues in C25 and C29 are so friendly, so I can get accustomed to the life in UK quickly.

China Scholarship Council and Cancer Research UK are gratefully acknowledged for providing the financial support for my study.

Finally, I am extremely thankful to my parents and my girlfriend, Xue Wu, for their support and encouragement in the period of my PhD study.

List of Abbreviations

A

Ala	Alanine
aq.	Aqueous
AR	Androgen receptor
Arg	Arginine
Asp	Aspartic acid
Asn	Asparagine
ATP	Adenosine triphosphate
APAF1	Apoptotic protease-activating factor 1
AKT	Protein kinase B
ARKs	Aurora kinases

B

BAX	Bcl-2-associated X protein
B-CLL	B-chronic lymphoid leukaemia
Bcl-2	B-cell lymphoma family proteins
BAK	Bcl-2 antagonist/killer
BH3	Bcl-2 homology domain 3
BID	BH3 interacting-domain death agonist
Brd4	Bromodomain-containing protein 4
n-ButLi	*n*-Butyllithium
t-BuOK	Potassium *tert*-butoxide
Boc	*tert*-Butyloxycarbonyl
Boc_2O	Di-*tert*-butyl dicarbonate

C

CAK	CDK-activating kinase

CDK	Cyclin-Dependent Kinase
CTD	Carboxy-terminal domain
CLL	Chronic lymphocytic leukaemia
CK2α2	Casein kinase 2 alpha subunit
COSY	Correlation spectroscopy
CPC	Chromosomal passenger complex
Cys	Cysteine
D	
DCM	Dichloromethane
1,2-DCB	1,2-Dichlorobenzene
DMAP	*N,N*-Dimethyl-4-aminopyridine
DMF	*N,N*-Dimethylformamide
DMSO	Dimethyl sulfoxide
DMA	Dimethylacetamide
DNA	Deoxyribonucleic acid
DSIF	DRB-sensitive-inducing factor
DFG	Asp-Phe-Gly residues sequence
DMF-DMA	Dimethylformamide dimethyl acetal
E	
ECM	Extracellular matix
EGFR	Epidermal growth factor receptor
ER	Endoplasmic reticulum
ESI	Electrospray ionisation
EtOAc	Ethyl acetate
F	
FASL	Fas ligand
FADD	FAS-associated death domain protein

G

Glu	Glutamic acid
Gln	Glutamine
Gly	Glycine
GI_{50}	Half growth inhibitory concentration
Grubbs II	The second-generation Grubbs catalyst

H

His	Histidine
HATU	(1-[Bis(dimethylamino)methylene]-1*H*-1,2,3-triazolo[4,5*b*]pyridinium 3-oxid hexafluorophosphate)
HRMS	High resolution mass spectra
HPLC	High-performance liquid chromatography
HOAt	1-Hydroxy-7-azabenzotriazole
Hoveyda-Grubbs II	The second generation Hoveyda-Grubbs II catalyst

I

IAP	Inhibitors of apoptosis proteins
IC_{50}	Half maximal inhibitory concentration
Ile	Isoleucine

K

K_i	Dissociation constant

L

Leu	Leucine
Lys	Lysine
Lyn	Lck/Yes novel tyrosine kinase
LDA	Lithium diisopropylamide
LOK	Lymphocyte-oriented kinase

M

Mcl-1	Myeloid-cell leukaemia 1
MeOH	Methanol
MYC	c-Myc, a protein encoded by c-Myc oncogene
Mdm-2	Mouse double minute 2 homolog
MOMP	Mitochondrial outer membrane permeabilization
mRNA	Messager RNA
MeCN	Acetonitrile

N

NELF	Negative elongation factor
NF-κB	Nuclear factor kappa-light-chain-enhancer of activated B cells
NCI	The US National Cancer Institute (NCI)
NMR	Nuclear magnetic resonance
NOESY	Nuclear Overhauser effect spectroscopy

P

pRb	Retinoblastoma protein
$Pd_2(dba)_3$	Tris(dibenzylideneacetone)dipalladium
PE	Petroleum ether
PI3K	Phosphoinositide 3-kinase
PKA	Protein kinase A
P-TEFb	The positive transcription elongation factor b
Phe	Phenylalanine

R

RCM	Ring closing metathesis
RNA	Ribonucleic acid
RT	Room temperature
RNAPII	RNA polymerase II

S

Ser	Serine
SAR	Structure-Activity Relationship
SMAC	Second mitochondria-derived activator of caspase
SPhos	2-Dicyclohexylphosphino-2, 6-dimethoxybiphenyl

T

TEA	Triethylamine
TFA	Trifluoroacetic acid
TLC	Thin layer Chromatography
THF	Tetrahydrofuran
Thr	Threonine
TMS	Tetramethylsilane
TRAILR	TNF-related apoptosis-inducing ligand receptor
TNF	Tumour necrosis factor
TFIIH	General transcription initiation factor IIH
TMSCl	Trimethylsilylchloride

V

Val	Valine
VEGF-A	Vascular endothelial growth factor-A

X

XIAP	X-Linked inhibitor of apoptosis protein
XPhos	2-Dicyclohexylphosphino-2, 4, 6-triisopropylbiphenyl

Table of Contents

Abstract I

Acknowledgements IV

List of Abbreviations V

Chapter One: Introduction 1

1.1 Cancer 1

1.1.1 The definition of cancer 1

1.1.2 The clonality of tumour 2

1.1.3 Types of cancer 4

1.1.4 Hallmarks of cancer 6

1.1.5 Chronic lymphocytic leukaemia (CLL) 10

1.1.6 Apoptosis pathway and the related apoptotic proteins 11

1.2 Targeting cyclin dependent kinase for cancer treatment 14

1.2.1 Protein kinases 14

1.2.2 Cyclin dependent kinases 17

1.2.3 Introduction to CDK9 18

1.2.4 Rationale of CDK9 as an anti-cancer target 20

1.3 CDK9 inhibitors 22

1.3.1 Known CDK9 inhibitors 22

1.3.2 The introduction to ATP binding site 28

1.3.3 The binding mode of CDK9 with known inhibitors 31

1.3.4 Flexible elements in CDK9/cyclin T 36

1.4 The rationale of the design for macrocyclic ligands 37

1.4.1 The binding mode of lead compounds with CDK9 and CDK2 37

1.4.2 Aurora kinases (ARKs) as the off-target proteins 39

1.4.2 The design strategies for macrocyclic compounds 40

1.5 Aims and objectives 43

Chapter Two: Macrocyclic compounds containing amide linkers 44
2.1 Overview of synthetic route 44
2.1.1 Synthesis of enaminone **9** as the precursor for pyrimidine **14** 45
2.1.2 Synthesis of guanidine **13** as the precursor for pyrimidine **14** 46
2.1.3 Formation of 2,4-disubstituted pyrimidine **15** 47
2.1.4 Cyclisation of the precursor **15** using amide coupling chemistry 48
2.2 Results and discussion 49
2.2.1 Kinase assay result 49
2.2.2 Molecular docking 50
2.3 Conclusion 52
Chapter Three: Optimised macrocyclic compounds with an alkene linker 53
3.1 The optimisation of the synthesis for macrocyclic compounds with an alkene linker 53
3.2 Overview of the synthetic route towards macrocyclic compounds containing alkene linkers 60
3.2.1 Formation of allyl-substituted pyrimidine derivatives 60
3.2.2 Optimisation of Suzuki reaction for 4-phenol-substituted pyrimidine **47** ... 61
3.2.3 Optimisation of RCM reaction condition for compound **44** 62
3.2.4 The confirmation of the configuration of macrocyclic compounds **43** 64
3.3 Results and discussions 66
3.3.1 Kinase assay results 66
3.3.2 Molecular docking 67
3.4 Conclusion 70
Chapter Four: Highly selective macrocyclic CDK9 inhibitors 71
4.1 Three synthetic routes toward new modified macrocyclic compounds 72
4.2 Overview of synthesis 76
4.2.1 Selective nucleophilic aromatic substitution of 2,4-dichloropyrimidine **46** 76

4.2.2 Mild conversion of aryl fluoride to phenol 77
4.2.3 Optimisation of Suzuki-Miyaura reaction..... 77
4.3 Results and discussion 79
4.3.1 Kinase assay results..... 79
4.3.2 Molecular docking 81
4.4 Conclusion 84
Chapter Five: Design and initial synthesis of alternative macrocyclic pyrimidine derivatives..... 85
5.1 Strategy one: flexible alkyl linker..... 85
5.1.1 Design and synthesis of flexible alkyl linker macrocyclic compound..... 85
5.1.2 Kinase assay results..... 86
5.2 Strategy two: alternative macrocyclic compounds 87
5.2.1 Design of the alternative macrocyclic compounds with molecular docking 87
5.2.2 Initial synthesis of compound **89** 90
5.3 Conclusion 92
Chapter Six: Conclusion and Future work 93
6.1 Conclusion 93
6.2 Future work..... 97
Chapter Seven: Materials, methods, experimental section.....98
7.1 Chemistry..... 98
7.2 Experiment data 100
7.2.1 General synthetic procedure (1) for nitrobenzene derivatives (compounds **29**, **11**) 100
7.2.2 General synthetic procedures (2) for *N*- and *O*- substituted derivatives (compounds **30**, **48**, **63**, **67**, **81**, **76**, **59**, **41**)..... 101
7.2.3 Synthetic procedure for *N*-methyl-*N*-(3-nitrobenzyl)-prop-2-en-1-amine (**50**) 106
7.2.4 Synthetic procedure for 3-(3-(but-3-en-1-yloxy)phenyl)-3-oxopropanenitrile (**68**) 107

7.2.5 General synthetic procedure (3) for aniline derivatives (compounds **12**, **99**) 108

7.2.6 Synthetic procedure for 3-(4-allylpiperazine-1-yl) aniline (**31**)[198] 109

7.2.7 General synthetic procedure (4) for guanidine derivatives (compounds **13**, **32**) 110

7.2.8 General synthetic procedure (5) for thiazole derivatives (compounds **7**, **26**) 112

7.2.9 General synthetic procedure (6) for Boc-protection of amine derivatives (compounds **27**, **8**) 113

7.2.10 General synthetic procedure (7) for enaminones derivatives (compounds **9**, **38**, **88**) 114

7.2.11 Synthetic procedure for methyl 3-(2-(4-methyl-piperazine-1-carbonyl)-6-nitrophenyl)acrylate (**92**) 116

7.2.12 Synthetic procedure for (5-(2-chloro-pyrimidin-4-yl)-2 methoxyphenyl)methanamine (**96**) 117

7.2.13 Synthetic procedure for phenyl borate derivatives 117

7.2.14 General synthetic procedure (8) for Suzuki coupling (compounds **47**, **62**, **78**, **95**) 119

7.2.15 Synthetic procedure for *N*-(3-(4-allylpiperazin-1-yl)phenyl)-4-(5-(but-3-en-1-yloxy)-2-methyl-phenyl)pyrimidin-2-amine (**83**) 122

7.2.16 General synthetic procedure (9) for 2, 4-di-substituted pyrimidine derivatives (compounds **73**, **57**) 123

7.2.17 Synthetic procedure for *N*-(3-(4-allylpiperazin-1-yl)phenyl)-2-chloropyrimidin-4-amine (**101**) 126

7.2.18 General synthetic procedure (10) for pyrimidine derivatives (compounds **53**, **52**, **64**) 127

7.2.19 General synthetic procedure (11) for pyrimidine derivatives (compounds **14**, **33**, **39**, **55**, **71**) 130

7.2.20 Synthetic procedure for 2-bromo-4-hydroxybenzonitrile (**75**)[200] 134

7.2.21 General synthetic procedure (12) for acetamide derivatives (compounds **15** and **40**) 135

7.2.22 General synthetic procedure (13) for amide coupling (compounds **16c**, **16b**, **16a**) 136

7.2.23 General synthetic procedure (14) for macrocyclic compounds with amide linker (compounds **17a**, **17b**, **17c**, **97**) 139

7.2.24 Synthetic procedure for (2-bromo-3-nitrophenyl)(4-methylpiperazin-1-yl)methanone (**91**)[201] 143

7.2.25 General synthetic procedure (15) for macrocyclic compounds with alkene linker (compounds **43**, **44**, **60**, **65**, **72**, **79**, **84**) 143

7.2.26 Synthetic procedure for 6-methyl-12-oxa-3,6-diaza-2(4,2)-pyrimidina-1,4(1,3)-dibenzenacyclodo-decaphane (**86**) 151

7.3 Molecular docking 153

7.4 Kinase assays 155

References 156

Chapter One: Introduction

1.1 Cancer

In 2014, around 357,000 new cases of cancer appeared in the UK, and 163,444 deaths from cancer, which equates to 450 deaths every day.[1] The number of new cancer diagnoses is increasing, and has risen by more than 25% since 2001.[1]

1.1.1 The definition of cancer

Cancer is a serious disease caused by abnormal cells that can grow and divide, or accumulate uncontrollably, invading normal tissues, organs and spreading throughout the body.[2,3] Rather than responding to signals that control normal cell division, differentiate or die, cancer cells do not respond to these signals and develop the autonomy of uncontrolled proliferation or survival. Almost 90% of deaths caused by cancer are due to the spreading of cancer cell, namely metastasis.[4]

The prevailing theory of how cancer develop this autonomy is that cancer cells with the mutated cell genome can result in mutated proteins to disrupt the balance between cell proliferation and cell death.[4,5]

1.1.2 The clonality of tumour

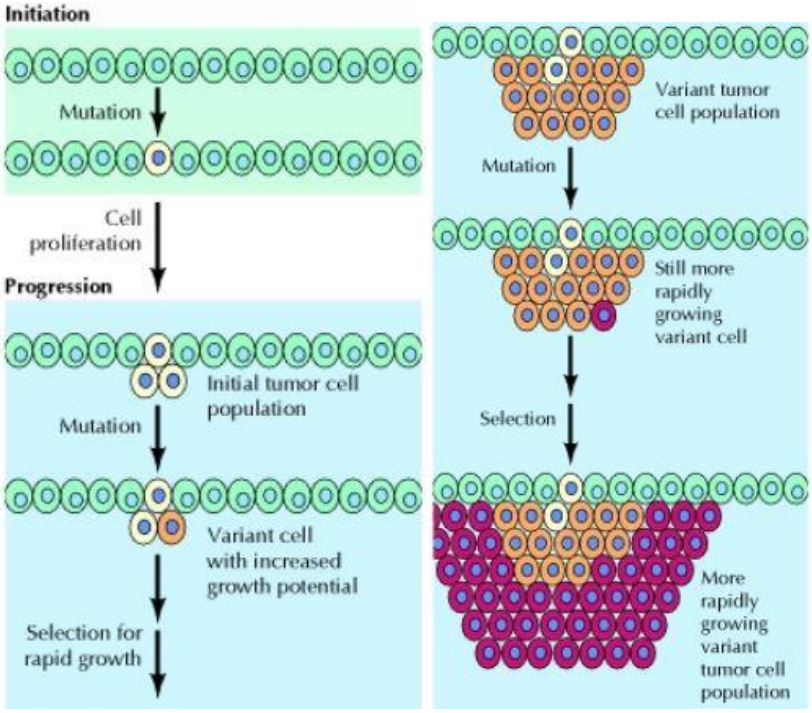

Figure 1.1 Stages of tumour development.[2]

A fundamental feature of cancer is tumour clonality.[6] Cancer originates from a single abnormal cell (clonal origin) with genes mutated. Uncontrolled proliferation of the abnormal cells leads to tumour progression and accumulation of additional random mutations.[7] Selective advantage will be conferred upon some of the cells by certain mutations, such as proliferative or survival advantage; the tumour cell with such mutation will accumulate and be dominant in the tumour population. This is called clonal selection.[2] Clonal selection continues with continued tumour cell proliferation. Therefore, tumour cells become more malignant. Uncontrolled mutation and selective expansion of tumour cells leads to tumour growth and progression, and will erode the membrane barrier, escaping into the connective tissue to invade other organs, blood and

lymphatic vessels, and eventually metastasise throughout the body (**Figure 1.1**).[6-8]

The clonality of tumours has been demonstrated by the analysis of X chromosome inactivation (**Figure 1.2**).[2,8] In female cells, one of the X chromosome pair becomes inactivated during embryonic development and the inactivation occurs randomly on the X-chromosome pair, so the normal tissue is composed of cells with different inactive X chromosomes. Nevertheless, the tumour tissue shows the same heterozygous X chromosome gene, which indicates cells in a tumour are derived from an original cell, because the pattern of X chromosome inactivation has been fixed before the proliferation of the (initial aberrant) mutated cancerous cell.[2]

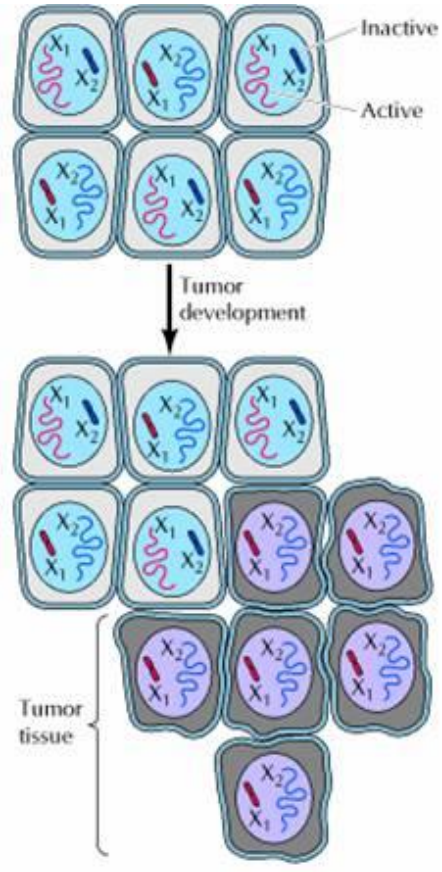

Figure 1.2 Tumour clonality-analysis of X-chromosome inactivation.[2]

1.1.3 Types of cancer

There are > 200 types of cancer, which result from the uncontrolled proliferation of any kind of abnormal cells in the body.[9] These cancers can be different from the behaviour and response to the treatment. A tumour can be either benign or malignant, and they are the two main classifications of tumours.[2]

1.1.3.1 Benign and malignant tumours

A benign tumour is confined to its original location and does not invade surrounding normal tissue. Contrastingly, a malignant tumour, penetrates and destroys adjacent tissue and metastasises to distant parts of the body *via* the circulatory or lymphatic systems (**Figure 1.3**).[10, 11] A malignant tumour, which is also referred to cancerous tumour, is innately dangerous because of the ability to invade and metastasise. Often, a benign tumour does not need any treatment, but it can be removed through surgery if necessary.[2,11]

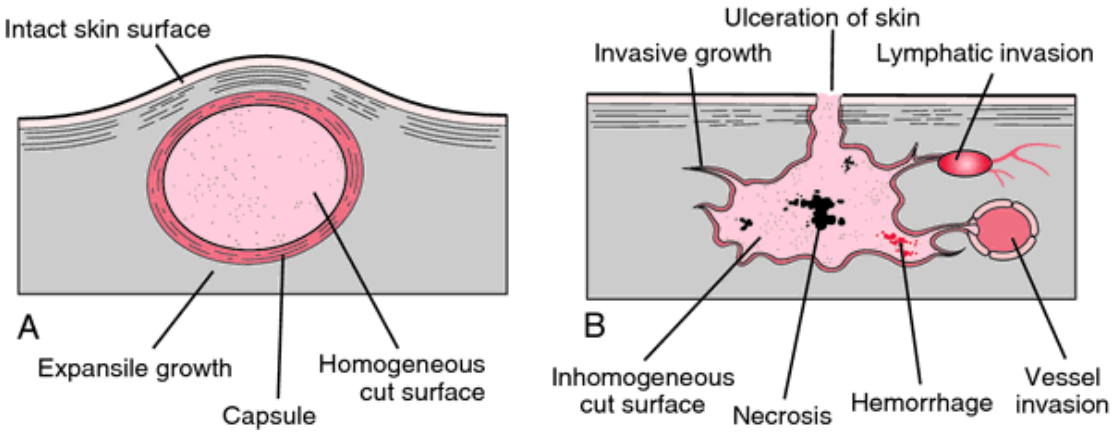

Figure 1.3. Gross appearance of benign and malignant tumours.[12]

1.1.3.2 Five main types of tumours

Both benign and malignant tumours can also be classified depending on the type of cell that is initial altered. Most cancers fall into five main types of tumours: carcinomas, sarcomas, leukaemia, lymphoma and myelomas.[13] Carcinomas, comprise 90% of human cancers, result from malignant epithelial cells, which cover the surface of the skin and internal organs. Sarcomas, which are solid tumours, result from cancerous change in muscle, bone, and connective tissue. Leukaemia and lymphomas, accounting for about 8% of human cancers, arise from malignant white blood cells and from cancer cells of the lymphatic system, respectively. Myelomas result from specialised white blood cells of the immune system that make antibodies.[12]

1.1.3.3 Grading system of tumours

Tumour cells can further be classified according to "grade" to predict the behaviour of the tumour and guide the treatment. The grading systems are different according to the type of cancer, but generally there are five grades depending on the degree of abnormality.[14]

GX: Grade cannot be assessed (undetermined grade)

G1: Well differentiated (low grade)

G2: Moderately differentiated (intermediate grade)

G3: Poorly differentiated (high grade)

G4: Undifferentiated (high grade)

1.1.4 Hallmarks of cancer

Normal cells have the intrinsic self-defenses against cancerous process, and there are many changes occurring when they start to grow uncontrollably to form cancer. In 2011, eight hallmarks of cancer and two enabling characteristics underlying the development of cancer were proposed by Hanahan and Weinberg (**Figure 1.4**).[15]

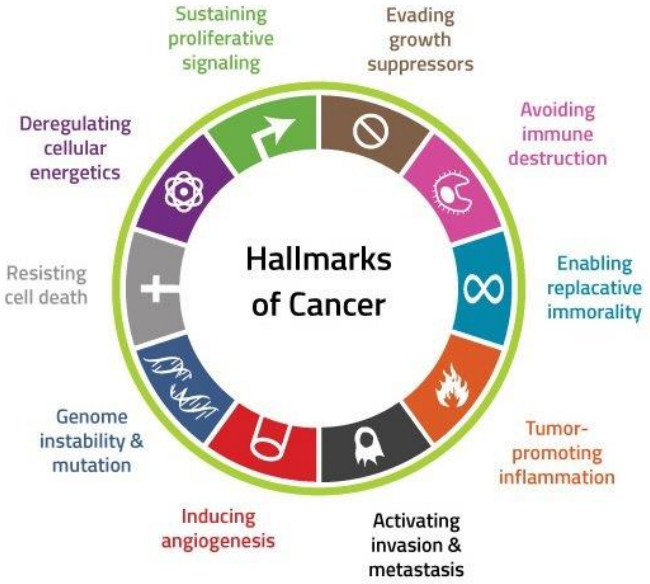

Figure 1.4 The eight hallmarks of cancer and two enabling characteristics.[15]

1.1.4.1 Sustaining proliferative signaling

Unlike normal cells, which carefully control the production and release of growth-promoting signals to ensure a homeostasis of cell number and maintenance of normal tissue architecture and function, cancer cells generate growth signals themselves to support the uncontrolled proliferation.[16] Additionally, cancer cells become resistant to anti-growth signals by overexpression of the signal receptors at the cell surface to ignore

normal signaling that limits the growth of cells.

1.1.4.2 Evading growth suppressors

Growth suppressors produce signals that inhibit abnormal cell growth and proliferation. Cancer cells acquire the ability to circumvent the regulation of tumour suppressors by mutations or alterations to tumour suppressor genes. Retinoblastoma protein (pRb) and TP53 (p53) are two prototypical tumour suppressors that determine whether to proliferate or activate the apoptotic programs of cells.

1.1.4.3 Resisting cell death

Apoptosis serves as a natural barrier to programmed cell death when facing various physiological stresses, such as DNA damage and elevated level of oncogene signaling.[17] Cancer cells avoid the normal cell death cycle and accumulate in the body by increasing expression of anti-apoptotic proteins (Mcl-1, Bcl-2) or survival signals (lgf1/2), or by downregulation of proapoptotic proteins (Puma, BAX).[15]

1.1.4.4 Enabling replicative immortality

Telomeres are small portions of DNA at the ends of each chromosome to protect the end of chromosomal DNAs from end-to-to fusion.[18-20] In normal cell division, telomeres are shortened each time DNA is copied (i.e. every cell division); eventually telomeres lose the protective function. Therefore, the replication of normal cells will only be a

limited number of times. However, cancer cells can activate telomerase to maintain telomeres and allow the uncontrolled proliferation of cancer cell.[21]

1.1.4.5 Inducing angiogenesis

Like the normal tissue in the body, a tumour mass also needs a blood supply to sustain the neoplastic growth and to eliminate metabolic wastes. However, solid tumours need greater and greater blood supply to support their growth to a clinical visible size, it must form its own blood vessel to extend and grows into the tumour.[22] This process is called angiogenesis, which is encouraged by interactions between the environment and the tumour. Vascular endothelial growth factor-A (VEGF-A), a well-known angiogenesis inducer, can be upregulated by cancer cells to encourage the growth of new vessels into the tumour mass.[23]

1.1.4.6 Activating invasion and metastasis

Unlike normal differentiated cells, cancer cells invade normal host tissue and circulate to other sites in the body to form new tumours (metastasis), which ultimately kills cancer patients.[24] Cancer cells in this process alter their shape and become detached from neighboring cells as well as from the extracellular matrix (ECM). E-cadherin, a key cell-to-cell adhesion molecule, serves as an antagonist against the invasion and metastasis of cancer cells. The downregulation and inactivation of E-cadherin are frequently observed in human cancers.[25,26]

1.1.4.7 Deregulating cellular energetics

Cancer cells have been observed to limit their energy metabolism to anaerobic glucose metabolism (glycolysis) even under aerobic conditions, whereas normal cells undergo distinct glucose metabolism pathway under aerobic and anaerobic condition. [27, 28,29] Activated oncogenes (e.g., *RAS*, *MYC*) and mutant tumour suppressors (e.g., p53) are shown to be involved in this glycolytic switch in cancer cells.[30,31]

1.1.4.8 Avoiding immune destruction

Through persistent monitoring of cells and tissues, the immune system of the body detects and eliminates abnormal cells and nascent tumours. Evidence shows that cancer cells can somehow avoid the detection of the immune system and continue uncontrolled proliferation.[32]

1.1.4.9 Two enabling characteristics underlying cancer development

The eight hallmarks distinguish cancer cells from normal cells, which possibly result from two characteristics that enable the alterations underlying cancer development:

1.1.4.9.1 Genome Instability and Mutation

Genes provide all the instructions for cellular activity. Cancer cell often increase the mutation rates of genes to acquire the hallmark characteristics of cancer, transforming cells into malignant cells. Because the genome maintenance and repair systems can

detect and resolve the mistakes in DNA replication, mutation rates are very low. The mutation rate of genes of cancer cells can be increased by increasing the sensitivity to mutagenic agents or destroying the DNA repair pathways.[15]

1.1.4.9.2 Tumour-promoting inflammation

The tumour-associated inflammatory response can enhance tumourigenesis and progression, and it also help the incipient neoplasia to acquire hallmark capabilities. It is achieved by supplying bioactive molecules, such as growth factors, survival factors.[33,34,35] Inflammatory cells can also release DNA-damaging reactive oxygen species to accelerate their genetic evolution toward the malignant stage.[15,36]

1.1.5 Chronic lymphocytic leukaemia (CLL)

Chronic lymphocytic leukaemia (CLL), also known as B-chronic lymphoid leukaemia (B-CLL), is the most common type of leukaemia in Western countries, with more than 3000 people diagnosed in the UK every year.[37]

CLL, originating in the bone marrow, is a type of blood cancer that affects B cell lymphocytes. CLL is characterised by uncontrolled accumulation of B cells and accumulation in the bone marrow and blood.[38] The co-expression of pan-T-cell marker CD5 and pan-B-cell marker CD19 is the phenotypic hallmark of classical CLL.[39, 40] CLL is also characterised by a typical defect in apoptosis through overexpression of key antiapoptotic protein (members of the Bcl-2 and IAP families), particularly Mcl-1.[41, 42]

1.1.6 Apoptosis pathway and the related apoptotic proteins

1.1.6.1 Apoptosis pathway

Apoptosis is a genetically encoded cell suicide program that is essential for the regulation of cell death in our bodies.[43] "Evading Apoptosis" defined as the third hallmark of cancer represents an important mechanism for cancer cells to resist the self-therapy in the body. The role of anti-apoptosis in tumorigenesis has been reported.[44, 45] To support uncontrolled proliferation, cancer cells perturb not only the growth pathways of normal cell, but also the apoptotic pathways.[46] Therefore, apoptosis-induction has been viewed as a therapy endpoint for treatment of cancer.

There are several pathways that apoptotic signalling can exert oncogenic effects. The two majors well-studied are the extrinsic pathway (death receptor) and the intrinsic pathway (mitochondrial) (**Figure 1.5**).[43]

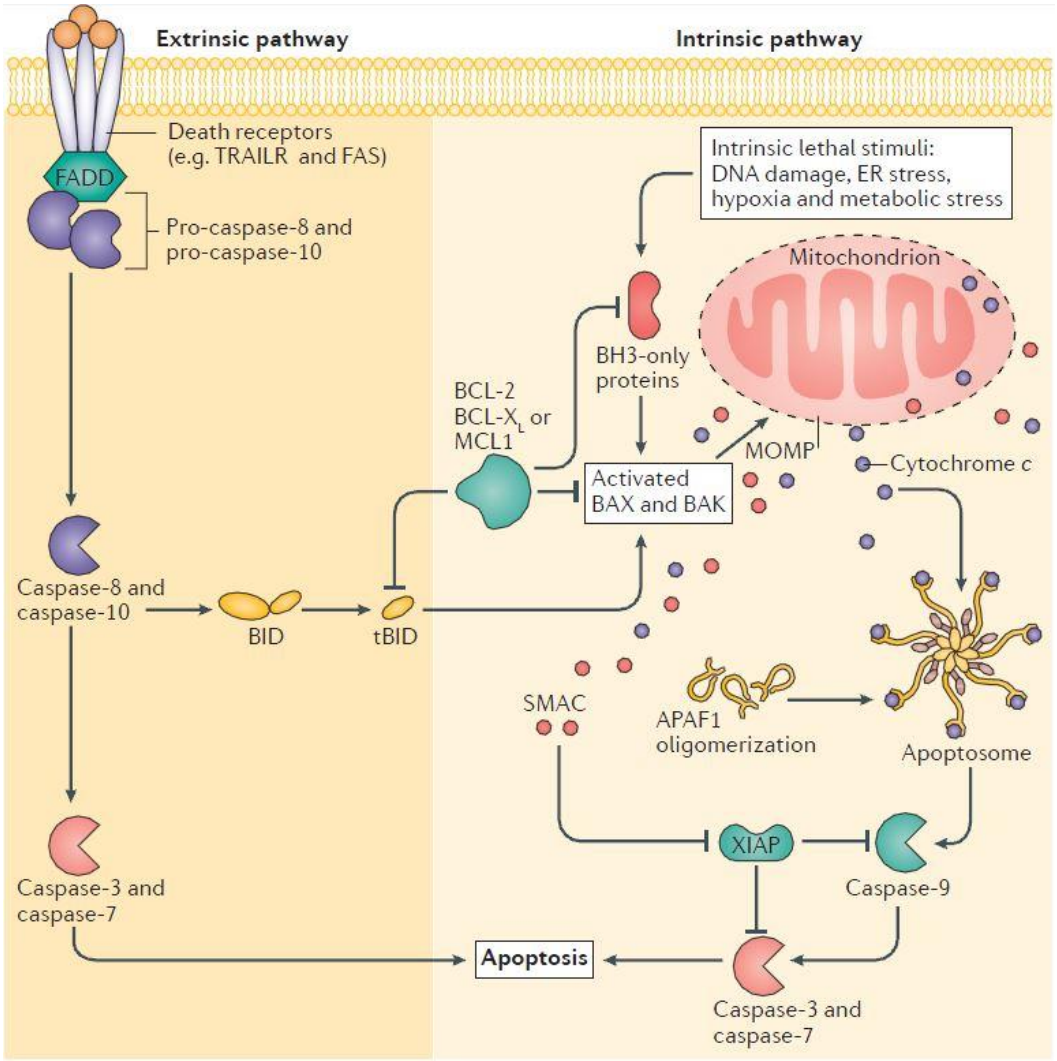

Figure 1.5 Extrinsic and intrinsic apoptotic signalling pathways.[43]

The extrinsic pathway starts with the binding of death receptors (such as tumour necrosis factor related apoptosis-inducing ligand receptor (TRAILR) and FASL receptor with their cognate ligands, which can activate initiator caspases (caspase-8, caspase-10) through dimerization mediated by FADD (FAS-associated death domain protein, an adaptor protein). Caspase-3 and caspase-7 are then cleaved and activated by Caspase-8 and caspase-10, eventually leading to apoptosis.[47,48 ,49]

The intrinsic pathway of apoptosis is triggered by intrinsic lethal stimuli (such as

DNA damage, ER stress), which first activate BCL-2 homology domain 3 (BH3)-only proteins. The BH3-only proteins then activate BAX and BAK, leading to mitochondrial outer membrane permeabilization (MOMP). BCL-2, as an anti-apoptotic protein, counteracts this. Upon MOMP, mitochondrial intermembrane space proteins, second mitochondria-derived activator of caspases (SMAC) and cytochrome c, are released from mitochondria into the cytosol. Cytochrome c binds with apoptotic protease activating factor 1 (APAF1), forming a complex termed apoptosome. The apoptosome then activates caspase-9, leading to the activation of caspase-3, caspase-7 and apoptosis.[48,50,51]

X-linked inhibitor of apoptosis protein (XIAP) regulates the apoptotic pathway by blocking caspase-3 and caspase-7. The BH3-only protein BH3-interacting death domain agonist (BID) is cleaved by caspase-8 and enables crosstalk between the intrinsic and extrinsic apoptotic pathways.[48]

1.1.6.2 Anti-apoptotic proteins in CLL

The leukaemic cells accumulated in the bone marrow and lymph nodes are unable to initiate the apoptotic program due to several factors including defects in apoptotic pathways and excessive survival signals.[52-56] The survival signaling pathways, such as NF-kB, which activates the transcription of antiapoptotic proteins (such as Mcl-1 and IAPs) or PI3K/AKT that phosphorylates several protein targets of relevance to apoptosis, are activated in leukaemic cells.[57] Key antiapoptotic proteins (Bcl-2 and IAP families)

are overexpressed, a consequence of transcription in these survival pathways. XIAP, which belongs to the inhibitor of apoptosis proteins (IAPs), has a significant role in caspase inactivation.[58] Both Mcl-1 and Bcl-2 play a crucial role inhibiting apoptosis in CLL cells.[59, 60] Through transcriptional up-regulation of antiapoptotic proteins Mcl-1 and XIAP, survival of CLL cells are ensured.[61]

1.2 Targeting cyclin dependent kinase for cancer treatment

1.2.1 Protein kinases

Protein kinases are kinase enzymes that transfer the terminal phosphate of ATP to substrates (phosphorylation). Phosphorylation of substrates (the target protein) can lead to a functional change, such as enzyme activity, cellular location, or association with other proteins.[62] To date, the human genome encodes 560 protein kinase genes.[63] Protein kinases can regulate cellular pathways through modification of the signal transduction.

Eukaryotic protein kinases share a common catalytic fold in which the active site is sandwiched by an N-terminal lobe and a larger C-terminal lobe (**Figure 1.6**).[62] The N-terminal lobe is composed of a β-sheet and a single α-helix (the "C helix"). The N- and the C-terminal lobes are connected by a five- to six-residue sequence which is termed the hinge region. Between the strands β1 and β2, there exists the glycine-rich loop which is a flexible part of the molecule. It participates in the ATP conformation, contributing to catalysis.[64-66]

According to their binding mode, kinase inhibitors can be classified into four

types.[67,68] Typle-1 inhibitors can recognise the active conformation of the kinase and is ATP-competitive. Most kinase inhibitors belong to this type. CDK9 inhibitors in this project are type-1 inhibitors and directly compete with ATP.[69] Type-2 inhibitors target an inactive conformation of the kinase, with access to a hydrophobic pocket adjacent to the ATP-binding site. The third class comprises the allosteric inhibitors, which bind to an allosteric site outside the ATP-binding site, and are ATP-non-competitive. Because of exploitation of binding sites and regulatory mechanisms, the third class tends to be more selective than types 1 and 2. The fourth class, covalent inhibitors, can form an irreversible and covalent bond with a nucleophilic cysteine residue in the kinase active site through an addition reaction.

All kinases have a conserved 20-35 residues activation loop. It plays a significant role in regulating kinase activity and is located between a conserved DFG motif and a less conserved APE motif (the abbreviations of three amino acids) (**Figures 1.6** and **1.7a**).[70,71]

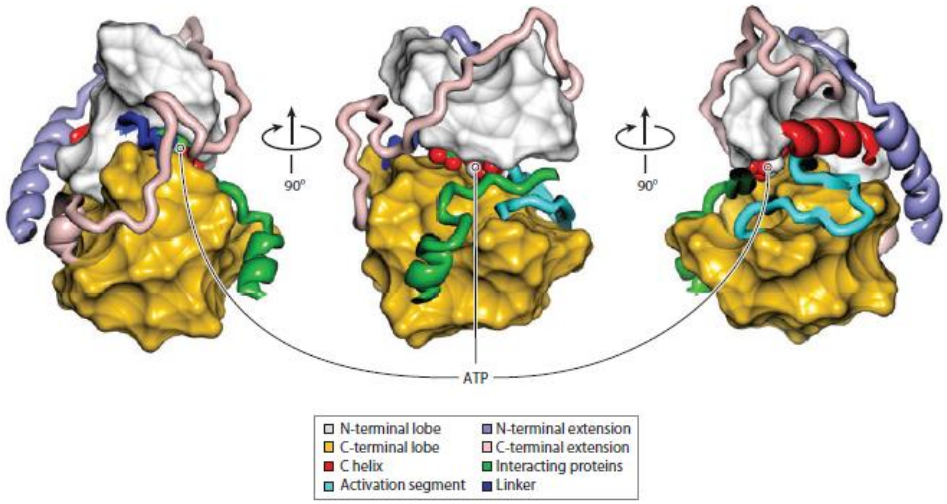

Figure 1.6: Architecture of a prototypical protein kinase.[72]

In the active conformation, the N-terminal lobe is packed by the C helix. Meanwhile the aspartate of the DFG orientates the ATP substrate by chelating a Mg^{2+} ion (**Figures 1.6** and **1.7b**). However, this interaction cannot exist in the inactive conformation because of the different position of the phenylalanine in the DFG motif (**Figure 1.7c**).[73]

Compared to inactive kinases, which are structurally diverse, active kinases do not have catalytic requirements to constrain the fold, so they share a common catalytic component.[73,74]

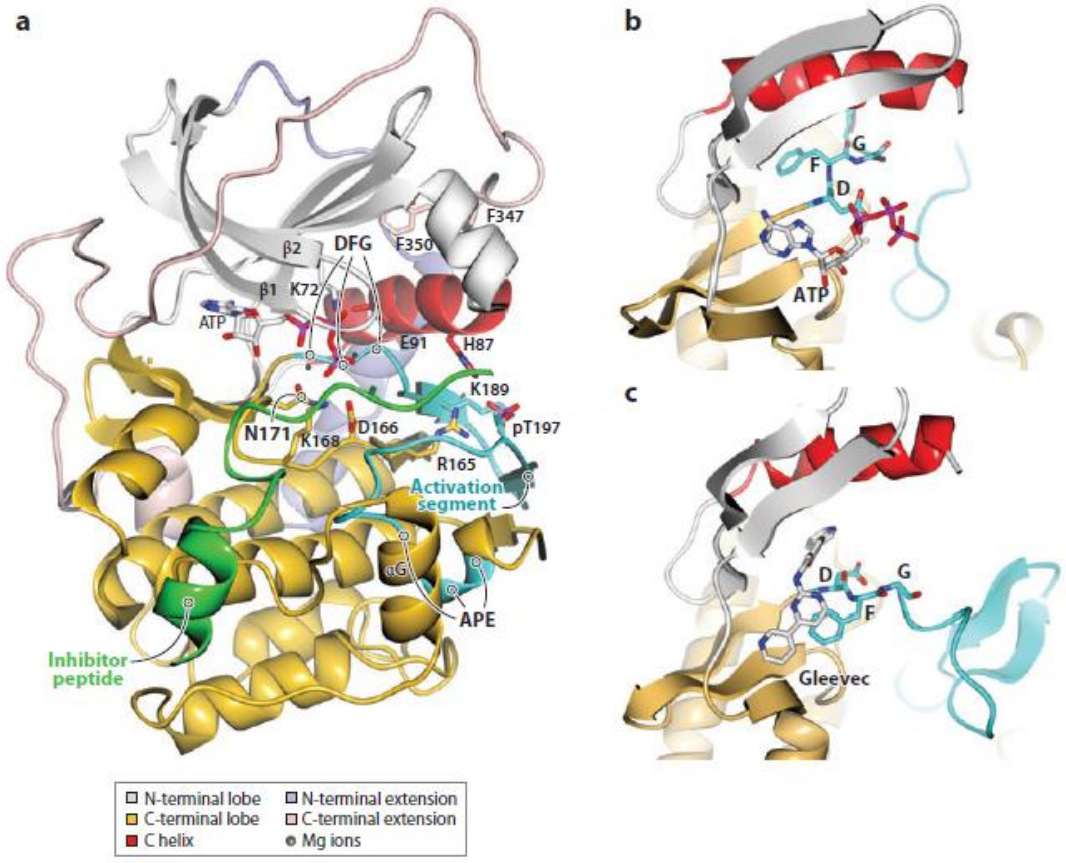

Figure 1.7: Active and inactive kinases. (*a*) The conserved residues at the active catalytic site of protein kinase A. (*b*) The C helix and DFG motif at the activation segment for PKA in the active conformation. (*c*) The C helix and DFG motif at the activation segment for Abl tyrosine kinase in the inactive conformation.[72]

1.2.2 Cyclin dependent kinases

CDKs (EC 2.7.11.22) are the members of the serine/threonine protein kinases family and play a key role in many physiological processes. To date, 20 types of CDKs have been identified in the human genome.[75] CDKs are generally classified into cell cycle CDKs and transcriptional CDKs based on their physiological roles.

Some CDKs, such as CDK1, CDK2, CDK3, CDK4 and CDK6, play a direct role in the regulation of cell cycle transitions by the monitoring and control of the major conformational and regulatory changes. (**Tab. 1.1**) CDK activity is regulated by cyclins as regulatory subunits. The cell cycle CDKs are usually classified as either G1 (CDK4 and CDK6/cyclin D, CDK2/cyclin E), S (CDK2/cyclin A, CDK1/cyclin A), or G2/M (CDK1/cyclin B) phase specific (**Figure 1.8**).[76,77]

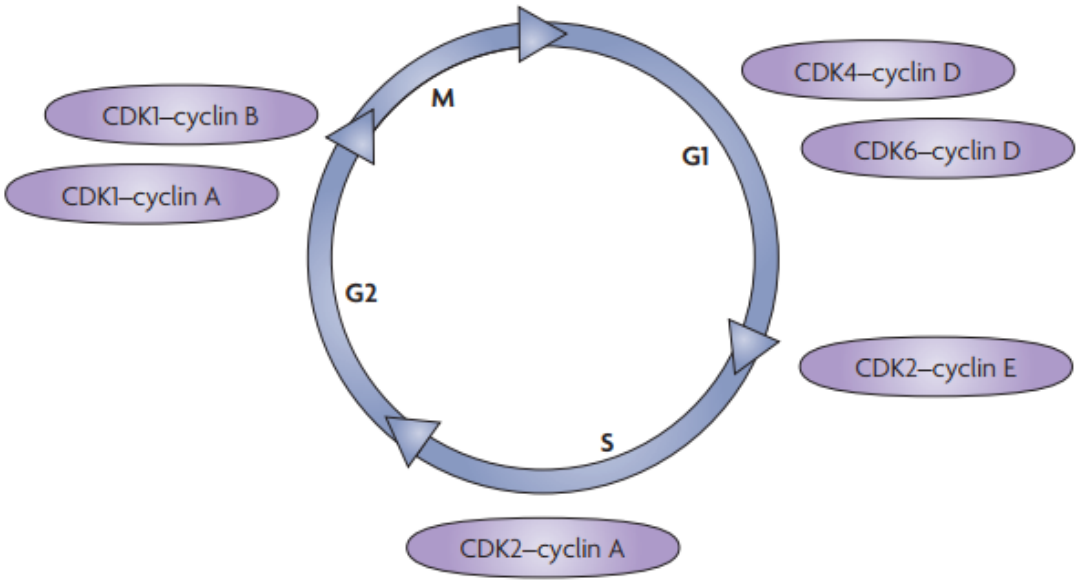

Figure 1.8 CDKs involved in cell cycle.[78]

Apart from the role in cell cycle regulation, CDKs also involve many other

physiological processes. **Table 1.1** gives a summary of physiological functions of CDKs1-14 and their main binding partners.[79,80] Transcriptional CDKs have attracted medicinal chemists, especially CDK8 and CDK9, which play key roles in the control of transcription by RNA polymerase II.[81-84] They are only involved in transcriptional regulation. Others CDKs have dual or multiple roles.

Table 1.1: The known CDKs, their main binding partners and their physiological functions.[80]

CDK	Main binding partners	Cellular functions
CDK1	cyclin A1; A2; B1; B2	G2-M (cell cycle)
CDK2	cyclin A1; A2; E1; E2	G1-S (cell cycle)
CDK3	cyclin E1; E2; A1; A2; C	G0-G1(cell cycle)
CDK4	cyclin D1; D2; D3	G1-S (cell cycle)
CDK5	p35; p39	Senescence, post-mitotic neurons
CDK6	cyclin D1, D2, D3	G1-S (cell cycle)
CDK7	cyclin H and MAT	CDK-activating kinase (CAK); transcription
CDK8	cyclin C	Transcription
CDK9	cyclin T1, T2a, T2b, K	Transcription
CDK10	cyclin M	Transcription; G2M (cell cycle)
CDK11	cyclin L1; L2	Transcription, pre-mRNA splicing; M (cell cycle)
CDK12	cyclin L1; L2; K	Transcription; regulation of RNA splicing
CDK13	cyclin L1; L2; K	Transcription; regulation of RNA splicing
CDK14	cyclin D1; D2; D3; Y	G1-S (cell cycle)

1.2.3 Introduction to CDK9

Cyclin-dependent kinase 9 (CDK9) is a cdc2-like serine/threonine kinase which complexes with T and K types cyclins.[85] There exist two CDK9 isoforms (CDK9-42

and CDK9-55) and four kinds of regulatory cyclins (T1, T2a, T2b and K). CDK9 is ubiquitous in almost all the human tissues.[86] Whereas the CDK9-42 isoform is localised in the cell nucleus and cytoplasm, the CDK9-55 isoform is mainly present in the cell nucleus.[87]

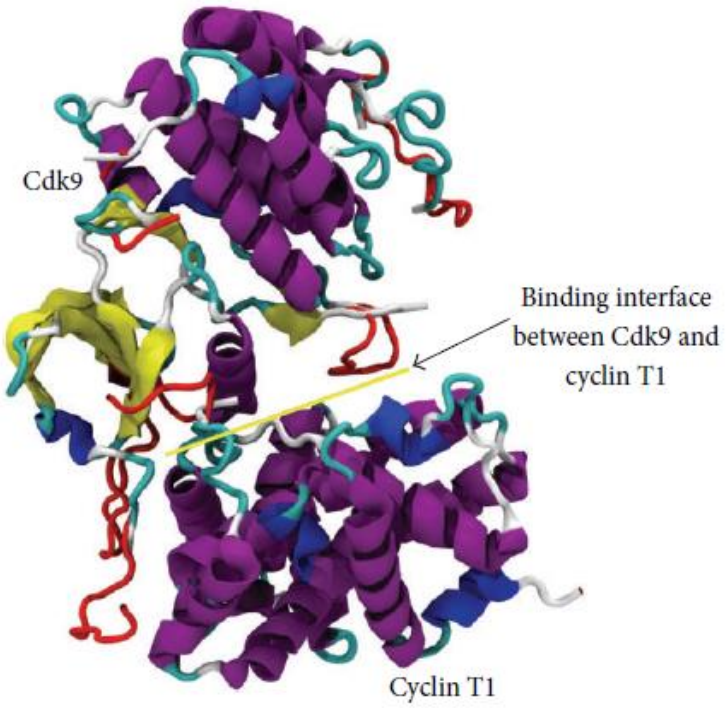

Figure 1.9: The CDK9/cyclinT1 complex. The yellow line shows the binding interface between Cdk9 and cyclin T1.[80]

Both CDK9 isoforms can form heterodimers with the four kinds of cyclins, in which CDK9 functions as the catalytic domain and cyclins constitute the regulatory subunit (**Figure 1.9**).[86,88] In contrast to monomeric CDK9, the heterodimer (CDK9/cyclinT) is more stable.[87,89] Additionally, CDK9 and cyclinT are subunits of the positive transcription elongation factor (P-TEFb), which regulates RNA pol II-based transcription.

The transcription cycle is triggered through phosphorylation of Ser 5 of CTD

heptapeptide repeats by CDK7 (a component of the TFIIH complex). Due to the association between RNA pol II and the two negative elongation factors (NELF, DSIF), non-phosphorylated RNA pol II is not able to support the full elongation of the nascent RNA transcript. The P-TEFb complex first phosphorylates negative elongation factors (NELF and DSIF), which promote release of NELF and convert DSIF to a positive elongation factor. Subsequently, the P-TEFb phosphorylates Ser2 residue of CTD of the RNA pol II, allowing the productive elongation of the nascent RNA transcript (**Figure 1.10**).[90-92]

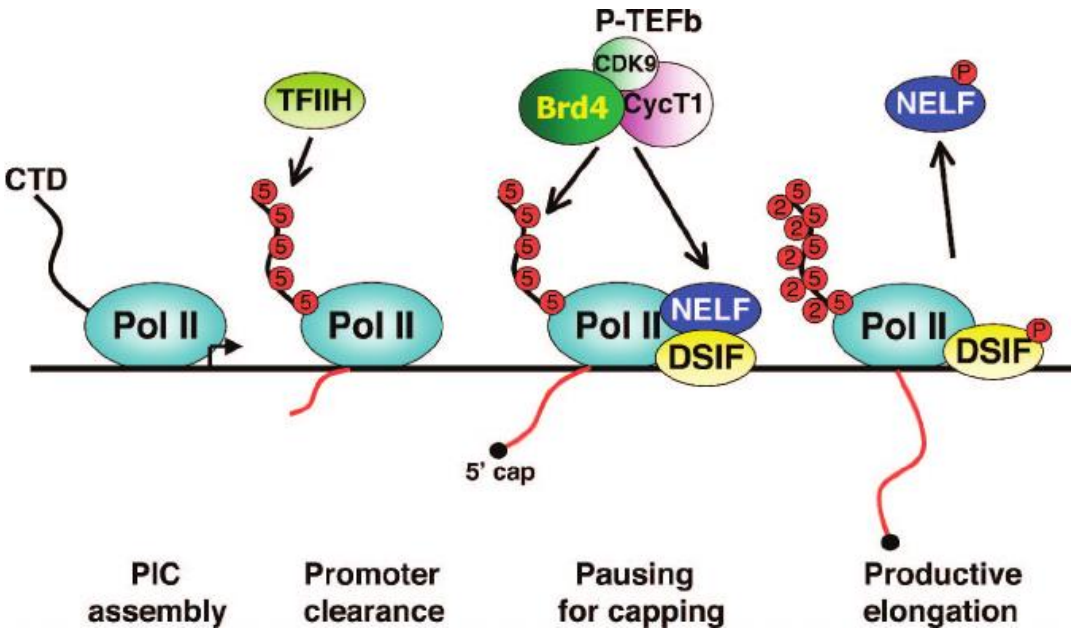

Figure 1.10: The role of the P-TEFb in transcription cycle.[93]

1.2.4 Rationale of CDK9 as an anti-cancer target

Resistance to apoptosis is a key characteristic of cancer.[15] Cancer cells need continuous production of antiapoptotic proteins to support survival and uncontrolled proliferation, which provide a therapeutic window for developing transcriptional

inhibitors to treat cancer. CDK9 is ubiquitously expressed and only involved in transcriptional elongation. Inhibition of CDK9 can downregulate the transcriptionally inducible genes, such as cell cycle regulators and antiapoptotic factors.[94]

1.2.4.1 Inhibition of anti-apoptotic proteins and Cyclin D

Inhibition of transcription (CDK9) can induce a rapid decrease of D-type cyclins and antiapoptotic proteins XIAP and Mcl-1, leading to apoptosis, which can be demonstrated by CLL cell death induced by flavopiridol, roscovitine and other CDK9 inhibitors.[95-97] Mc1-1 is an anti-apoptotic/pro-survival protein, which is highly expressed in numerous cancer cells. It is reported that downregulation of Mcl-1 alone is sufficient to promote apoptosis in CLL cells.[61] Cyclin D1 is the regulatory partner for CDK4 and CDK6,[98] the overexpression of which can cause hyper-phosphorylation of pRb and eventually lead to uncontrolled proliferation of cancer cells.[99, 100]

1.2.4.2 Inhibition of transcriptional factors

Positive transcriptional elongation factor b, which is composed of CDK9 and cyclin T can interact with transcriptional factors, such as the androgen receptor (AR), to promote transcriptional elongation. Additionally, AR is also reported to increase the growth of prostate cancer.[101, 102] Therefore, through inhibition of CDK9, AR transcription can be decreased, causing inhibition of proliferation rates of cancer cells.[102]

1.2.4.3 Inhibition of angiogenesis

Inhibition of CDK9 can also lead to an anti-angiogenesis in cancer cells. Some CDK inhibitors (such as flavopiridol, SNS-032 and roscovitine) have been shown to inhibit of angiogenesis due to the potent activity against CDK9.[103-105] Anti-angiogenesis of CDK9 is reported to be ascribed to downregulation of both VEGF mRNA and protein, the most potent tumour angiogenic factor.[106, 107]

1.2.4.4 Activation of *p53*

p53 is a key tumour suppressor protein and is mutated in 50% of human cancers. It is reported that transcriptional inhibition of *p53* by CDKs inhibitors (flavopiridol, roscovitine, and DRB) can induce apoptosis in cancer cells.[108, 109] Through transcriptional regulation of related genes in the *p53* network, it can also lead to DNA repair, cell-cycle arrest, and senescence in cancer cells.[110-112] For example, Mdm-2 is a negative regulator of *p53*, its downregulation by CDK9 inhibitors can activate *p53*, resulting in cancer cell apoptosis.[113-115]

1.3 CDK9 inhibitors

1.3.1 Known CDK9 inhibitors

CDK9 belongs to a family which comprises at least 13 closely related kinases. To maximise the therapeutic margin of CDK9 inhibitors, CDK9 inhibitors with high selectivity over other CDKs are required. Most broad-range CDK inhibitors display

activity against CDK9, and primary mechanistic studies show that to a large extent inhibition of CDK9 contributed to their anti-tumour activities. Some of these CDK inhibitors are in clinical trials and discussed below.[116-119] To date, only few selective CDK9 inhibitors have been reported.

1.3.1.1 **BAY 1143572** and **BAY 1251152**

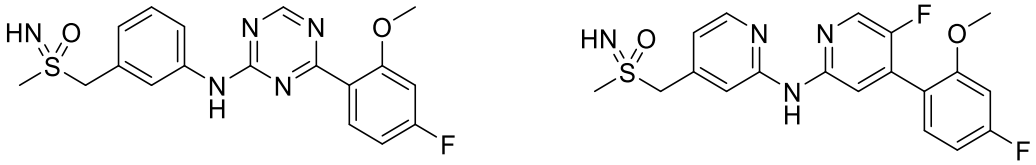

Figure 1.11 Chemical structures of potent and selective CDK9 inhibitors BAY 1143572 and BAY 1251152.

BAY 1143572 is reported as a potent and highly selective CDK9 inhibitor, which currently is being investigated in a Phase I clinical trial to determine the safety, tolerability and recommended Phase II dose in patients with advanced cancer or acute leukemia.[120, 121] It shows IC_{50} value for CDK9 of 25 nM, and more than 50-fold selectivity over other CDKs in enzymatic assays. Treatment with BAY 1143572 results in a transient inhibition of MYC (short-lived anti-apoptotic survival proteins) levels and an induction of apoptosis. BAY 1143572 also exhibits significant antitumour activity against primary adult T-cell leukaemia/lymphoma cells *in vitro*.[122]

Extensive structural optimisation of BAY 1143572 led to the identification of BAY 1251152. BAY 1251152 shows increased enzymatic activity (IC_{50} value for CDK9 of 3 nM) and cellular potency ((IC_{50} value for MOLM13 of 29 nM), and increased selectivity

against CDK2 (more than 100-fold) as well as high permeability and no efflux. BAY 1251152 is currently in a Phase I clinical trial to determine the safety, tolerability, pharmacokinetics and initial pharmacodynamic biomarker response in patients with advanced cancer.[123]

1.3.1.2 Flavopiridol

Flavopiridol and roscovitine (**Figure 1.12**), as two pan-selective CDK inhibitors, are the most studied CDK inhibitors. Flavopiridol has a preferred inhibition of CDK9 (K_i < 3 nM) over other CDKs (K_i values of 40 to 70 nM).[124]

Flavopiridol as a single agent in a phase-I clinical study for treatment of CLL has achieved high response rates.[125, 126] According to mechanism studies, flavopiridol can reduce the levels of anti-apoptotic proteins, especially MCL-1 and XIAP, in CLL and induce CLL cell death through transcriptional inhibition of CDK9.[97] Thus, providing proof of concept for the use of CDK9 inhibitors in the treatment of CLL.

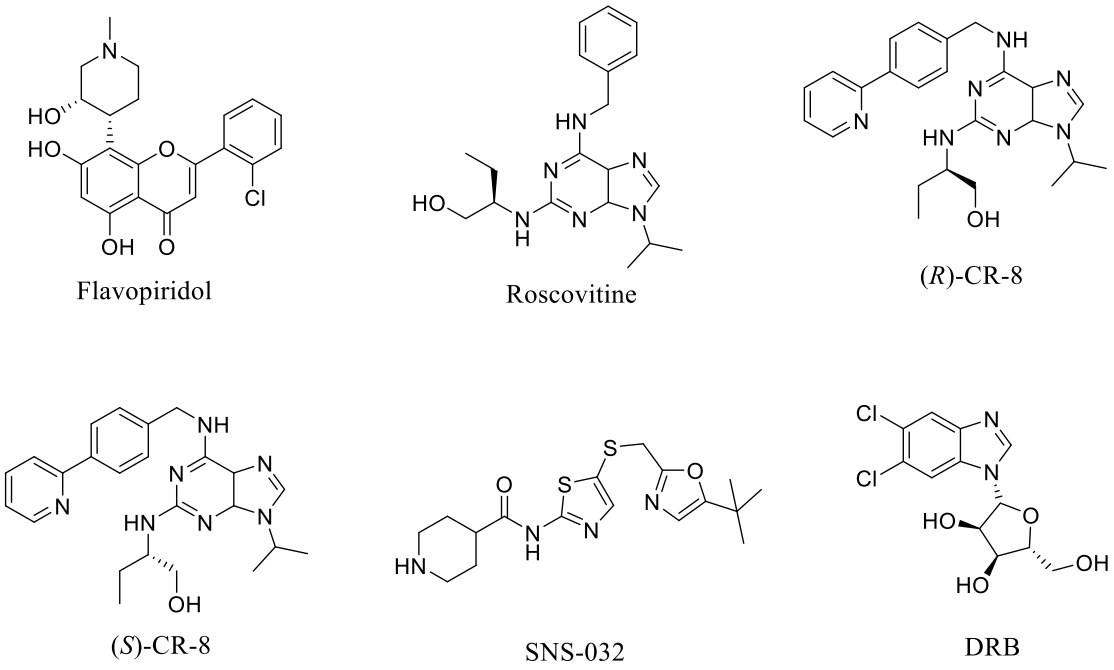

Figure 1.12 Chemical structures of representative CDK9 inhibitors

1.3.1.3 (*R*)-Roscovitine and its analogue CR-8

Roscovitine inhibits CDK1, 2, 5, 7 and 9 within the low micromolar range.[127] It has been reported that (*R*)-roscovitine can be used to treat distinct types of cancer, such as non-small cell lung cancer,[128] CLL,[95] and breast cancer.[129] Because of its short half-life and low potency against cancer cell lines, the large quantities which are needed to treat patients may limit its development as an anti-cancer drug.[130-132] Subsequently, a second-generation analog CR-8 (**Figure 1.12**) has been reported to exhibit 2- to 4-fold more activity than roscovitine against CDK1/2/3/5/7/9. (*S*)-CR8 also shows 102-fold more potency than (*R*)-roscovitine in the NCI 60 cell line panel.[133] Transcriptional inhibition by (*R*)-roscovitine can trigger the down-regulation of anti-apoptotic protein Mcl-1 in cancer cell, and thus lead to apoptosis, which has been demonstrated by *ex vivo*

treatment of patient CLL cells.[134]

1.3.1.4 DRB and SNS-032

DRB (**Figure 1.12**), a nucleoside analog, is an inhibitor of the transcriptional CDKs (CDK7 and CDK9). Although the half maximal inhibitory concentration (IC_{50}) of DRB for CDK9 is only 0.34 μM, it shows more than 28-fold selectivity for CDK9 over both CDK2 and CDK7.[135, 136] Due to the poor physicochemical properties and low potency against cancer cell lines, DRB is generally used as a chemical tool for chemical biology studies.

SNS-032 was designed as a CDK2 inhibitor, but it turned out to be potent against CDK9/cyclin T (IC_{50} = 4 nM). In a panel of 208 kinases, SNS-032 is highly selective for CDKs, and only four non-CDK proteins were inhibited. SNS-032 has been demonstrated to have a potential for antitumour activity in both solid and haematological cancers.[137] It was studied in Phase I clinical trial for treatment of CLL, multiple myeloma and metastatic refractory solid tumours.[138]

1.3.1.5 Pyrimidine derivatives

2-aminopyrimidine core is widely used as a pharmacophore in lots of CDK inhibitors, which commonly has different substitutions on 4-pyrimidine position. AstraZeneca reported two 4-imidazole ring substituted analogues, **1** and **2**.[139, 140] Both compound **1** (CDK1 IC_{50} = 16 nM, CDK2 IC_{50} = 6 nM, CDK5 IC_{50} = 14 nM, CDK9 IC_{50} = 20 nM)

and compound **2** (CDK1 IC_{50} = 2 nM, CDK2 IC_{50} = 2 nM) exhibited potent inhibitory activity against CDKs. Nevertheless, the clinical development of compound **1** has been stopped because of its short half-life and low tolerability.[141] Further study of compound **1** showed it can be employed as a potent radiosensitizer in non-small-cell lung cancer (NSCLZ) model.[142]

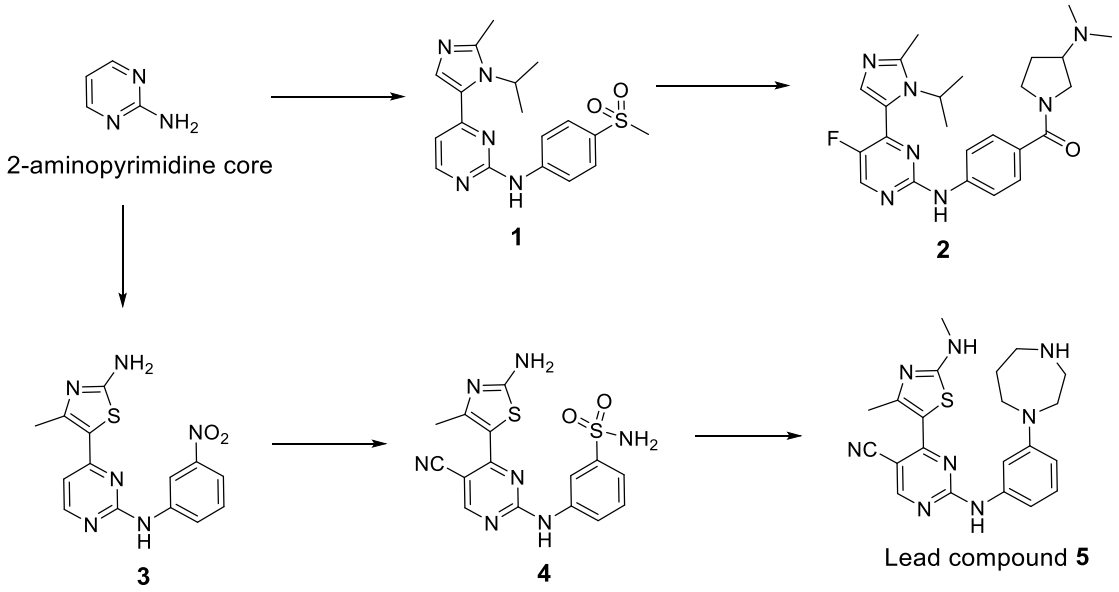

Figure 1.13 The development of a potent pyrimidine lead compound **5**.

A series of 2-aniline-4-(thiazol-5-yl)pyrimidine derivatives were reported as the highly potent and selective CDK9 inhibitors.[143-145] Through introducing electron-withdrawing substituents to the meta- position of the aniline and H-bond acceptor groups such as primary amino to 2-thiazole position, it can increase the inhibitory potency against CDK2. Compound **3** was reported as a potent CDK2 inhibitor (K_i = 2 nM). Further structural optimization of compound **3** led to another potent CDK inhibitor **4** (CDK1 K_i = 12 nM, CDK2 K_i = 4 nM, CDK9 K_i = 6 nM) by replacing the nitro group with the sulphonamide group and add a cyano group to the pyrimidine ring. Compound

5 was achieved by introducing a bulky diazepane group instead of the sulphonamide group and it shows > 80-fold selectivity for CDK9 (K_i = 7 nM) over CDK2 (K_i = 568 nM), and demonstrates potent anticancer activity against primary chronic lymphocytic leukaemia cells.[144] Compound **5** is adopted as the lead compound in this project.

1.3.2 The introduction to ATP binding site

Although the ATP-binding site of protein kinases is highly conserved, there are still some key areas of diversity within the architecture of the ATP-binding site. It can be divided into the following five regions.[146-148]

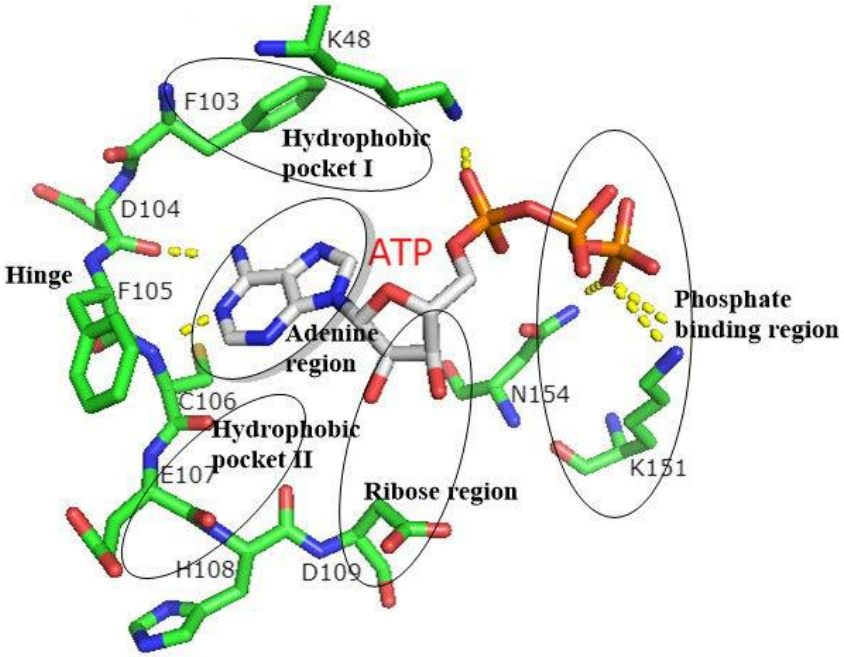

Figure 1.14: The ATP binding site of CDK9 complexed with ATP (PDB code 3BLQ). Hydrogen bonds are shown in yellow dash.[149]

1.3.2.1 Adenine binding site

The adenine binding site is mostly hydrophobic in character. According to the binding pose of CDK9 with ATP in **Figure 1.14**, N1 and N6 nitrogen of the adenine ring of ATP are engaged in two hydrogen bond donor-acceptor systems by interactions with the backbone NH and carbonyl groups of the hinge region. The hydrogen bonds formed with hinge region are common in most potent kinase inhibitors. The adenine ring of ATP is typically replaced by a heterocyclic ring system in CDKs inhibitors, and the substituents of the heterocyclic ring can extend to the adjacent hydrophobic pockets I and II.[67]

1.3.2.2 Hydrophobic pocket I

The hydrophobic pocket I locates at the extending direction of N7 nitrogen of adenine. It is not used by ATP in most of the protein kinases, but it can be exploited to gain binding affinity and improve selectivity. The size of this pocket varies in different kinases and is determined by the gatekeeper residue. The gatekeeper residue partially or fully blocks the hydrophobic region I and contributes to the selectivity of kinases for small molecule inhibitors.[150] Kinase inhibitors have been reported to gain affinity or selectivity by exploiting the difference in gatekeeper residues.[151-153]

1.3.2.3 Hydrophobic pocket II

This region is a hydrophobic slot which is opened to solvent. It is not occupied by

ATP and can be used to gain binding affinity. It has been reported a selective CDK4 inhibitor was designed based on the differences of hydrophobic II between CDK2 and CDK4.[154]

1.3.2.4 Ribose region

It is also called the sugar region, which is hydrophilic in most protein kinases, except EGFR. This peculiarity has been exploited to design potent and selective EGFR inhibitors.[155]

1.3.2.5 Phosphate binding site

Due to high solvent exposure, the phosphate binding site is less important in terms of binding affinity. But it can also be exploited to gain some additional affinity or to improve selectivity by taking advantage of the less conserved amino acids in this region.[148]

1.3.3 The binding mode of CDK9 with known inhibitors

1.3.3.1 Flavopiridol

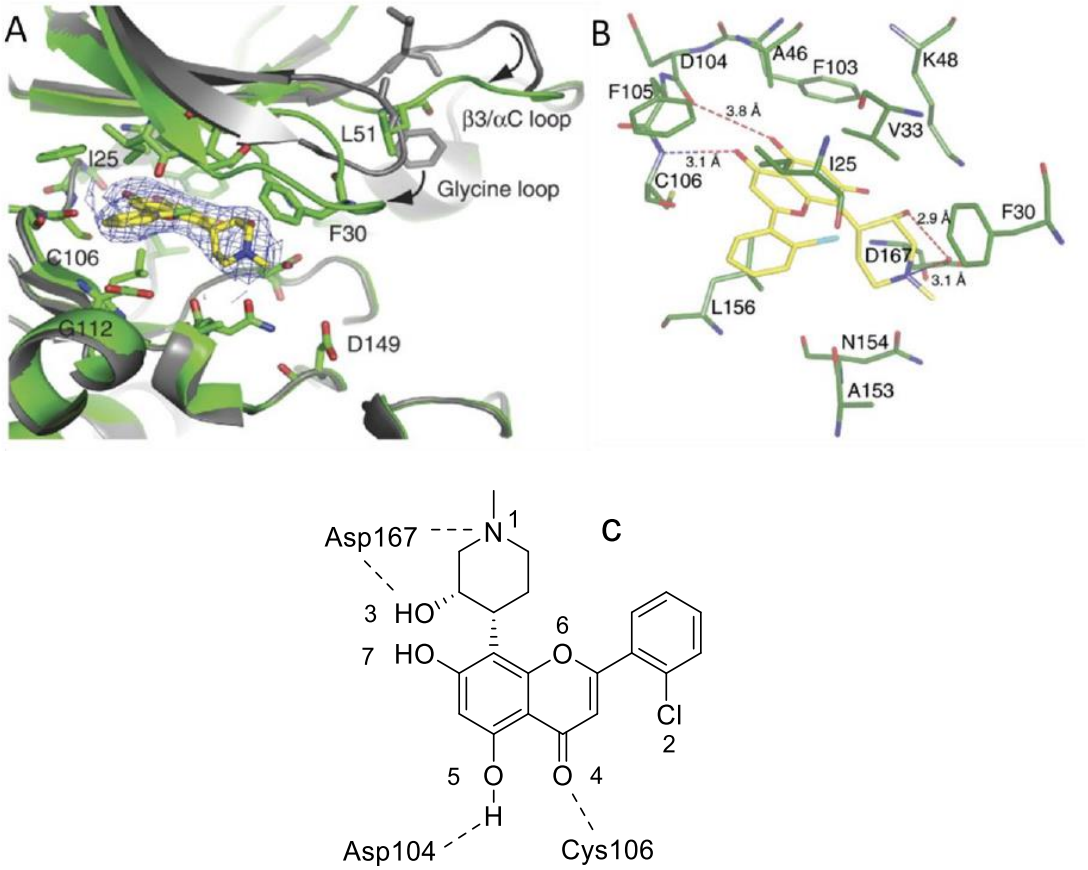

Figure 1.15: (A) Flavopiridol binding mode in CDK9 (PDB ID: 3BLQ). (B) Details of interactions of flavopiridol with CDK9. (C) A schematic representation of flavopiridol with related amino acid residues.[156]

Several known CDK inhibitors were co-crystallised with CDK9 and will be discussed here. To date almost all CDK inhibitors compete with ATP in the ATP-binding pocket,[157] and flavopiridol is the most studied inhibitor.

The co-crystallisation of flavopiridol with CDK9/cycin T1 was reported by Baumli *et al*. in 2008 (**Figure 1.15**).[156] Hydrogen bonds are formed between the O4 oxygen, O5

hydroxyl of flavopiridol and Cys106 NH and Asp 104 O of hinge region. The protonated piperidinyl group N1 and the O3 hydroxyl also form hydrogen bonds with the Asp167 (Asp145 in CDK2) side chain.

Analysis of the superposition of CDK2 and CDK9 with flavopiridol (**Figure 1.16**) shows that the CDK9-flavopiridol complex shows more intermolecular hydrogen bonds. The benzopyran ring is at the same position in both complexes.[158] There are two strong salt bridges existing between Glu92-Lys20 and Glu92-Lys29 in the CDK9-flavopiridol structure. This strong electrostatic interaction, involving residues from two different lobes in CDK9, makes the two lobes closer and leads to more contact area for the ligand and protein kinase.

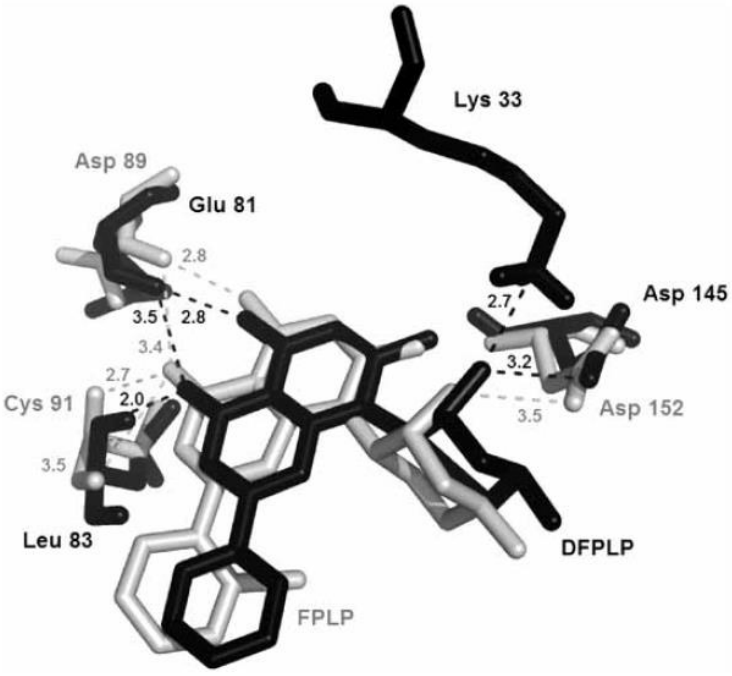

Figure 1.16 Details of superposition of the complexes of deschloroflavopiridol with CDK2 and flavopiridol with CDK9.[158]

1.3.3.2 DRB

DRB shows 30-fold more selectivity against CDK9 over CDK2. DRB adopts different orientations when binding to the ATP-binding site of CDK9 and CDK2 (**Figure 1.17**).[159] In CDK9/cycin T, the planar benzimidazole moiety is sandwiched between residues Ile25 and Leu156. The two chlorine atoms of the DRB benzimidazole, Cl1 and Cl2, form halogen bonds with Asp104 and Cys106 in the CDK9 hinge region. There still exists polar contact between DRB and CDK9, which is mediated by a water molecule between the benzimidazole N2 and the backbone NH group of Asp167.

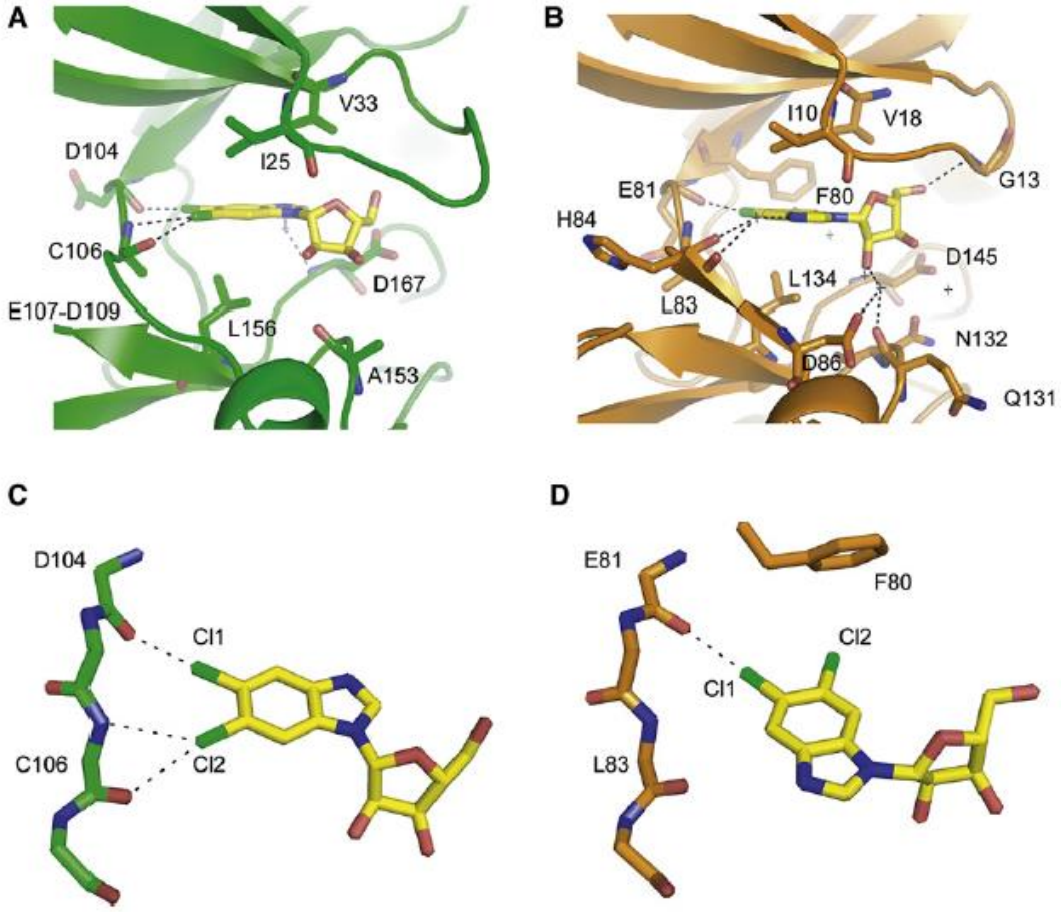

Figure 1.17 DRB binding to CDK9 and CDK2 (A) Details of the CDK9/cyclin T (B) Details of the CDK2/cyclin A inhibitor; carbon atoms, yellow; Contacting

residues, stick models; Halogen and hydrogen bonds, dotted lines; Waters, crosses. (C and D) Detailed views of the halogen bonds of DRB bound to CDK9 and CDK2, respectively.[160]

DRB binds to CDK2 in a different orientation (**Figure 1.17 B** and **D**).[160] Cl1 contacts the carbonyl group of Glu81 in the hinge region, and forms a hydrogen bond. Cl2 contacts the π-electrons of the phenylalanine ring of gatekeeper residue Phe80. The ribofuranoside adopts a similar orientation in the CDK2-bound structure as that in CDK9 except a hydrogen bond forms between the ribofuranoside to the main chain nitrogen of Gly13. Several water-mediated interactions of DRB are also observed with CDK2, which is formed by N2 of benzimidazole with the carbonyls of Leu83 and His84, and the O of ribofuranoside with the carbonyls of Asp86 and Asn132, **Figure 1.17**, **B**).[160]

1.3.3.3 (*S*)-CR8

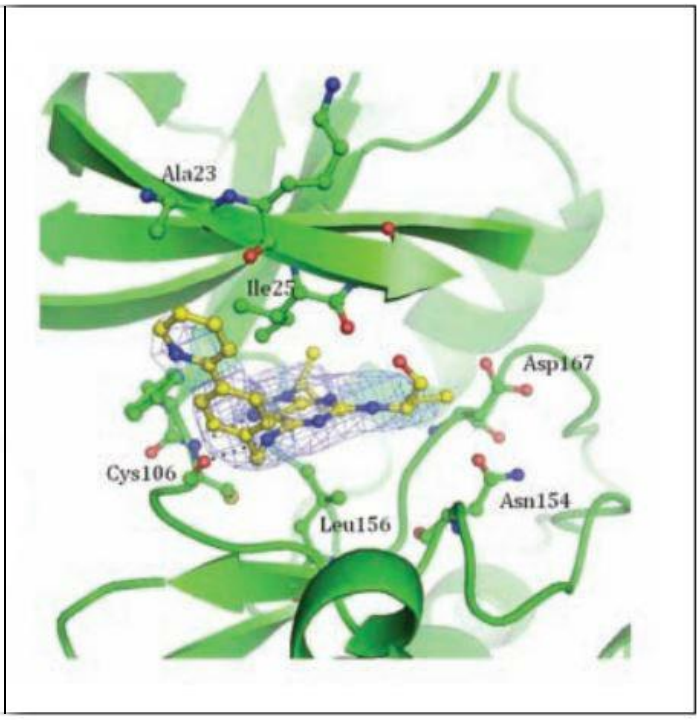

Figure 1.18 The co-crystal structure of (*S*)-CR8 with CDK9/cyclin T.[37]

(*S*)-CR-8 is a potent CDK9 inhibitor (IC_{50} = 110 nM).[37] **Figure 1.18** is cocrystal structure of (*S*)-CR8 bound to the ATP binding pocket of CDK9/cyclin T. The purine ring of (*S*)-CR8 occupies the adenine binding site and is sandwiched between residues Ile25 and Leu156.

Two hydrogen bonds are formed by N7 of the purine ring and the 6-amino group with Cys106 of the hinge region. This orientation of (*S*)-CR8 makes the phenyl-pyridine ring out of the ATP binding site and forms a favorable interaction with Phe105, Ile25, and Ala23. The Phenyl-pyridine moiety shows a weaker electron density than the purine ring, which indicates the flexibility of the phenyl-pyridine ring within the crystal.[37]

1.3.4 Flexible elements in CDK9/cyclin T

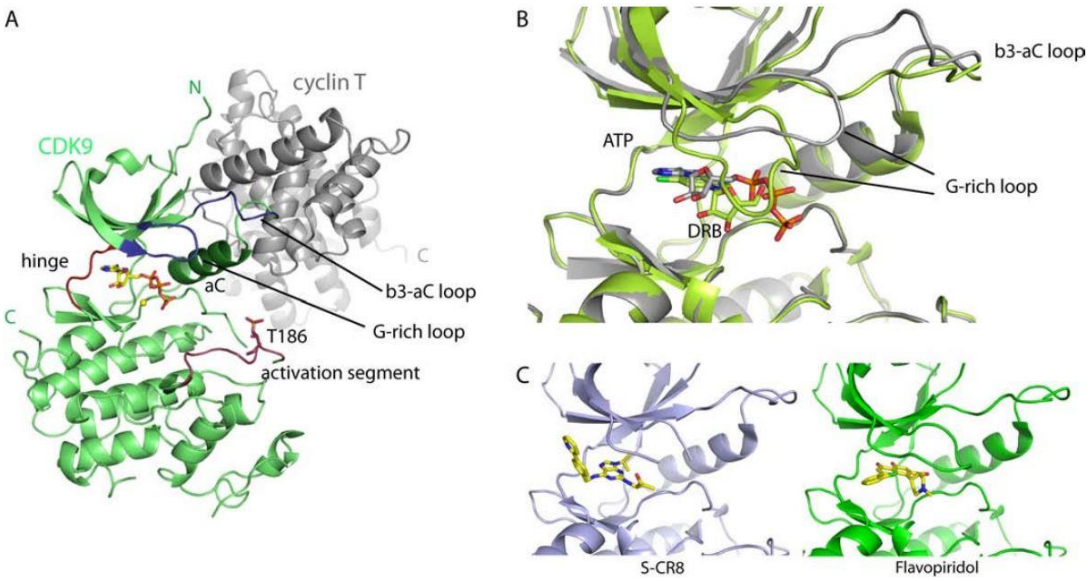

Figure 1.19 A: Ribbon model of ATP bound to CDK9/cyclin T (PDB ID: 3BLQ). **B**: Overlay of CDK9/cyclin T ATP (grey, PDB code: 3BLQ) and DRB (lime green, PDB code: 3MY1) bound structures. **C**: Structures of (*S*)-CR8 (PDB code: 3LQ5) and flavopiridol (PDB code: 3BLR) bound to CDK9. All proteins are represented as ribbon models, inhibitors as stick models.[161]

Compared to other CDK inhibitors, CDK9 inhibitors are more specific as they are able to exploit the conformation flexibility of the glycine-rich loop and the β3-αC loop.[156] Although DRB makes more polar contacts with CDK2 than it does with CDK9, it is able to exploit the greater flexibility of CDK9/cyclin T by a downward movement of the glycine-rich loop.[156, 160] Meanwhile, the β3-αC loop moves to the original position of the glycine-rich loop and further stabilises this conformation. The same downward movement of the glycine-rich loop is observed in the crystal structure of CDK9/cyclin T with flavopiridol. Nevertheless, this conformational change is not present in the crystal structure of deschloroflavopiridol and DRB with CDK2/cyclin A, which

indicates this conformational change is specific for CDK9.[160, 162] The flexible glycine-rich loop as a specific structure of CDK9, can be exploited to design potent and selective CDK9 inhibitors.[146]

1.4 The rationale of the design for macrocyclic ligands

1.4.1 The binding mode of lead compounds with CDK9 and CDK2

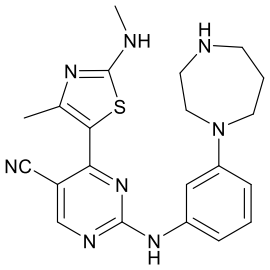

Lead compound 5

K_i = 7 nM for CDK9
K_i = 568 nM for CDK2
K_i = 63 nM for aurora-A
K_i = 58 nM for aurora-B

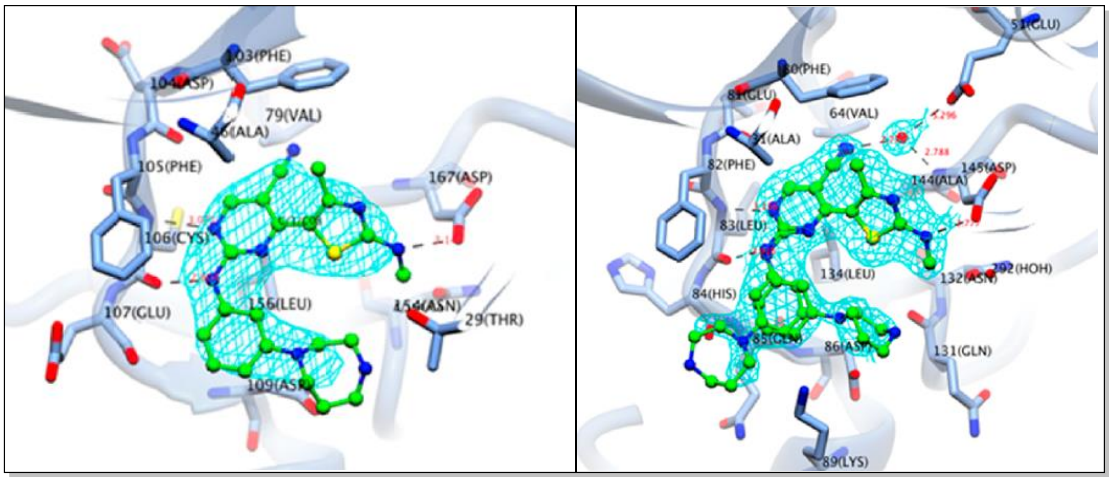

Figure 1.20 Cocrystal structures of lead compound **5** bound to (A) CDK9/cyclin T (PDB code 4BCG) and (B) CDK2/cyclin A (PDB code 4BCP).[144]

Lead compound **5** was reported as a potent and selective CDK9 inhibitor (over 80 fold selectivity for CDK9 versus CDK2) in the previous CDK9 project.[144] It was optimised from another small pyrimidine derivative **4** through introducing a bulky diazepane to the meta- aniline (**Figure 1.13**). Through inhibiting cellular RNAPII

transcriptional activity, lead compound **5** can down-regulate the antiapoptotic protein Mcl-1 and triggers apoptosis of cancer cells. Notably, lead compound **5** shows excellent antitumor activity in primary CLL cells, and it only shows little toxicity in healthy normal B- and T-cells.[144] The disadvantage of lead compound **5** is the lack of selectivity over Aurora kinases (ARKs) (8-fold selectivity for CDK9 over ARKs).

Lead compound **5** was co-crystallised with CDK9/cyclin T (left) and CDK2/cyclin A (right) in **Figure 1.20** to explain the difference of two binding poses.[144] From the co-crystal structures, **5** adopts the similar binding poses within the ATP binding sites of these two CDKs. In the kinase hinge regions, the N1-pyrimidine and C2-NH of the pyrimidine ring form two hydrogen bonds with the NH of Cys106 (Leu83 in CDK2) and the carbonyl of Cys106 (Leu 83 in CDK2). A favourable lone pair-π-interaction is formed by the C5-carbonitrile group with the gatekeeper residue Phe103 (Phe80 in CDK2) in the hydrophobic pocket I. Notably, an extra water molecule is trapped near the C5-carbonitrile in the CDK2, and a water-mediated hydrogen-bonds network is formed with residue Asp145 and Glu51. The N-H of 2-thiazole methylamine can also form a hydrogen bond with Asp167 in (Asp145 in CDK2) in both binding poses.

Within the cocrystal structures in **Figure 1.20**, the bulky substituent, 1,4-diazepane, adopts two distinct orientations. One has the position toward the thiazole group and is close to the ribose region in the ATP binding pocket, which is termed the “inward” conformation. The other orientation of 1,4-diazepane termed the “outward” conformation” has a 180^{o} rotation and is away from the thiazole group.

1.4.2 Aurora kinases (ARKs) as the off-target proteins

ARKs belong to a small family of serine/threonine kinases, which play key functions in mitotic events.[163] Mammalian cells express three classes of aurora kinases, namely aurora A, aurora B, and aurora C. Aurora A, which positions to the centrosome and spindle poles, promotes centrosome maturation and spindle assembly.[164, 165] Aurora B as the component of the chromosomal passenger complex (CPC) is required for phosphorylation of histone-H3, the spindle assembly checkpoint, and cytokinesis.[163,164] Aurora C is reported as a chromosome messager, but its functional role is still unknown.[165] Auroras A and B have been demonstrated to be over-expressed in primary breast[166] and colon tumour cells.[167]

According to the Diversity Kinase Panel screening, lead compound **5** is a potent and selective CDK9 inhibitor, except ARKs as the main off-target.[168]

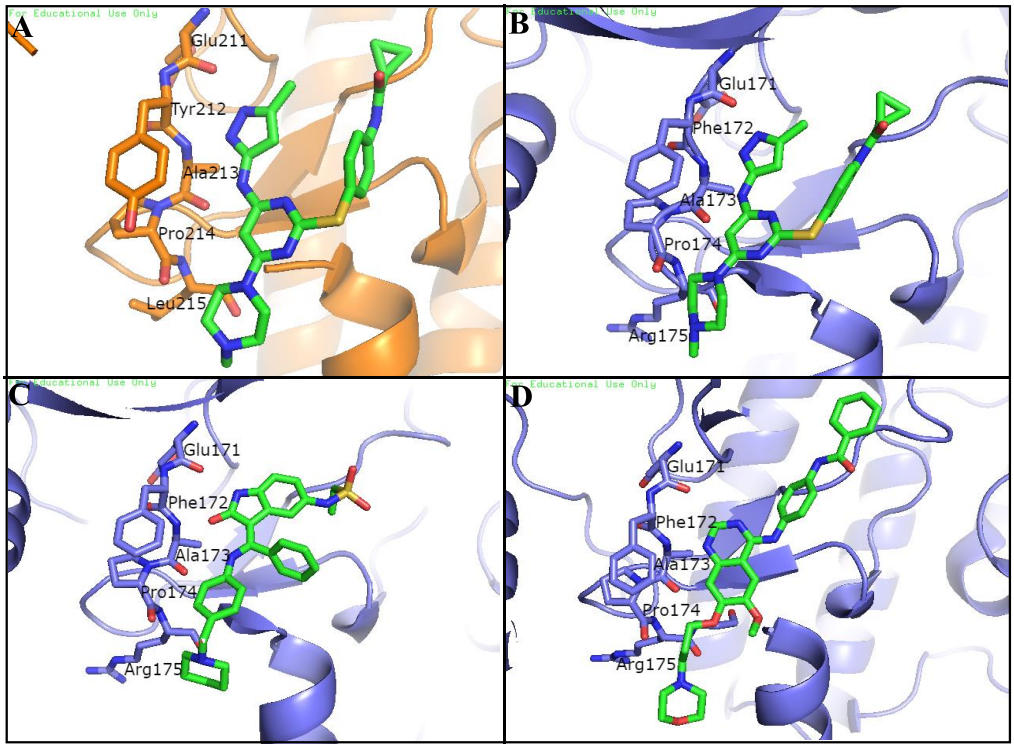

Figure 1.21 Cocrystal structures of known ARKs inhibitors bound to Aurora A and Aurora B. (A) VX680 with Aurora A (PDB code 3E5A),[169] (B) VX680 with Aurora B (PDB code 4B8M),[169] (C) Hesperadin with Aurora B (PDB code 2BFY),[164] (D) ZM447439 with Aurora B (PDB code 2VRX).[170]

Figure 1.21 shows the cocrystal structures of the known ARKs inhibitors, ZM447439, Hesperadin and VX-680, bound to the ARKs with the "outward" conformation.[163, 164, 169, 170] It is similar as the docking pose of lead compound **5** bound to CDK2.

1.4.3 The design strategies for macrocyclic compounds

1.4.3.1 Macrocyclic structure

Figure 1.20 shows that lead compound **5** adopts two alternative conformations, "inward" and "outward", in the CDK2/cyclin A complex. However, the 1, 4-diazepane ring in the CDK9 complex clearly only adopts an "inward" conformation, suggesting the ATP binding pocket of CDK2 is too crowded for the "inward" conformation of **5**. Meanwhile, in **Figure 1.21**, ARKs inhibitors all adopt the same "outward" conformation binding poses in the ATP binding site of ARKs. Therefore, a locked "inward" conformation, macrocyclic structure, has the potential to improve the selectivity of CDK9 inhibitors over CDK2, ARKs.

Amide linkers and alkene linkers are two common used strategies in cyclisation reaction. Therefore, macrocyclic compounds in this project were synthesised using the amide coupling and ring closing metathesis (RCM).

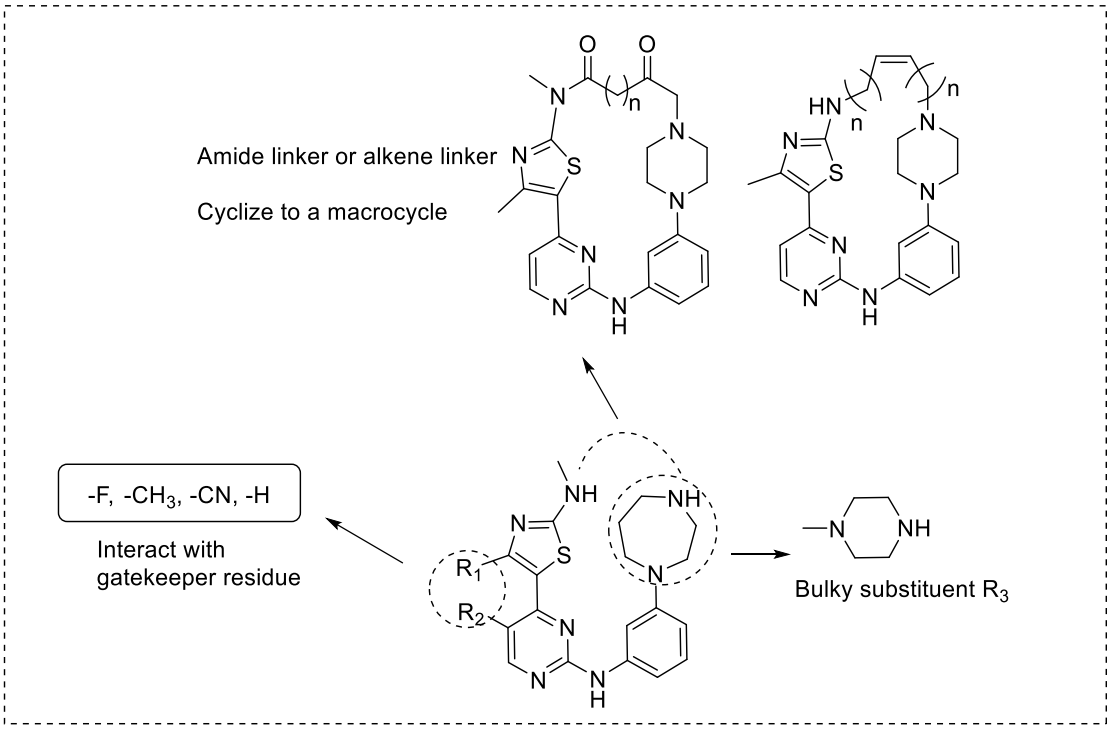

Figure 1.22 The design strategies for macrocyclic compounds.

1.4.3.2 R^1 and R^2 substituents

The gatekeeper residue in hydrophobic pocket I is crucial for the kinase inhibitor to improve the binding affinity. This pocket in CDK9 is relatively small because of the small gatekeeper residue Phe103. Therefore, through exploring the interaction between R^1, R^2 and gatekeeper residue Phe103, it should be possible to gain binding affinity and improve the selectivity for CDK9 over other kinases, such as CDK2 and ARKs.

1.4.3.3 Bulky R_3 substituent

Because of the flexible glycine-rich loop in CDK9, CDK9 inhibitors favour an "in-conformation" in the ATP binding site, and a bulky R^3 substituent (heteroatom

substituted ring) can generate a polar contact with Thr29 in the glycine-rich loop. However, this interaction cannot be observed in the “out-conformation” in other CDKs. Thus, a bulky R^3 substituent, like piperazine, has the potential to improve the selectivity of CDK9 inhibitors.

1.5 Aims and objectives

This project aims to:

1) Design and synthesise macrocyclic pyrimidine analogues using structure-based design strategies, and improve the selectivity of the designed compounds against CDK9 over other kinases, like CDK2 and ARKs.

2) Analyse the observed SAR data and give a rational guide for the compound design with molecular docking.

Chapter Two: Macrocyclic compounds containing amide linkers

2.1 Overview of synthetic route

The first series of macrocyclic compounds was synthesised using the amide linker in **Scheme 2.1**. The pyrimidine ring of compound **14** was formed by treating enaminone **6** with *N*-phenyl-guanidine **10** under microwave condition. After deacetylation, the resulting precursor **15** was converted to macrocyclic compounds **17a-c** in a two-step process using two successive amide coupling reactions.

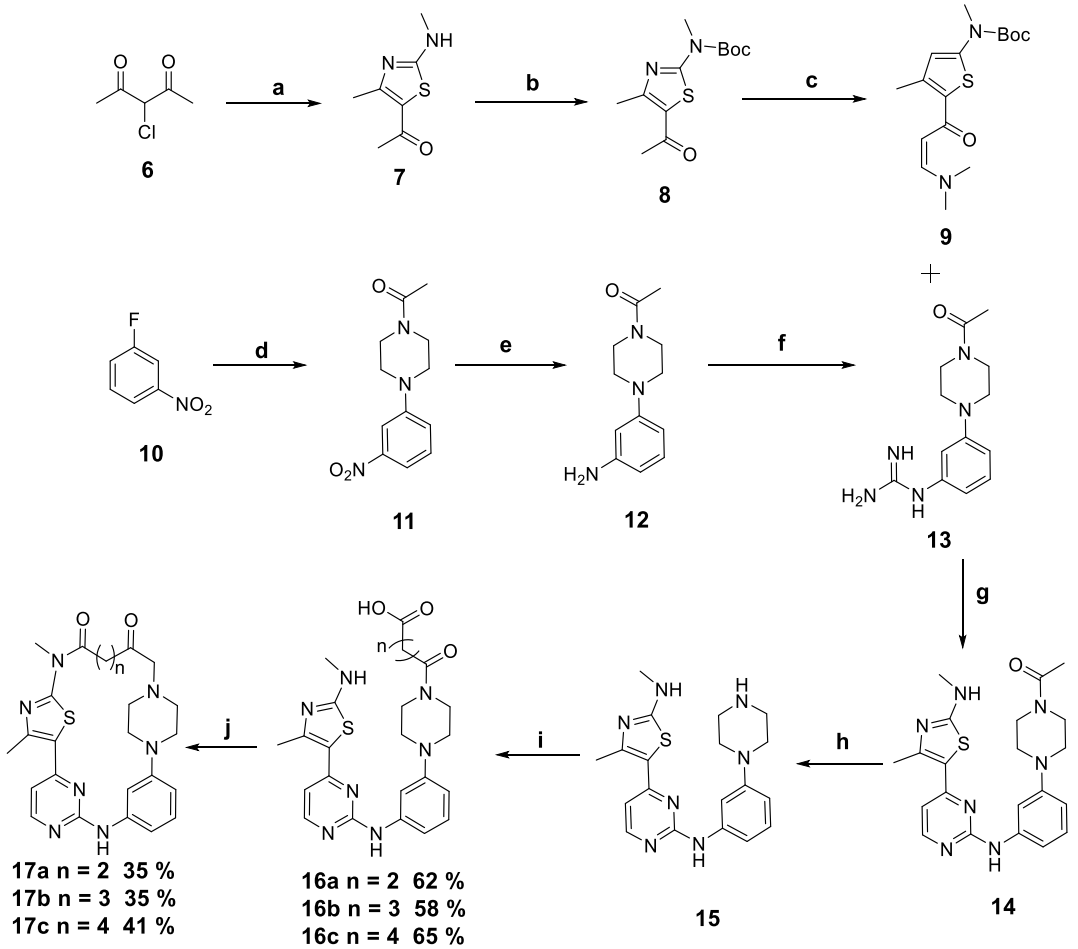

Scheme 2.1 Synthetic route towards macrocyclic pyrimidine analogues **17a-c**. Reagents and conditions: (a) 1-methylthiourea, pyridine, MeOH, 4 h, 90%; (b) Boc_2O, DMAP, DCM, RT, 2 h, 95%; (c) DMF-DMA, 120 ºC, 12 h, 55%; (d) 1-acetylpiperazine, DMSO, 100 ºC, 72 h, 70%; (e) H_2, 10% Pd/C, MeOH/ H_2O, RT, overnight, 95%; (f) cyanamide, TMSCl, MeCN, reflux, 6h, 70%; (g) 2-methoxyethanol, microwave 299W, 140 ºC, 45 min, 60%; (h) 2 M HCl, MeOH, reflux, 90%; (i) adipic acid for **16c** (glutaric acid for **16b** and succinic acid for **16a**), 2-chloro-4,6-dimethoxy-1,3,5-triazine, *N*-methyl-morpholine, DCM, RT, overnight; (j) DMAP, Et_3N, HATU, DMF, 50 º C, 20 h.

2.1.1 Synthesis of enaminone 9 as the precursor for pyrimidine 14

The synthetic route for 1-thiazole substituted enaminone **9** is shown in **Scheme 2.1**. Treatment of 1-methylthiourea with 3-chloropentane-2,4-dione **6** resulted in thiazole **7**. The *N*-methylamine group was protected, followed by alkylation reaction with excess DMF-DMA overnight to afford enaminone **9**.

DMF-DMA can react with compound **8** in two different reaction pathways, one leading to the methylation product following the reaction with acetyl group and the other leading to the condensation product following the reaction with *N*-methyl amine group.[171] Therefore, the *N*-methylamine group of **7** was Boc-protected to avoid the methylated by-product. **Scheme 2.2** gives the condensation reaction mechanism of compound **8** to enaminone **9**.

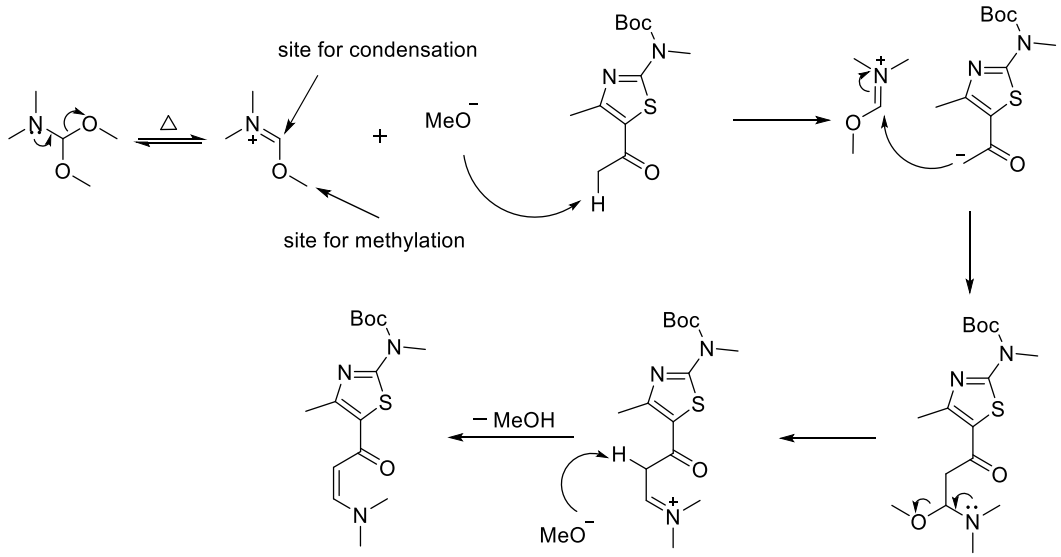

Scheme 2.2 Reaction mechanism of the enaminone **9**. From ref.[171]

2.1.2 Synthesis of guanidine 13 as the precursor for pyrimidine 14

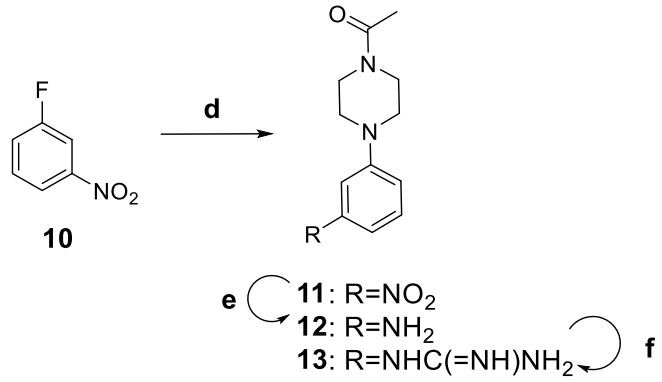

Scheme 2.3 Synthesis of compound **13**.

The *meta*-nitrobenzene compound **11** was synthesised by heating 1-fluoro-3-nitrobenzene **10** and 2 equivalents of 1-acetylpiperazine in DMSO in the presence of potassium carbonate, as shown in **Scheme 2.1**.[172] This method is optimised from the reaction for *para*-nitrobenzene as below (**Scheme 2.4**).

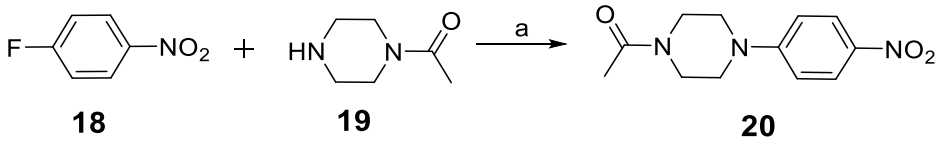

18 19 20

Scheme 2.4 Synthesis of *para*-nitrobenzene derivative. Reagents and conditions: (a) K_2CO_3/DMF, 100 ºC, overnight. 99%.

When this condition was applied to the *meta*-nitrobenzene compound, only a modest yield of 10% was achieved. Comparing to the *para*-substituted compound, the *meta*-substituted compound **11** is much more difficult to synthesise, which can be explained by the extra resonance stabilisation of the intermediate anion by the *para*-nitro-group.[172]

Pd/C was chosen as the catalyst to synthesise compound **12**, after which compound **12** was refluxed with cyanamide and TMSCl in acetonitrile. Unfortunately, neither crystallisation nor chromatography column was able to purify guanidine **13** because of its strong basicity. Therefore, it was used in the next step directly without purification.

2.1.3 Formation of 2,4-disubstituted pyrimidine 15

2,4-Disubstituted pyrimidine **14** was synthesised from enaminone **9** and phenylguanidine **13** in the microwave at 140 ºC for 1 h in **Scheme 2.1**. Reflux conditions were also used in this reaction, but it took > 12 h. Microwave-assisted conditions seemed to be more effective for this condensation.

Under the employed pyrimidine formation step, the Boc group was cleaved. Compound **14** was deacetylated to afford the piperazine analogue **15**, which was achieved by heating the compound **14** in 2 M aqueous HCl solution at 100 ºC overnight (**Scheme 2.1**).

2.1.4 Cyclisation of the precursor 15 using amide coupling chemistry

As is shown in **Scheme 2.1**, carboxylic acids are coupled with two terminal amines of compound **15** to afford the product **17a-c**. The amide couplings are divided into two separate steps. A selective amide coupling reaction was reported to convert carboxylic acid and piperazine into mono-amidated piperazine derivatives **16a-c** using 2-chloro-4,6-dimethoxy-1,3,5-triazine (**Scheme 2.5**).[173]

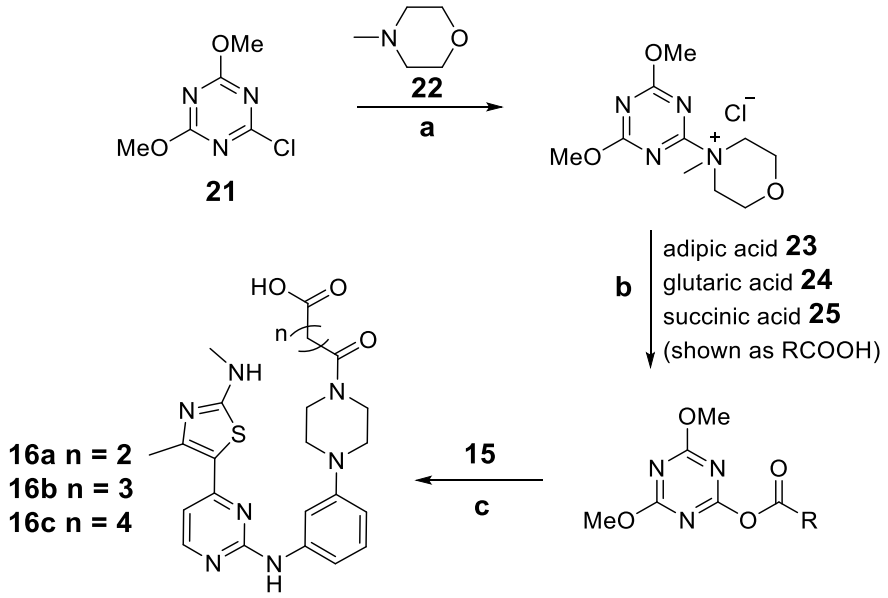

Scheme 2.5 A rapid and mild condition for amide formation. From ref.[173] Reagents and conditions: (a) *N*-methyl-morpholine, DCM, RT, 30 min; (b) DCM, RT, 1 h; (c) DCM, RT, overnight.

By introducing the 4,6-dimethoxy-1,3,5-triazine group, the reactivity of the carbonyl group was enhanced, and the piperazine was easily acylated to afford the mono-amidated product. Following that, typical amide coupling reagent HATU was employed to form the other amide bond and give the macrocyclic products **16a-c**.[174, 175]

2.2 Results and discussion

2.2.1 Kinase assay result

Kinase assays were carried out by Eurofins Kinase Screening & Profiling service using the radiometric assay. The inhibition of kinase activity was tested on three macrocyclic compounds **17a-c** against aurora-A, aurora-B, CDK2 and CDK9 at two concentrations (0.1 μM and 1 μM). **Table 2.1** shows the kinases activity inhibition (%).

Table 2.1. CDK2, CDK9, and aurora kinase inhibition activity of compounds **17a-c**.

Compound		Kinase inhibition (%)[a]			
No.	concentration (μM)	aurora A	aurora B	CDK2–cyclin A	CDK9–cyclin T1
17a	0.1	58	74	5	7
	1	93	98	22	35
17b	0.1	51	33	0	8
	1	44	70	0	23
17c	0.1	41	27	11	10
	1	85	53	26	36

[a]Data are mean values derived from two replicates.

All three compounds **17a-c** inhibit CDK9 activity by 7 - 10% at 0.1 mM concentration, which represents a poor activity against CDK9. A possible explanation is that the macrocycles might be too large and rigid to reside inside the ATP binding site of CDK9 from the structure difference between **17a-c** and lead compound **5**, and it will be discussed in the molecular docking part later. Interestingly, compound **17a** inhibits

aurora-A and aurora-B activity by 58% and 74% at 0.1 μM, but it shows < 10 % inhibition against CDK2 and CDK9. It could be further studied as an aurora-B inhibitor.

2.2.2 Molecular docking

The molecular docking work described in the following section can be used to predict the binding mode of the macrocyclic compounds with CDK2, CDK9, aurora-A and aurora-B kinases. It also can help better understand the SAR analysis to further optimise the designed compounds.

Lead compound **5**, and test compounds **17a**, **17b** and **17c** were docked into the CDK9 protein (PDB code 4BCG). The binding poses with the lowest Glide scores are shown in **Figure 2.1**.

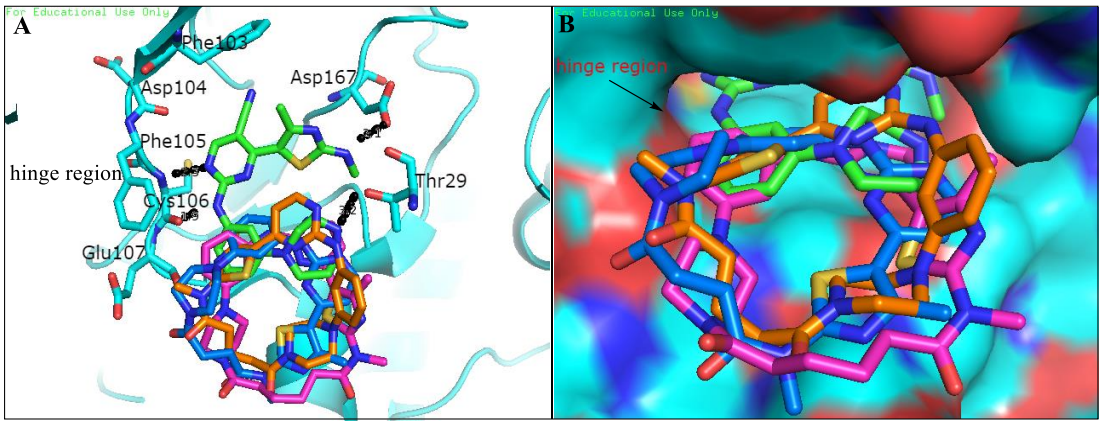

Figure 2.1: Superposition of the binding poses of compounds **5** (green), **17a** (blue), **17b** (brown) and **17c** (pink) with CDK9 (PDB code 4BCG). (A) CDK9 shown in sticks (B) CDK9 shown in surface.

Figure 2.1 shows the superposition of the binding modes of ATP binding site of CDK9 with four ligands, lead compound **5** and **17a-c**. Compound **5** in (A) occupies the ATP binding site, and shows a tightly binding with the hinge region (as it is discussed

in **section 1.4.1**). Compounds **17a-c** in (A) are all away from the hinge region and no interaction is found, resulting the poor inhibitory activity against CDK9 (7 - 10% inhibition at 0.1 μM concentration).

(B) shows a surface view of the ATP binding pocket of CDK9 and four ligands. Compound **2** (in green carbon) fully resides in the ATP binding pocket, while **17a-c** (in blue, brown and pink carbon) fail to go inside the pocket. The macrocyclic structures of **17a-c** are too large for the ATP binding pocket of CDK9.

2.3 Conclusion

The first series of macrocyclic compounds (**17a**, **17b**, **17c**) containing an amide linker was synthesised. Although the kinases activity assay showed these compounds exhibited poor inhibitory activity against CDK9, molecular docking was employed to explore the cause of the poor activity. The docking poses of the macrocycles bound to CDK9 confirmed all these three macrocyclic compounds are too large to reside into the ATP binding pocket. The alkene linker as another cyclisation strategy was adopted to synthesise a new series of macrocyclic compounds.

Chapter Three: Optimised macrocyclic compounds with an alkene linker

3.1 The optimisation of the synthesis for macrocyclic compounds with an alkene linker

Ring closing metathesis (RCM) is widely used to synthesise unsaturated rings in organic chemistry.[176-180] It was employed to synthesise macrocyclic compounds in the following synthetic routes.

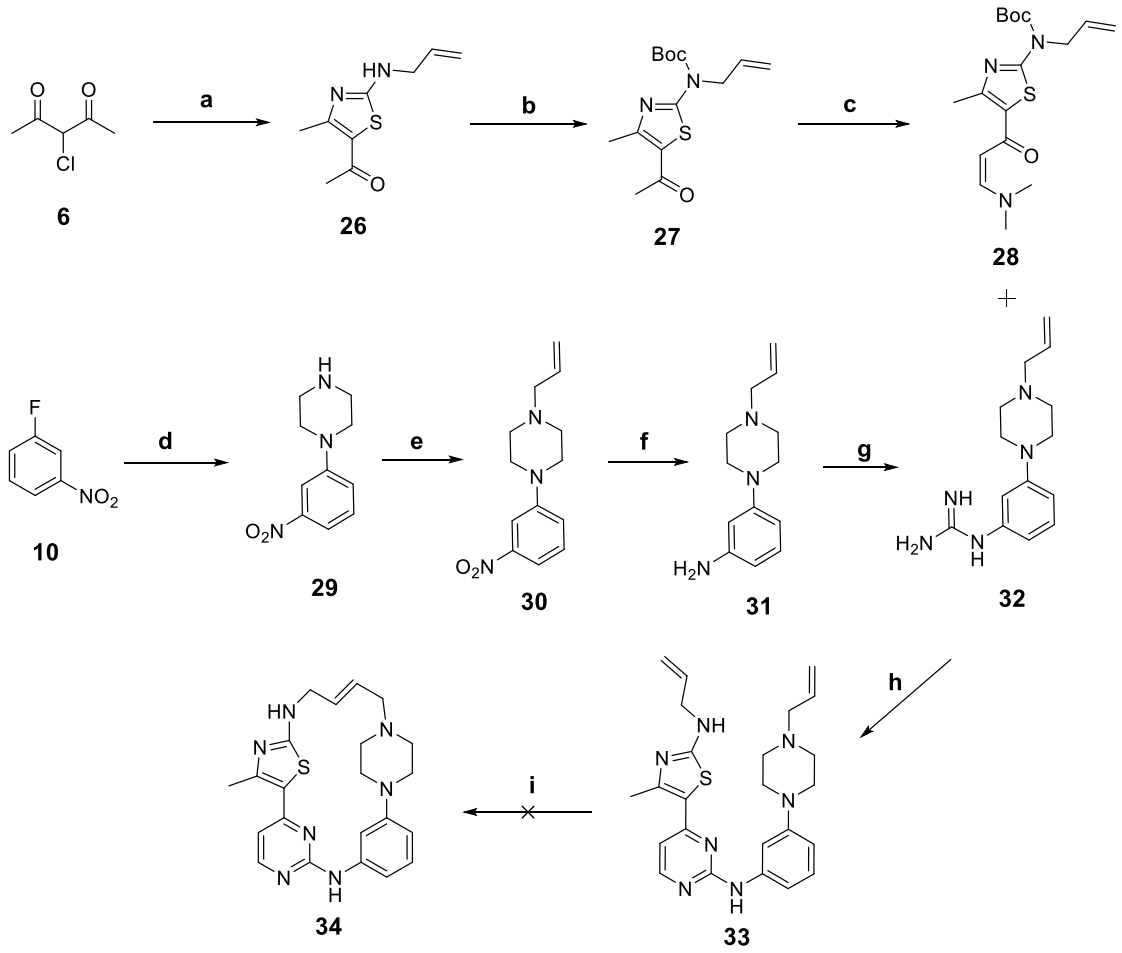

Scheme 3.1 The intended synthetic route for macrocyclic pyrimidine analogue **34**.

Reagents and conditions: (a) 1-allylthiourea, MeOH, RT, 4-6 h; (b) Boc_2O, DMAP, CH_2Cl_2, RT, 2 h; (c) DMF-DMA reflux overnight; (d) piperazine, DMSO, 100 ºC, 72 h; (e) allyl bromide, K_2CO_3, DMF, 100 ºC, 24 h; (f) $SnCl_2$, MeOH/H_2O, RT, overnight; (g) cyanamide, TMSCl, MeCN, reflux, overnight; (h) DMA, microwave, 200 º C, 299W, 60 min. (i) different reaction conditions (see **Table 3.1**).

The second-generation Grubbs catalyst (Grubbs II) and the second-generation Hoveyda-Grubbs catalyst (Hoveyda-Grubbs II) are a series of ruthenium carbene complexes used as catalysts for olefin metathesis. Grubbs II is not only stable against moisture and air, but also functional group-tolerant.[179] It has been demonstrated to be highly efficient in the RCM of sterically demanding dienes.[181] Compared to Grubbs II, Hoveyda-Grubbs II shows improved thermal stability and air-, moisture-tolerance. However, it is more expensive and slower to initiate than Grubbs II.[179]

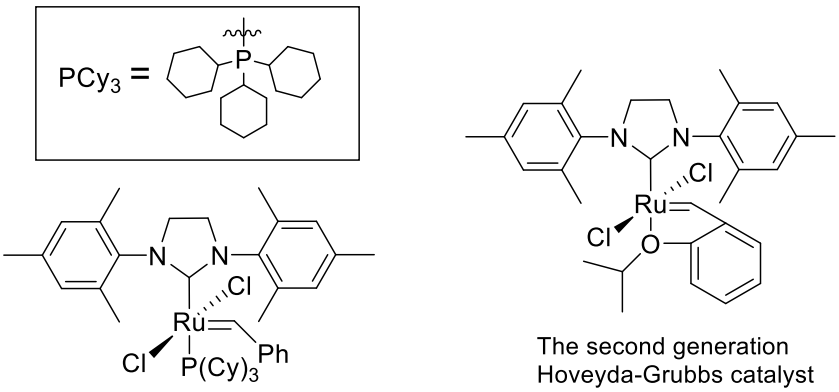

Figure 3.1 The chemical structure of Grubbs II and Hoveyda-Grubbs II catalysts.

Scheme 3.1 shows an intended synthetic route for macrocyclic compound **34**. The allyl groups were introduced into the two intermediate compounds **26** and **30**, and the key intermediate **33** was synthesised through the condensation of compounds **28** and **32** under microwave conditions. However, precursor **33** failed to be cyclised. **Table 3.1**

shows different RCM reaction conditions which were explored to synthesise compound **34**.

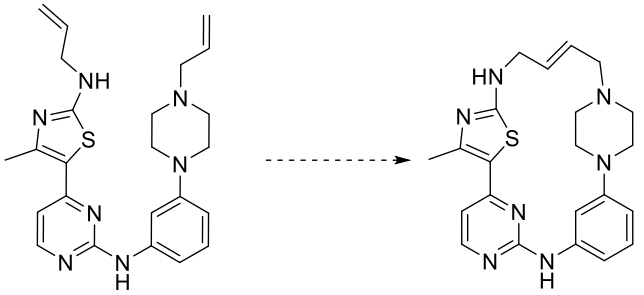

33 **34**

Table 3.1 The reaction conditions of ring closing metathesis

Entry	Catalyst	Reagent and Solvent	Temperature and time	Result (From TLC and LC-MS)
1	20 % Hoveyda-Grubbs II	DCM	reflux, 24 h	No desired product and only starting material observed
2	20 % Hoveyda-Grubbs II	1,2-DCB	200 ^{o}C, 5 min (Microwave)	Many by-products and no desired product observed
3	20 % Grubbs II	DCM	reflux, 24 h	No desired product and only starting material observed
4	20 % Grubbs II	1,2-DCB	200 ^{o}C, 10 min (Microwave)	Many by-products and no desired product observed
5	20 % Grubbs II	HCl (4.0 M) in DCM	reflux, 24 h	No desired product and only starting material observed
6	20 % Grubbs II	HCl (4.0 M) in dioxane	50-100 ^{o}C, 24 h	No desired product and only starting material observed

Catalysts (Grubbs II and Hoveyda-Grubbs II) and different boiling point solvents 1,4-dioxane, DCM and DCB were employed in **Table 3.1**,[178-180] but none of them succeeded

in cyclising compound **33**.

The yield of RCM is often highly dependent on the nature of the N-substituent. It is reported that a steric bulk substituent around the nitrogen leads to a favorable transition state for ring closure.[178, 182, 183] Therefore, compounds **35** and **36** with different *N*-substituted groups were designed, and the conditions in **Table 3.1** were employed.

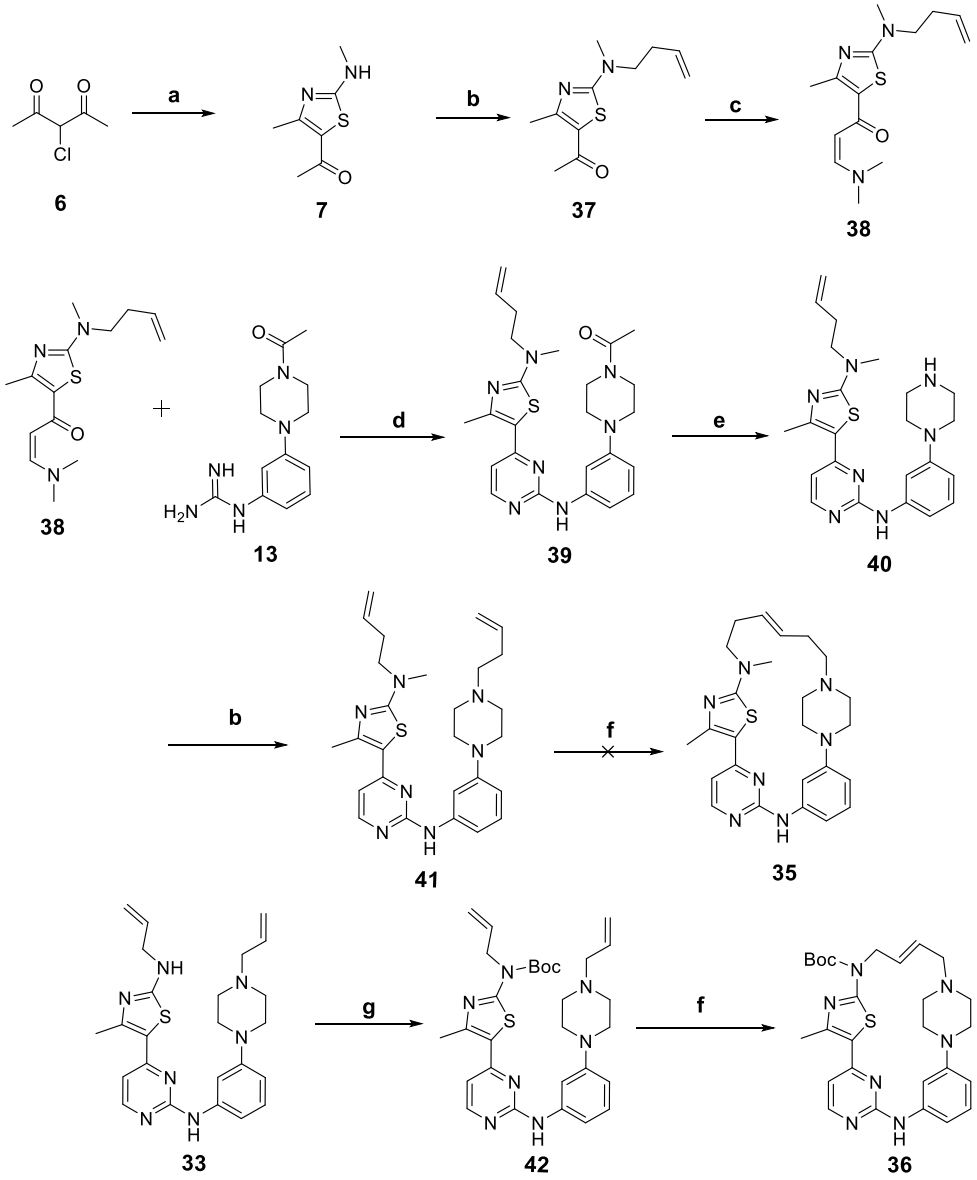

Scheme 3.2 The synthetic route for compound **35** and **36**. Reagents and conditions: (a) 1-methylthiourea, MeOH, RT, 4-6 h; (b) 4-bromo-butene, K_2CO_3, DMF, 120 °C, 24

h; (c) DMF-DMA, reflux overnight; (d) DMA, microwave, 200 ºC, 299W, 60 min. (e) 2M HCl, MeOH, reflux, overnight; (f) different RCM reaction conditions (see **Table 3.1**), (g) Boc_2O, DMAP, CH_2Cl_2, RT, 2 h.

For compound **35**, 1-methylthiourea was used as the starting material to synthesise *N*-methyl substituted thiazole intermediate **7**. Instead of 1-allylbromide, 1-bromo-butene was added to two terminal amine to afford precursor **41**. Compound **33** was Boc-protected to yield precursor **42** by using Boc anhydride. However, both precursors **41** and **42** failed to be cyclised and only starting materials were recovered. Other factors, like ring size, functional groups were then considered as the possible reasons which might interfere with the formation of the macrocycle.

Compound **43** (shown in **Scheme 3.3**), a novel pyrimidine-based macrocycle, was reported as a potent inhibitor of CDK 1, 2, 3, 5, 9, JAK2 and FLT3.[184, 185] It most potently inhibits CDK isoforms, with IC_{50} values of 3 - 9 nM for CDK 1, 2, 3, 5, 9. Compound **43** also potently inhibits the Janus Kinase 2 (JAK2) and Fms-like tyrosine kinase 3 (FLT3) with IC_{50} value both of 19 nM. Comparing the reference inhibitor that only block one of the kinase targets (CDK or JAK2), compound **43** shows the benefit of combined CDK and JAK2 targeting and is more consistently anti-proliferative in human tumour cell lines. Compound **43** is currently being evaluated in Phase I clinical trial in patients with advanced haematological malignancies.[185]

Compound **43** shows a similar ring size (18-membered) and structure to the designed compound **34** (19 membered), thus it can be used as a model compound to optimise our

RCM reaction. From the structure difference between compound **34** and model compound **43**, the functional groups, thiazole and piperazine, are the major difference and could be the factor that interferes with the RCM reaction. As the design idea shown in **Scheme 3.3**, the phenyl and *tert*-amino groups of compound **43** will be replaced by the thiazole and piperazine groups of compound **34** to afford compounds **44** and **45** to verify which group underlies failure of RCM.

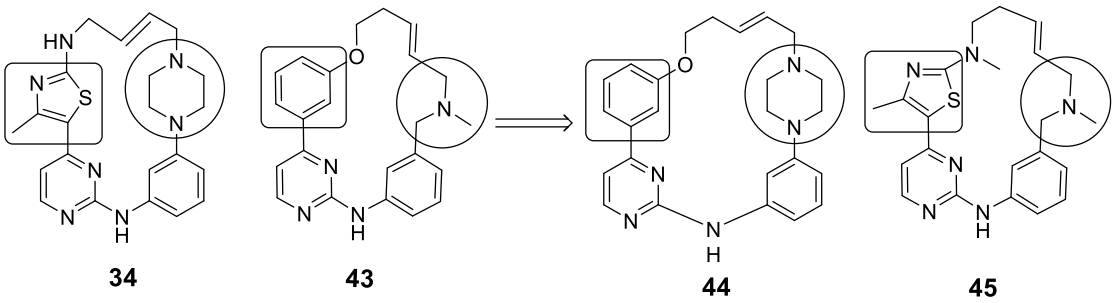

Scheme 3.3. The design idea of compound **44** and **45**.

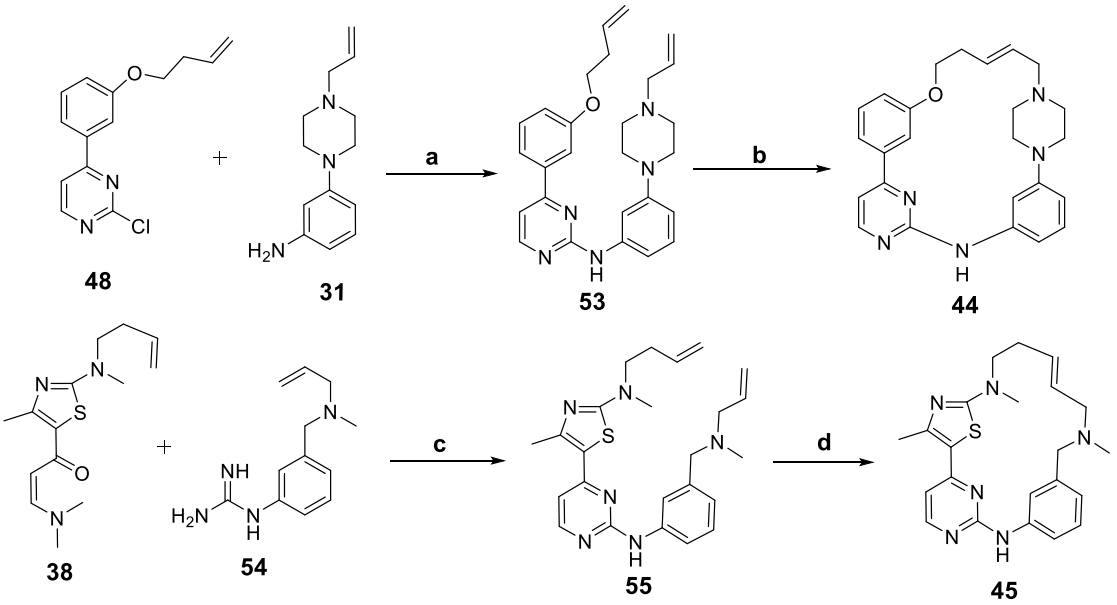

Scheme 3.4 Synthetic route for designed compounds **44** and **45**. Reagents and conditions: (a) 4 M HCl, n-BuOH, reflux, overnight; (b) Grubbs II, TFA, DCM, reflux,

12 h; (c) DMA, microwave, 200 ºC, 299 W, 60 min; (d) different RCM reaction conditions (see **Table 3.1**).

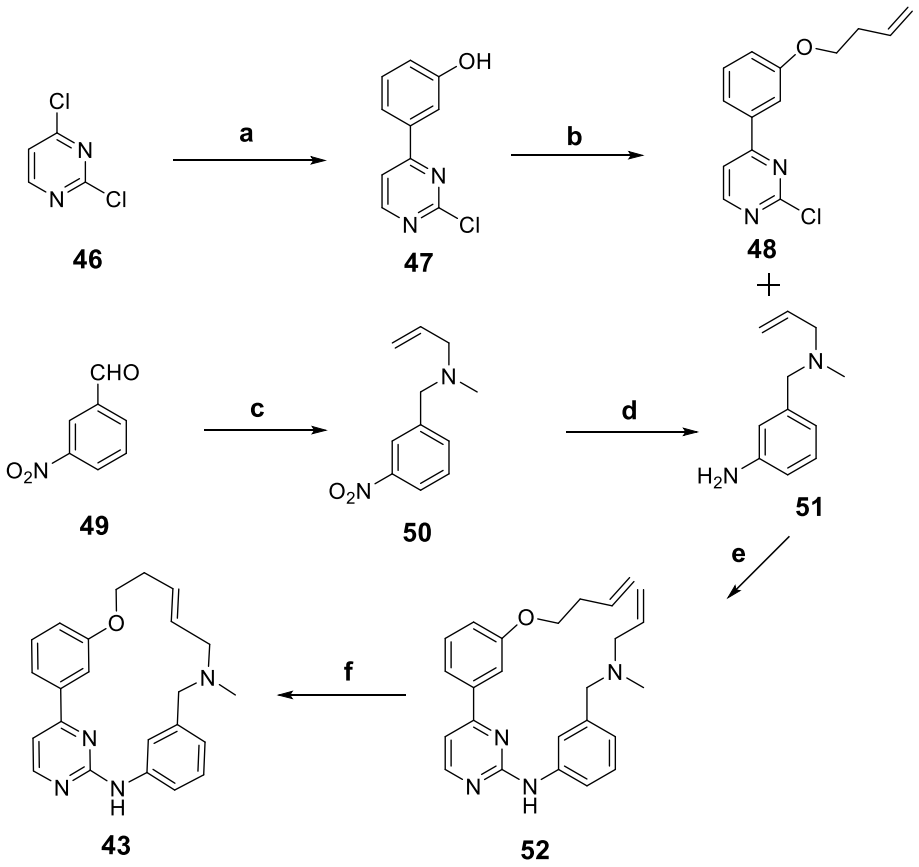

Scheme 3.5 Synthetic route for model compound **43**. Reagents and conditions: (a) 3-hydroxy-phenylboronic acid, $Pd(PPh_3)_4$, aqueous $NaHCO_3$, 1,2-dimethoxy-ethane, reflux, 12 h; (b) 4-bromo-1-butene, Cs_2CO_3, DMF, 100 ºC, overnight; (c) *N*-allylmethylamine, $NaBH(OAc)_3$, DCM, RT, overnight; (d) $SnCl_2{\cdot}2H_2O$, MeOH, H_2O, RT, 12 h; (e) 4 M HCl, n-BuOH, reflux, overnight; (f) Grubbs II, TFA, DCM, reflux, 12 h.

Scheme 3.4 and **3.5** show the synthetic route for model compound **43** and designed compounds **44** and **45**. Suzuki coupling of 2,4-dichloro-pyrimidine **46** and 3-hydroxyphenylboronic acid afforded the biaryl **47**. Alkylation of **47** with 4-bromo-butene and caesium carbonate furnished ether **48**. Compound **50** was constructed by

reductive amination of benzaldehyde **49** and *N*-allylmethylamine. Following selective reduction of the nitro-group of **50**, the two fragments **48** and **51** were coupled in hot butanol to afford the diene precursor **52**. RCM of **52** proceeded in the present of Grubbs II and TFA to obtain macrocyclic compound **43**. The two precursors **53** and **55** in **Scheme 3.4** were obtained by coupling of intermediates **48**, **31** and **38**, **54**.

It was found that compounds **43**, **44** with phenyl, *tert*-amine and piperazine groups succeeded to be synthesised, but compounds **34** and **45** with the thiazole group failed to be obtained from RCM. Although macrocyclic compounds containing a thiazole group can be synthesised from a RCM reaction in the reference,[186-188] it was the problem that cause the failure of RCM reactions in this project. Therefore, the thiazole group was replaced by a phenyl group in the further optimisation.

3.2 Overview of the synthetic route towards macrocyclic compounds containing alkene linkers

3.2.1 Formation of allyl-substituted pyrimidine derivatives

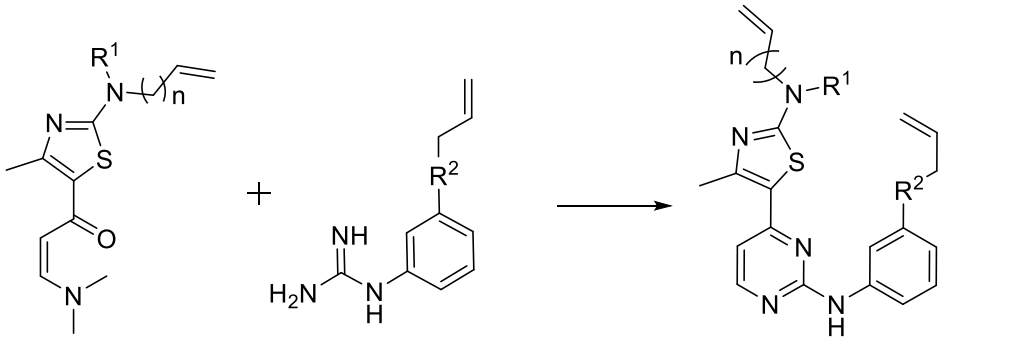

28 R^1=Boc, n=1
38 R^1=Methyl, n=2

32 R^2=Piperazine
54 R^2=*Tert*-amino

33 R^1=H, R^2=Piperazine, n=1
55 R^1=Methyl, R^2=*Tert*-amino, n=2

Scheme 3.6 Reagent and conditions: DMA, microwave, 200 ºC, 299W, 60 min. yield: 45% for **33**, 40% for **55**.

Following the synthetic conditions set up for the formation of pyrimidine **14** in **Scheme 2.1**, 2-methoxyethanol was employed as the solvent and the reaction was heated under microwave (140 ºC, 45 min). These conditions were applied to the allyl-substituted pyrimidines **33** and **55** (**Scheme 3.1** and **3.4**), but only 10% yield was achieved with 90% starting material recovered. Through optimising the reaction condition, it was found that high boiling point solvent DMA was necessary to raise the reaction temperature to facilitate the formation of the pyrimidine ring. The yield was raised to 45% for **33** and 40% for **55**.

3.2.2 Optimisation of Suzuki reaction for 4-phenol-substituted pyrimidine 47

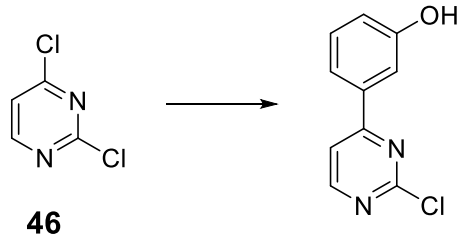

46 **47**

Scheme 3.7 Optimisation of suzuki reaction. Reagents and conditions: (Before optimisation) 3-hydroxyphenyl boronic acid, aqueous Na_2CO_3, $Pd(PPh_3)_4$, 1,2-dimethoxyethane, 80 ºC, 10%. (After optimisation) 3-hydroxyphenyl boronic acid, $KF{\cdot}2H_2O$, $Pd(PPh_3)_4$, 1,4-dioxane, reflux, 72%.

It was reported that 2,4-dichloropyrimidine **46** was coupled with 3-hydroxyphenyl boronic acid to give the compound **47** at 88% yield in the condition of aqueous Na_2CO_3

and $Pd(PPh_3)_4$ in 1,2-dimethoxyethane.[184] However, only 10% yield was achieved when the reaction was repeated. It was then optimised using different bases and reaction solvents. According to the results, the best reaction conditions were $KF \cdot 2H_2O$ and $Pd(PPh_3)_4$ in 1,4-dioxane, achieving a 72% yield.

3.2.3 Optimisation of RCM reaction condition for compound 44

In **Scheme 3.5**, an optimised reaction was reported for model compound **43**.[184] It adopted TFA to weaken ruthenium-phosphine chelation and facilitate the initiation of the catalytic cycle.[189] But the yield (10%) for compound **44** was much lower than the yield (86%) for model compound **43**. Therefore, we optimised the acid to HCl for compound **53**, improving the yield to 35%. Additionally, the concentration of the substrate was a key factor that affected the reaction yield, because the intermolecular olefin metathesis became competitive with intramolecular ring closure at a high concentration of substrate. Parallel experiments of substrate concentration from 5 to 40 mM were carried out. It was found that 10 mM compound **53** achieved the highest yield of 35%.

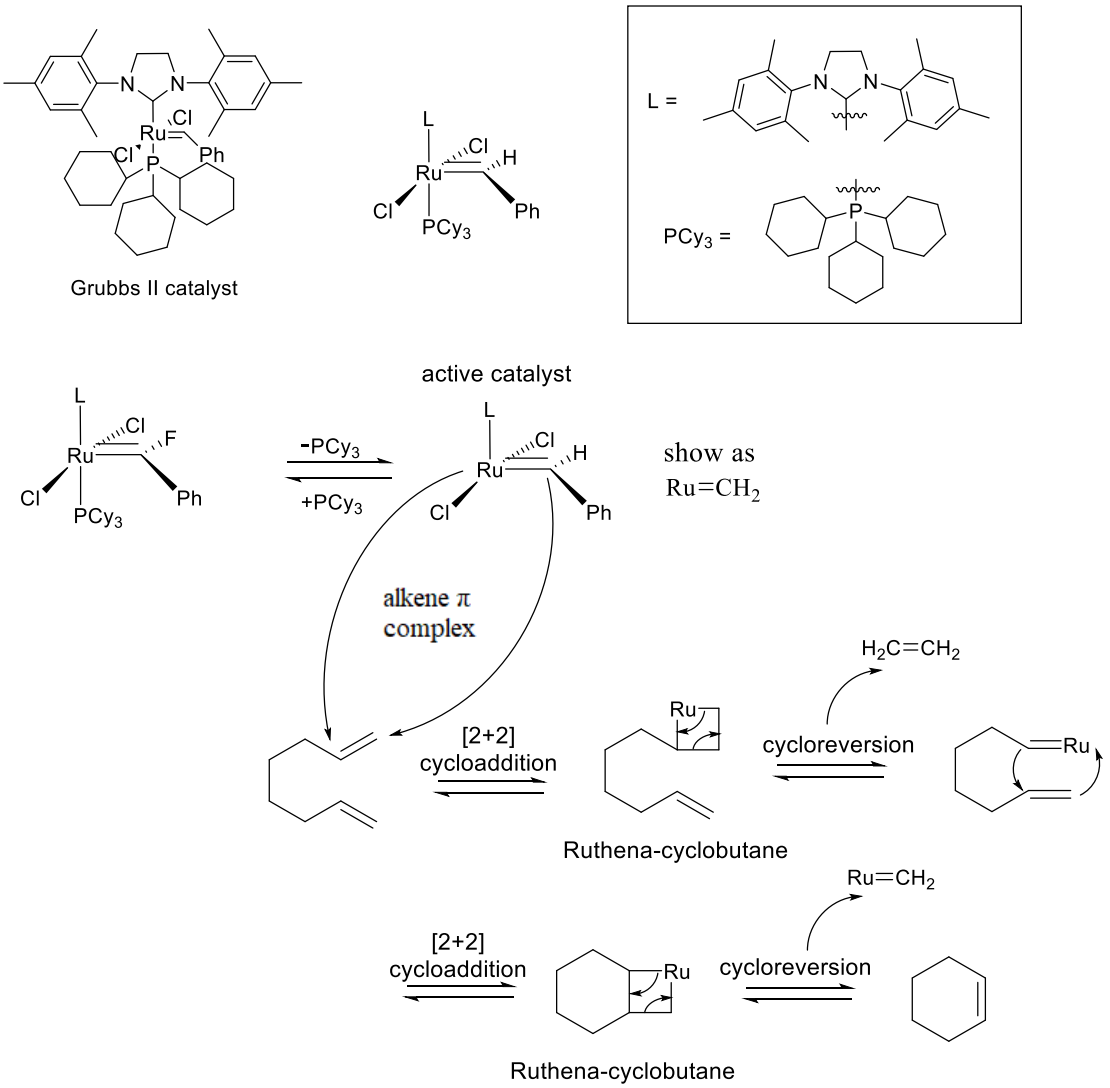

Figure 3.2 The structure of catalyst Grubbs II, and the general mechanism of RCM reaction with Grubbs II.[176, 190]

Figure 3.2 shows the structure of Grubbs II catalyst and the general mechanism of RCM reaction.[176, 190] The catalyst activation requires the tricyclohexyl phosphine to dissociate from the precatalyst complex to release a vacant site for the olefin substrate. One of the terminal alkenes of the substrate is coordinated with the active catalyst to form the Ruthena-cyclobutane. The cycloreversion is then involved and followed by another cycloaddition with the other terminal alkene to give the second Ruthena-

cyclobutane. A common side reaction happens through an intermolecular cycloaddition to form a polymerized byproduct. Cycloreversion of the second Ruthena-cyclobutane affords the desired RCM product and the alkylidene, Ru=CH_2, reenters the catalytic cycle.

3.2.4 The confirmation of the configuration of macrocyclic compounds 43

Figure 3.3 shows the COSY NMR for compound **43**. The chemical shift of alkene proton should be at 4.8-6.8 ppm. Alkene CH **2** couples with CH_2 **1** and alkene CH **3**, and alkene CH **3** couples with alkene CH **2** and CH_2 **4**. Meanwhile, compared to CH_2 **1**, CH_2 **4** is deshielded by N and moves to downfield. Therefore, in **Figure 3.3**, CH_2 **4** is localised and leads to the position of CH_2 **1**, alkene CH **2** and CH **3**.

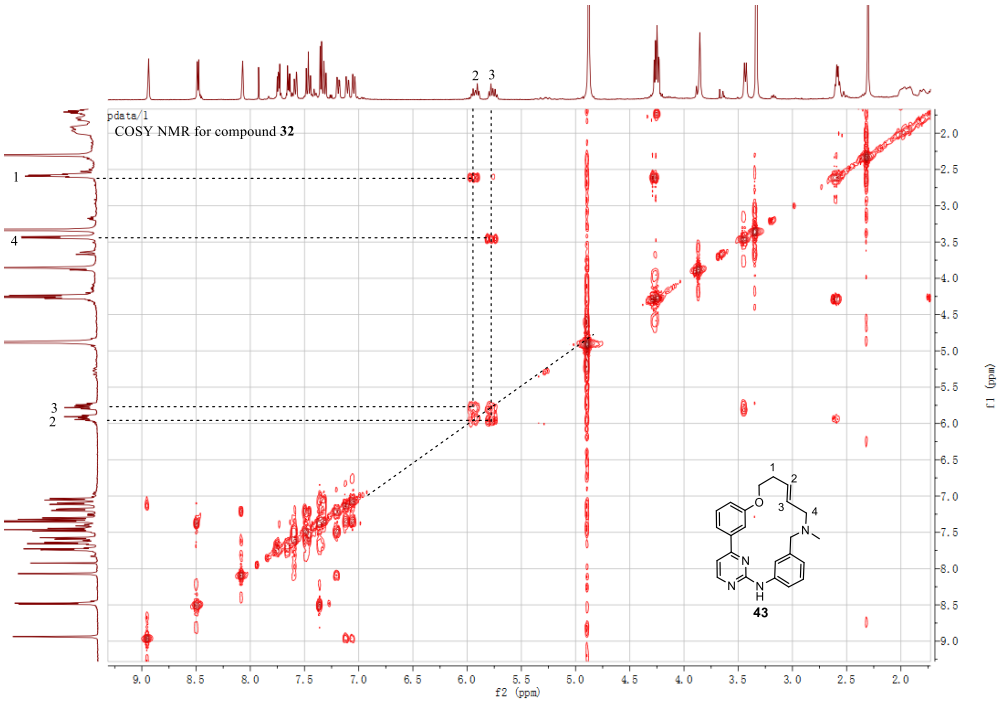

Figure 3.3 COSY NMR for compound **43**.

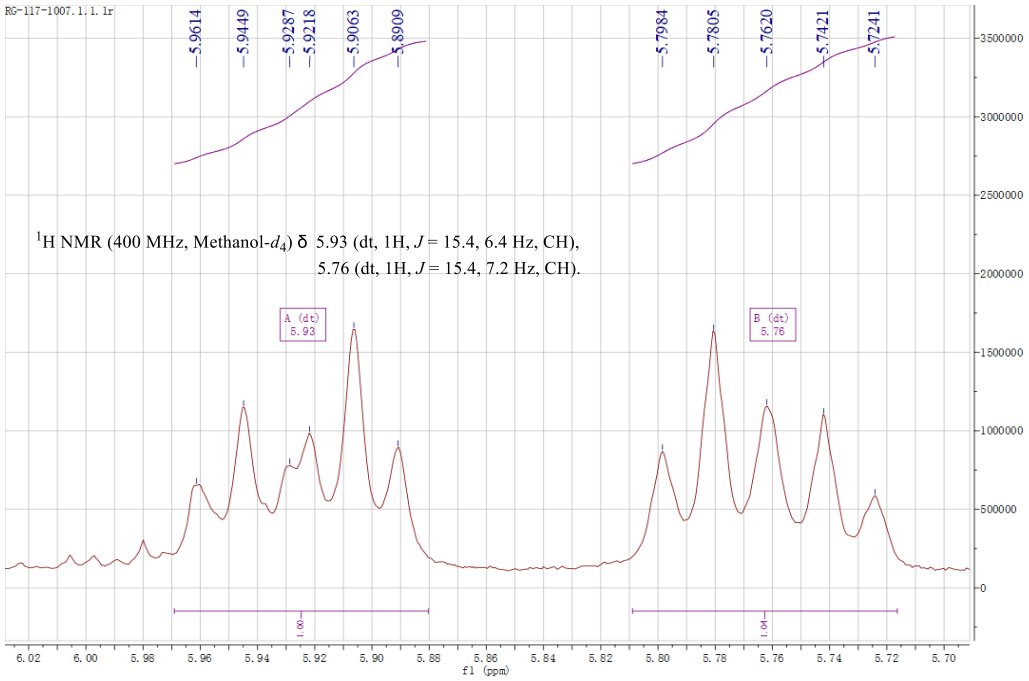

Figure 3.4 The coupling constants of the alkene protons.

The coupling constant for a (*Z*) isomer (6-14 Hz) is smaller than that for a (*E*) isomer (11-18 Hz). In **Figure 3.4**, ^{1}H NMR spectrum shows the double of triplets (dt) peaks for the two alkene protons, and the coupling constant is 15.4 Hz for both alkene protons, which indicates the trans configuration isomers for the alkene. A NOESY NMR experiment was also conducted to determine the isomer configuration, but the spectrum was not clear enough to allow conclusions to be drawn.

3.3 Results and discussions

3.3.1 Kinase assay results

The kinase inhibitory activity of two macrocyclic compounds **43** and **44** against Aurora-A, Aurora-B, CDK2 and CDK9 was examined. **Table 3.2** shows the K_i assay results.

Table 3.2 The kinases assay result (K_i) of two macrocyclic compounds **43**, **44**.

Kinase	Kinase inhibition K_i (nM)[a]	
	43	**44**
Aurora-A	4455	284
Aurora-B	2340	219
CDK2/cyclin A	19	346
CDK9/cyclin T1	1	18

[a]Data are mean values derived from two replicates. Apparent inhibition constants (K_i) were calculated from IC_{50} values and the appropriate K_M (ATP) values for each kinase.

In **Table 3.2**, the two designed compounds **43** and **44** exhibited potent inhibitory activity against CDK9 at 18 nM and 1 nM respectively. Although compound **43** demonstrates 1000-fold selectivity for CDK9 over Aurora-A and Aurora-B, it only shows 20-fold selectivity for CDK9 over CDK2. Notably, compound **44** shows poor inhibitory activity against CDK2, Aurora A and Aurora B. The disadvantage associated with compound **44** (compared to compound **43**) is its reduced potency (18 nM and 1 nM respectively) against CDK9. Therefore, optimisation of compound **44** was undertaken to raise its inhibitory activity against CDK9 and thus enhance selectivity for CDK9 over

CDK2 and aurora kinases.

3.3.2 Molecular docking

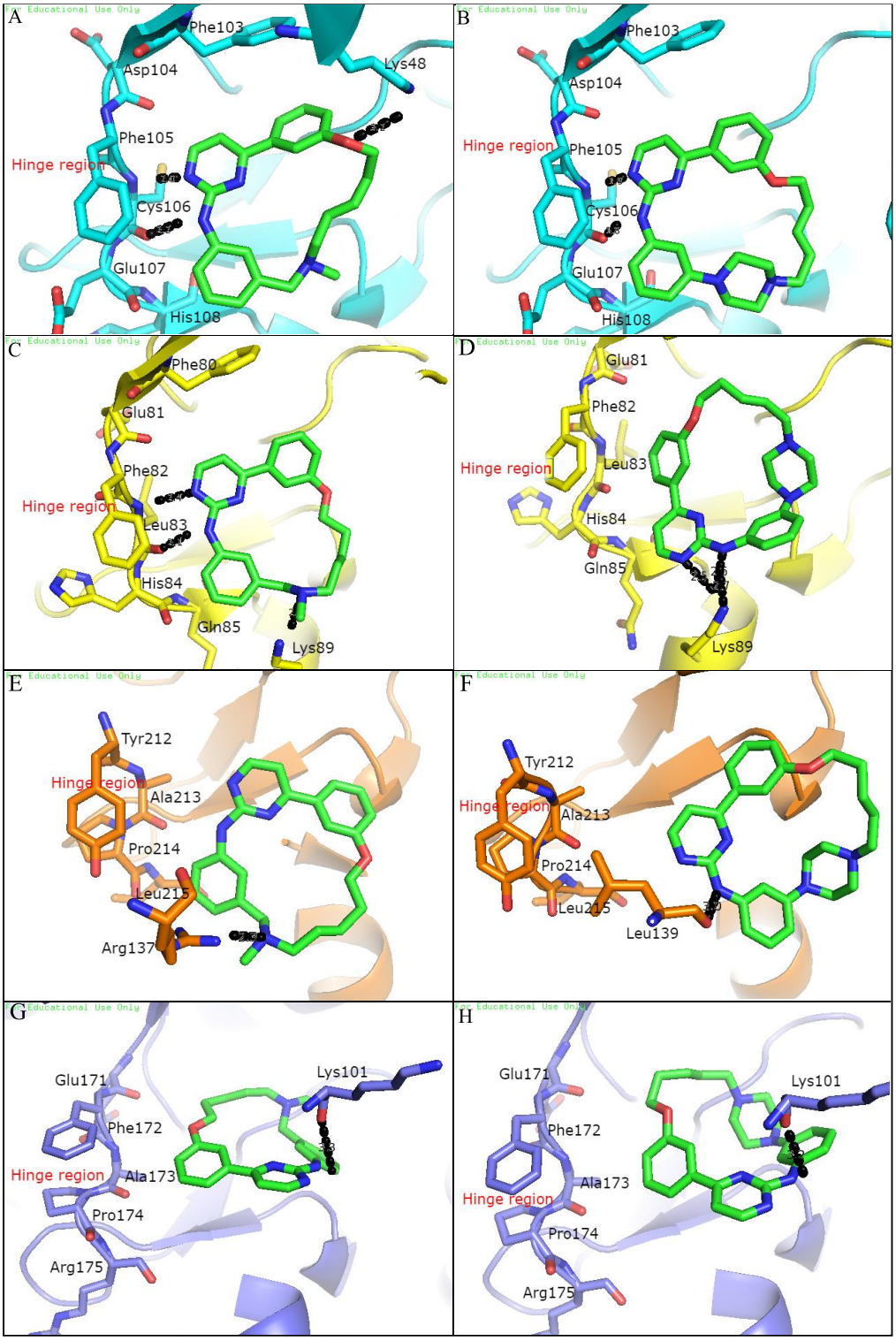

Figure 3.5: Docking poses for complexes of **43** and **44** with different kinases. (A) **43** with CDK9, (B) **44** with CDK9, (C) **43** with CDK2, (D) **44** with CDK2, (E) **43** with aurora-A, (F) **44** with aurora-A, (G) **43** with aurora-B, (H) **44** with aurora-B.

Compounds **43** and **44** were docked into proteins aurora-A, aurora-B, CDK2 and CDK9; the binding poses with the top Glide score are shown in **Figure 3.5**.

In **Figure 3.5**, the key residues of the hinge region are shown in distinct color sticks (sky blue for CDK9, yellow for CDK2, brown for aurora-A, dark blue for aurora-B). The ligands **43** and **44** are both depicted as green stick.

Compounds **43** and **44** in (A), (B) occupy the ATP binding site and form two strong hydrogen bonds with the hinge region of CDK9, which generate a stable binding mode. The docking results for the two poses are consistent with the related K_i result (1 nM for A, 18 nM for B) in **Table 3.2**.

(C) and (D) reveal the differences in the binding modes of compounds **43** and **44** with CDK2. Compound **43** in (C) has a tight binding with the hinge region and forms an extra hydrogen bond with Lys89, while **44** in (D) is away from the hinge region. This observation is in line with their distinct inhibitory activity against CDK2 (19 nM for A, 346 nM for B).

The remaining four binding poses of E, F, G, H show the ligands do not occupy the ATP binding site and only one hydrogen bond is observed in each pose. The docking result is consistent with the K_i result against ARKs (from 219 nM to 4455 nM) in **Table 3.2**.

Based on the poor inhibitory activity of compound **44** against CDK2 and ARKs (> 200 nM), the further optimisation is required to improve the inhibitory activity of **44** against CDK9 by developing the interaction between the ligand and CDK9. Since no interaction is observed near the hydrophobic pocket I in (B), extensive structure modification needs to be put in place to gain more interactions with gatekeeper residue Phe103.

3.4 Conclusion

The optimisation of the cyclisation reactions towards macrocyclic CDK9 inhibitors was described in this chapter. The key model compound **43** with a similar structure as lead compound **5** was introduced to synthesise the new designed macrocyclic compound **44**. Although compound **43** showed high selectivity against CDK9 over ARKs, no selectivity over CDK2 was observed. The new designed compound **44** showed a better selectivity profile against CDK9 over both CDK2 and ARKs than **43**. Therefore, further structural modification of compound **44** was the focus of Chapter 4 to increase the inhibitory activity against CDK9 and improve the selectivity for CDK9 over CDK2 and ARKs.

Chapter Four: Highly selective macrocyclic CDK9 inhibitors

The third series of macrocyclic compounds was synthesised based on compound **44**; structure optimisation was focused on R^1 and R^2 according to previously published SAR studies.[144]

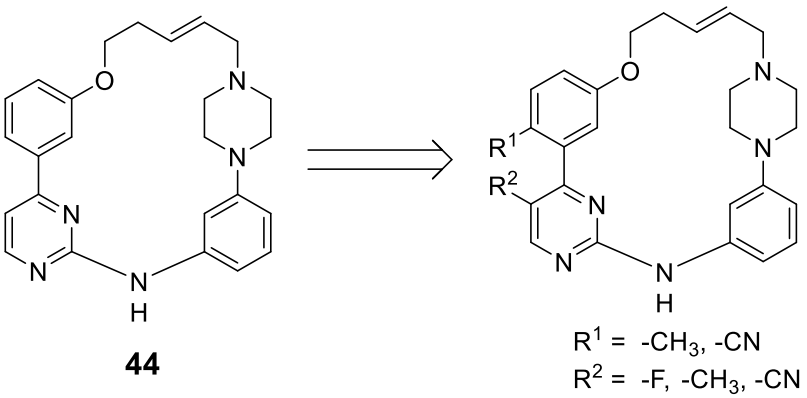

44

Cyano-, fluorine- and methyl-groups were reported to form hydrophobic interactions with the gatekeeper residue Phe103 in the hydrophobic pocket I and contribute to the high potency of inhibitors against CDK9.[144] The synthetic routes for the designed macrocyclic compounds are shown in **Scheme 4.1**-**4.5**. Because some of the starting materials were not commercially available, different routes were developed for these final compounds.

4.1 Three synthetic routes toward new modified macrocyclic compounds

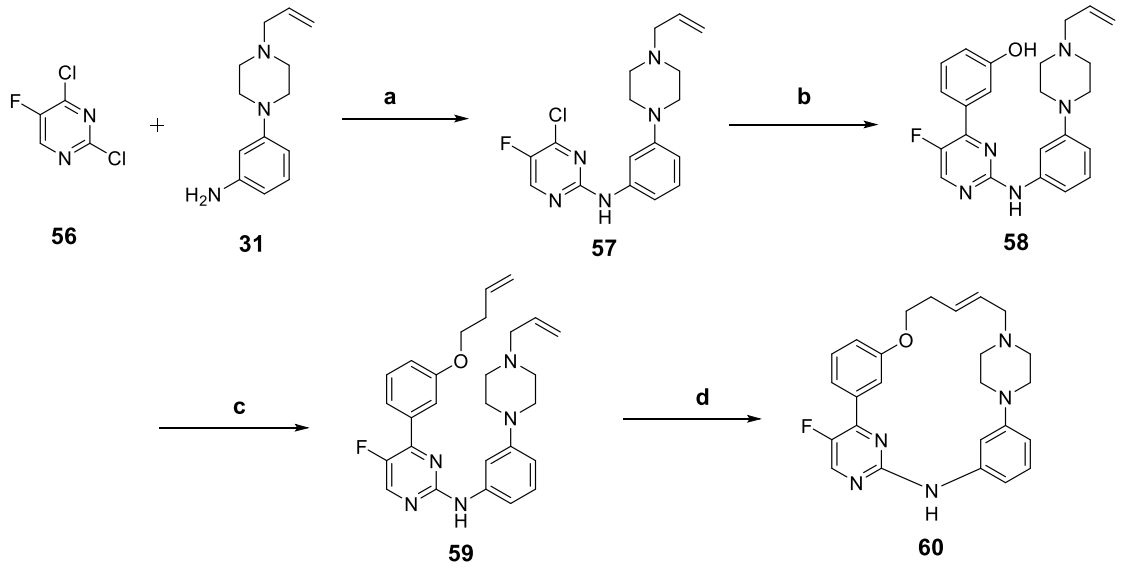

Scheme 4.1 Synthetic routes for compound **60**. Reagents and conditions: (a) Et_3N, $ZnCl_2$ in Et_2O, 1,2-dichloroethane and *N*-butanol, 50 ºC, 18 h, 65%; (b) 3-hydroxyphenylboronic acid, $Pd(PPh_3)_4$, Na_2CO_3, toluene and ethanol, reflux, 4 h, 70%; (c) 4-bromo-1-butene, K_2CO_3, DMF, 100 ºC, 24 h, 95%; (d) Grubbs II, 4 M HCl in dioxane, CH_2Cl_2, 45 ºC, 12 h, 20%.

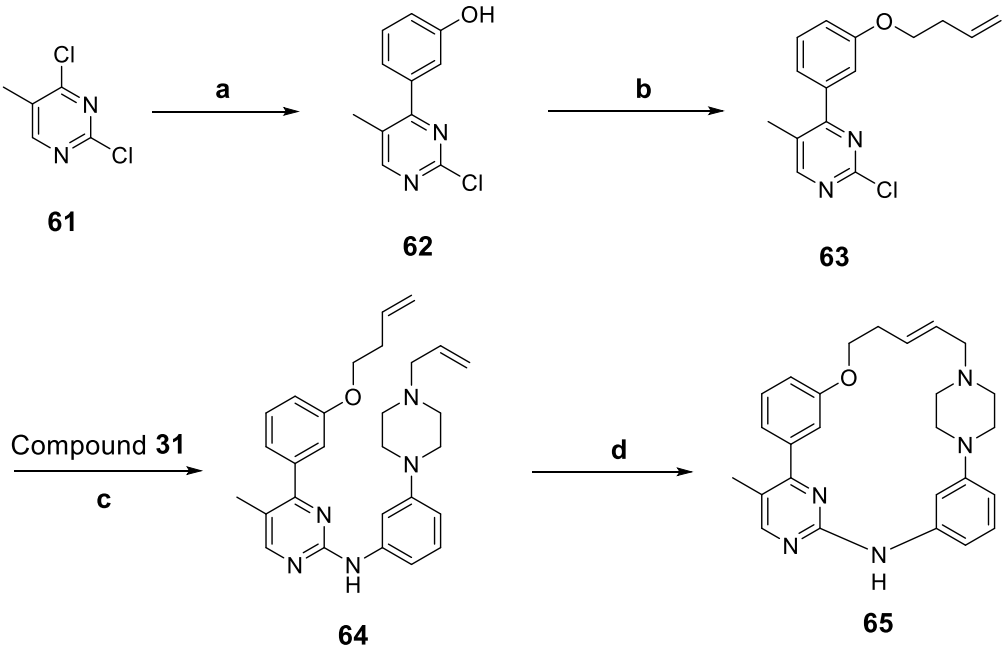

Scheme 4.2 Synthetic routes for compound **65**. Reagents and conditions: (a) 3-hydroxyphenylboronic acid, $Pd(PPh_3)_4$, Na_2CO_3, toluene and ethanol, reflux, 4 h, 70%; (b) 4-bromo-1-butene, K_2CO_3, DMF, 100 °C, 24 h, 95%; (c) 4 M HCl, *N*-butanol, 100 °C, overnight, 45%; (d) Grubbs II, 4 M HCl in dioxane, CH_2Cl_2, 45 °C, 12 h, 20%.

Compounds **60** and **65** were synthesised using two similar routes. 2,4-Dichloro-5-fluoro-pyrimidine **56** was coupled with aniline derivative **31** to afford intermediate **57**, which was coupled with 3-hydroxyphenylboronic acid via Pd-mediated Suzuki-Miyaura coupling reaction. Alkylation of the resulting phenol **58** gave the precursor **59**, followed by the RCM reaction to afford the macrocycle **60**. Compound **62** was prepared via Suzuki-Miyaura reaction of 2,4-dichloro-5-methyl-pyrimidine and 3-hydroxyphenylboronic acid, followed by alkylation with 4-bromo-1-butene to afford the intermediate **63**. Compound **63** was then coupled with compound **31** to give precursor **64**. The macrocyclic compound **65** was obtained by RCM of precursor **64**.

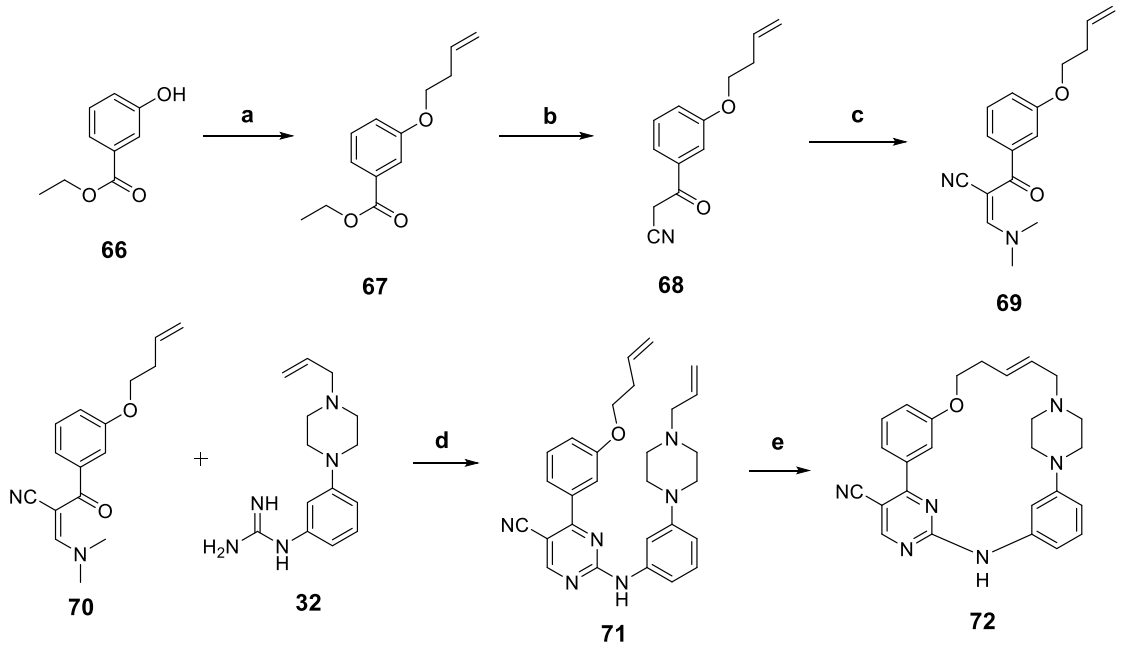

Scheme 4.3 Synthetic route for compounds **72**. Reagents and conditions: (a) Cs_2CO_3, 4-bromo-1-butene, CH_3CN, reflux, overnight, 90%; (b) *t*-BuOK, CH_3CN, THF, RT, 4 h, 55%; (c) DMF-DMA, reflux, overnight, 75%; (d) 2-methoxyethanol, microwave 299W, 140 ºC, 45 min, 35%; (e) Grubbs II, 4 M HCl in dioxane, CH_2Cl_2, 45 ºC, 12 h.

Alkylation of compound **66** with 4-bromo-1-butene afforded **67**, and the alkylation product was then treated with potassium *tert*-butoxide and acetonitrile in THF. Converting the resulting compound **68** to enaminone **69** was achieved by refluxing in DMF-DMA. Precursor **71** was prepared by condensation of compounds **70** and **32**, followed by RCM of **71** to give the desired macrocyclic compound **72.**

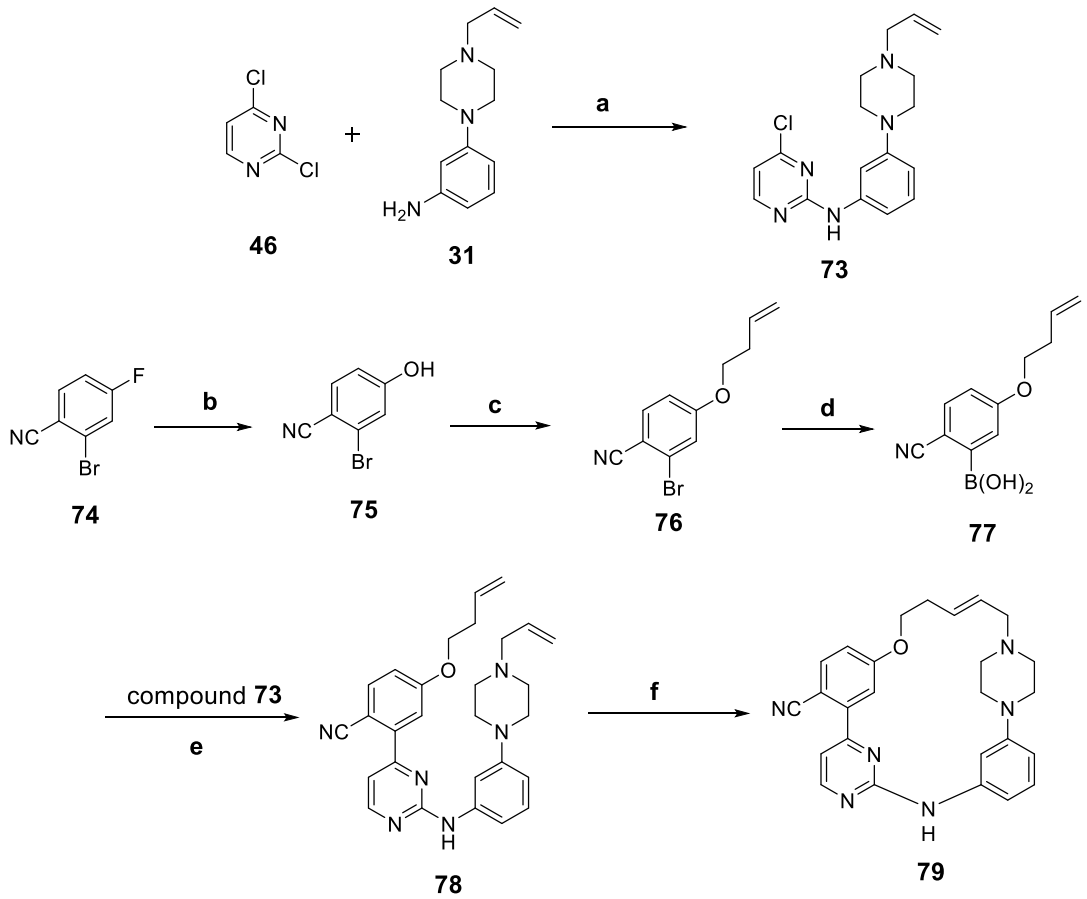

Scheme 4.4 Synthetic route for compound **79**. Reagents and conditions: (a) TEA,

$ZnCl_2$ in Et_2O, 1,2-dichloroethane and *N*-butanol, 50 °C, 18 h, 45%; (b) NaH, 2-methylsulfonylethanol, HCl, DMF, RT, overnight, 90%; (c) 4-bromo-1butene, Cs_2CO_3, DMF, 120 °C, 24 h, 83%; (d) *n*-BuLi, triisopropyl borate, 2 M HCl, THF, -78 °C, 78%; (e) 2 M sodium carbonate, $Pd(PPh_3)_4$, 1,2-dimethoxyethane, reflux, overnight, 55%; (f) Grubbs II, 4 M HCl in dioxane, CH_2Cl_2, 45 °C, 12 h, 20%.

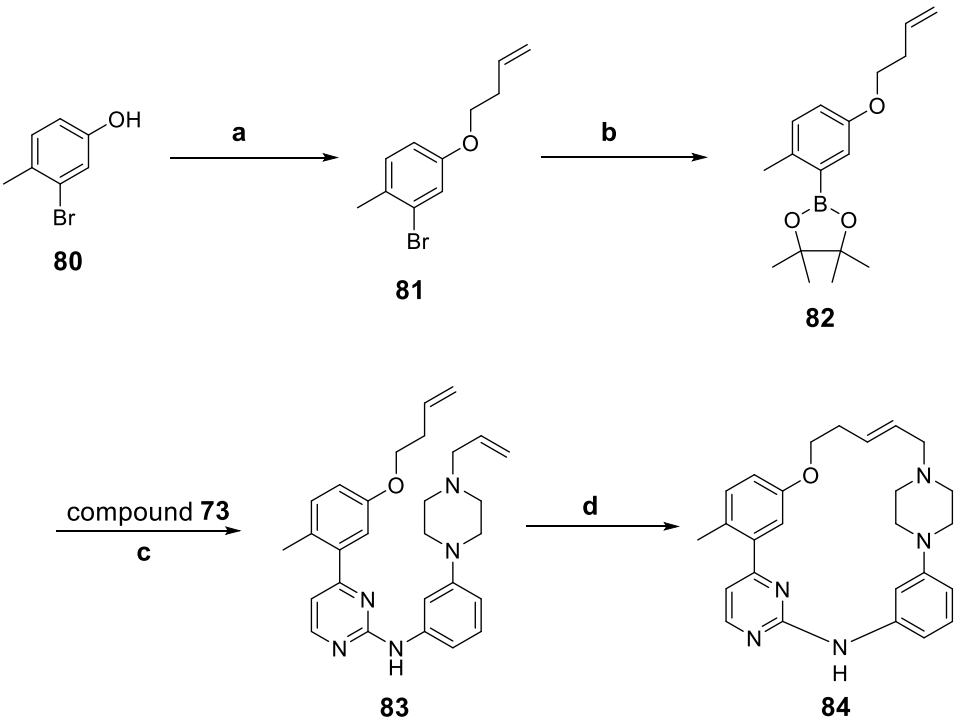

Scheme 4.5 Synthetic route for compound **84**. Reagents and conditions: (a) 4-bromo-1butene, Cs_2CO_3, DMF, 120 °C, 24 h, 83%; (b) KOAc, $Pd(dppf)Cl_2$, *bis*(pinacolato)diboron, dioxane, reflux, overnight, 60%; (c) $Pd_2(dba)_3$, SPhos, 5 M K_3PO_4, dioxane, microwave 299W, 150 °C, 20 min, 45%; (d) Grubbs II, 4 M HCl in dioxane, CH_2Cl_2, 45 °C, 12 h, 20%.

The key intermediate **73** was prepared by the coupling of 2,4-dichloropyrimidine **46** and aniline **31**. 2-bromo-4-fluorobenzonitrile **74** was hydrolysed to phenol **75** in the presence of sodium hydride and 2-methylsulfonylethanol, followed by alkylation of compound **75** with 4-bromo-1-butene to afford **76**. Converting **76** to phenylboronic acid

77 was achieved using *n*-BuLi and triisopropyl borate in THF at -78 ºC. Intermediate **73** was treated with compound **77** to form the precursor **78** under Suzuki-Miyaura reaction, which was then cyclised to the target compound **79**.

Alkylation of compound **80** and 4-bromo-1-butene afforded intermediate **81**, which was converted to boronate ester **82** using K_2CO_3, $Pd(dppf)Cl_2$ and *bis*(pinacolato)diboron in dioxane. Precursor **83** was obtained by Suzuki-Miyaura reaction of **73** and **83** in the presence of $Pd_2(dba)_3$, SPhos and K_3PO_4, followed by RCM to afford macrocycle **84**.

4.2 Overview of synthesis

4.2.1 Selective nucleophilic aromatic substitution of 2,4-dichloropyrimidine 46

2,4-Dichloropyrimidine **46** proceeded nucleophilic aromatic substitution to afford the key intermediate **73** (**Scheme 4.4**). For compound **46**, the amine addition occurs preferentially at the more reactive C-4 position of pyrimidine. Lewis acid $ZnCl_2$ was reported as an additive to improve the reaction selectivity for C-2 position over C-4 position.[191] Therefore, a selective method (triethylamine and $ZnCl_2$ in diethyl ether in 1,2-dichloroethane and N-butanol (1:1), 50 ºC) was employed,[192] giving a ratio of 4:1 of C-2 substituted product **73** and C-4 substituted products.

4.2.2 Mild conversion of aryl fluoride to phenol

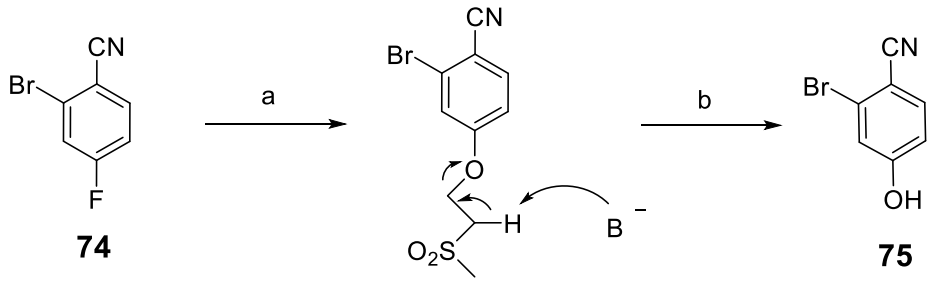

Scheme 4.6 Mechanism of hydrolysation reaction to convert aryl fluoride to phenol. Reagents and conditions: (a) NaH, 2-methylsulfonylethanol, DMF, RT, overnight (b) HCl.

In **Scheme 4.6**, aryl fluoride **74** was used to synthesise phenol **75**. A mild conversion was reported to convert aryl fluoride to phenol.[193] 2-Methylsulfonylethanol was first deprotonated by sodium hydride to form alkoxide, and then the alkoxide substituted the fluoro group of **74** to yield the ether intermediate. In the presence of another equivalent of sodium hydride, the ether intermediate was quickly decomposed to generate the product **75**.

4.2.3 Optimisation of Suzuki-Miyaura reaction

Phenyl borate derivatives **77** and **82** underwent Suzuki-Miyaura reactions to afford precursors **78** and **83** in **Scheme 4.3**. It was found that the commonly used Suzuki-Miyaura reaction condition (sodium carbonate and $Pd(PPh_3)_4$ in 1,2-dimethoxyethane) failed to react successfully with compound **82**. According to the structure difference between **77** and **82**, the boronic ester **82** is less active than boronic acid **77**, which makes the reaction rate very slow. $Pd_2(dba)_3$/ XPhos was reported to be a highly effective

catalyst for the Suzuki-Miyaura reactions, especially with the substrate phenyl boronic ester.[194] The yield of compound **83** was raised to 45%.

4.3 Results and discussion

4.3.1 Kinase assay results

Table 4.1. Kinase inhibitory activity of macrocyclic compounds **60**, **65**, **72**, **79** and **84** against CDK2, CDK9, aurora A and aurora B.

compound		kinase inhibition (%)			
No.	concentration (μM)	aurora A	aurora B	CDK2–cyclin A	CDK9–cyclin T1
60	0.1	6	0	5	0
	1	3	46	0	0
65	0.1	1	11	1	30
	1	50	16	25	86
72	0.1	0	1	8	12
	1	10	16	11	40
79	0.1	4	7	4	52
	1	28	18	26	93
84	0.1	5	0	10	25
	1	23	13	15	79

The kinases activity assays of macrocyclic compounds **60**, **65**, **72**, **79** and **84** were carried out against aurora-A, aurora-B, CDK2 and CDK9. **Table 4.1** and **Table 4.2** show the kinase activity inhibition (%) and inhibitory potency.

Table 4.2 The K_i test result of compound **79**

Kinase	Kinase inhibition K_i (nM)[a]	
	79	**5**
Aurora-A	2728	61
Aurora-B	2899	54
CDK2/cyclin A	1821	568
CDK9/cyclin T1	36	7

[a]The data given are mean values derived from two replicates. Apparent inhibition constants (K_i) were calculated from IC_{50} values and the appropriate K_M (ATP) values for

each kinase.

In **Table 4.1**, all compounds exhibit poor inhibitory activity against CDK2, aurora-A and aurora-B (0 - 11% inhibition at 0.1 μM); only compound **79** shows 52% inhibition against CDK9, demonstrating that compound **79** is highly selective for CDK9 over the other three kinases. Therefore, the K_i assay was carried out for compound **79** against four kinases to support this conclusion. In **Table 4.2**, compound **79** is shown to exhibit 60-fold selectivity for CDK9 over CDK2 and 90-fold selectivity for CDK9 over ARKs. Although compound **79** is less active than lead compound **5** against CDK9, it is still the most selective compound.

Compound **79** shows good selectivity for CDK9 over CDK2 and ARKs, but the selectivity of **79** over other kinases in the human genome is still unknown. Figure **4.1** is a Diversity kinase panel for compound **79** and it shows inhibition of kinase activity (%) with the substrate at a concentration of 0.2 uM.

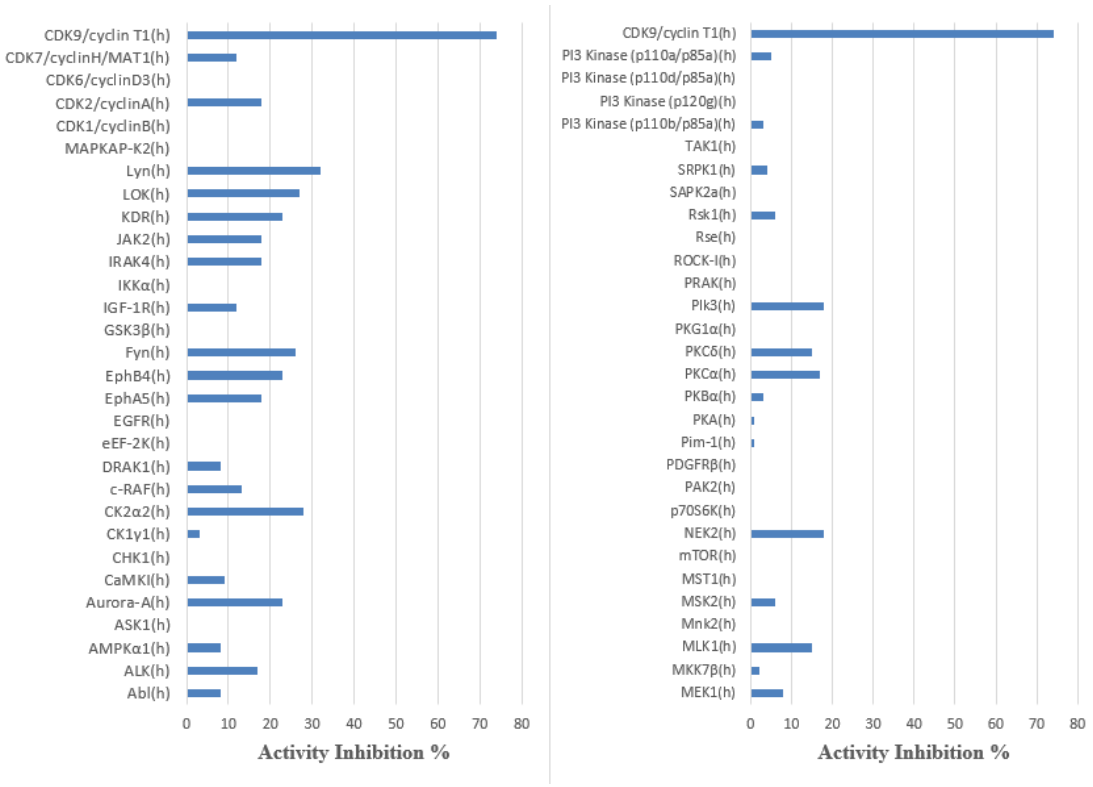

Figure 4.1: Diversity kinase profile screening of compound **79**.

Compound **79** exhibits a high selectivity in the kinase profile screen in **Figure 4.1**. Excluding inhibition against CDK9 (74%), only tyrosine-protein kinase Lyn(h) revealed > 30% inhibition after treatment with compound **79** at a concentration of 0.2 μM. In addition, there are three Serine/Threonine protein kinase, aurora-A(h), CK2α2(h), and LOK(h), showing > 20% inhibition. Lyn(h) could be the only off-target kinase markedly inhibited by compound **79**, but further K_i tests against Lyn(h) are necessary for future work.

4.3.2 Molecular docking

Table 4.3. The Glide score (kcal/mol) of docking poses for compounds **79** with aurora-A, aurora-B, CDK2 and CDK9.

Protein/Ligand	79
Aurora-A	-3.84
Aurora-B	-4.67
CDK2/cyclin A	-4.38
CDK9/cyclin T1	-7.86

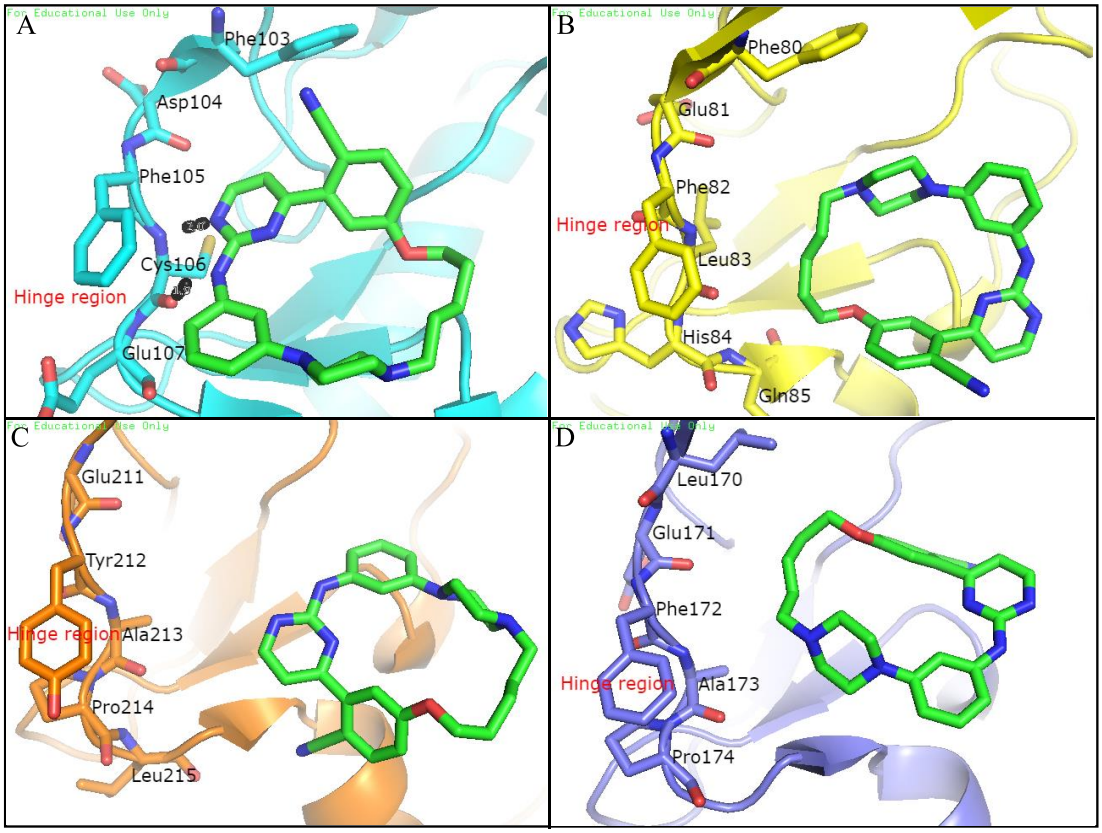

Figure 4.2: Docking poses for complexes of **79** with (A) CDK9, (B) CDK2, (C) Aurora-A, (D) Aurora-B.

Compound **79** was docked into proteins aurora-A, aurora-B, CDK2 and CDK9, and the top Glide scores of the best binding poses are listed in **Table 4.3**. In **Figure 4.2**, the key residues of the hinge region are shown in distinct color sticks (sky blue for CDK9, yellow for CDK2, brown for aurora-A, dark blue for aurora-B). The ligand **79** is shown in green.

Compound **79** in (A) occupies the ATP binding site and forms two strong hydrogen bonds with Cys106 of hinge region of CDK9 and a favourable lone pair-π-interaction is formed by cyano group and the gatekeeper residue Phe103 in the hydrophobic pocket I. This stable docking pose produced a relative low Glide score (-7.86) in **Table 4.3** and potent inhibition activity against CDK9 (36 nM) in **Table 4.2**.

Ligands in (B), (C), (D) are away from the hinge region and no hydrogen bond is observed. That could explain the poor affinity of compound **79** binding with CDK2 and ARKs. The generated docking Glide scores (-4.38 for CDK2, -3.84 for aurora A, -4.67 for aurora B) are at the same level as the K_i value in Table 4.2 (1821 nM for CDK2, 2728 nM for aurora A, 2899 nM for aurora B).

It was found that compound **79** only forms two hydrogen bonds with Cys106 of hinge region in (A), and no other hydrogen bond is observed to stabilise the binding mode in CDK9. Therefore, a flexible alkyl linker and alternative macrocyclic compounds are to be adopted as other optimisation strategies to explore more interactions of the ligands with the ATP binding site of CDK9 in the next chapter.

4.4 Conclusion

The third series of macrocyclic compounds was synthesised through four different synthetic routes. The optimisation work focused on the 5-position of the pyrimidine and the adjacent phenyl group. Compound **79** is the most selective CDK9 inhibitor over Aurora kinases and CDK2 among all the designed compounds. The diversity kinase profile screening of compound **79** also corroborated this conclusion, and only tyrosine-protein kinase Lyn revealed > 30% inhibition. Compound **79** exhibits 60-fold selectivity for CDK9 over CDK2 and 90-fold selectivity for CDK9 over aurora-A and aurora-B, although it is less active against CDK9 than lead compound **5**. In the next chapter, two different optimisation strategies were adopted to improve the activity against CDK9.

Chapter Five: Design and initial synthesis of alternative macrocyclic pyrimidine derivatives

Compound **79** in chapter four is the most selective CDK9 inhibitor among all designed macrocyclic compounds, but exhibits 5-fold less activity against CDK9 than lead compound **5**. In this chapter, two strategies were employed to improve the inhibitory activity of compound **79** against CDK9. Unfortunately, only part of the synthesis work has been finished.

5.1 Strategy one: flexible alkyl linker

5.1.1 Design and synthesis of flexible alkyl linker macrocyclic compound

Compound **43** was employed as the model compound in this section, because of its affordability and synthetic accessibility in gram scales. The docking study of compound **43** bound to CDK9 shows the ligand fails to reside in the ATP binding site of CDK9. Therefore, introducing a flexible alkyl linker instead of alkene to **43** can be an effective way to improve the affinity of the ligand with the ATP binding site.

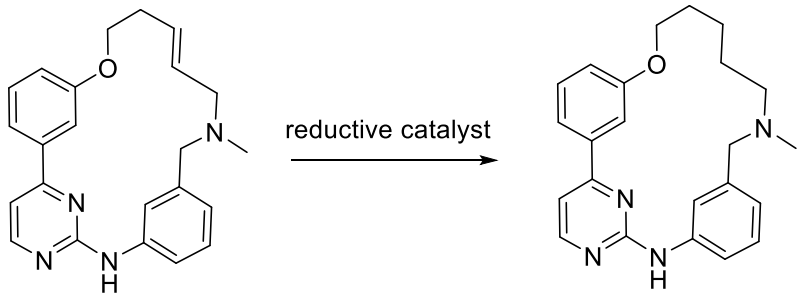

43 **85**

Reactions with different hydrogenation catalysts were carried out to reduce the alkene linker. It was found that commonly used catalysts, Pd/C, Pt_2O, ruthenium/C, rhodium/C, failed to give the desired product **85**, and only multiple reductive byproducts were observed in these experiments. Optimised reaction condition of $Pd(OH)_2$ in THF/*tert*-butanol at H_2 atmosphere was then employed, and the mono-reductive product **85** was achieved as the main product, giving a 25% yield.

5.1.2 Kinase assay results

Table 5.1 The kinase assay (K_i) of macrocyclic compounds **43** and **85.**

Kinases	Kinase inhibtion K_i (nM)[a]	
	43	**85**
Aurora-A	4455	>482
Aurora-B	2340	>473
CDK2/cyclin A	19	99
CDK9/cyclin T1	1	2

Table 5.1 shows the K_i value of compound **43** and **85** against four protein kinases. Compared to compound **43**, the reductive macrocyclic compound **85** maintains high affinity for CDK9, and the selectivity for CDK9 over CDK2 is raised from 20-fold to

50-fold. Therefore, for the CDK9 inhibitors, the flexible alkyl linker can be an effective way to improve the selectivity for CDK9 over CDK2.

5.2 Strategy two: alternative macrocyclic compounds

5.2.1 Design of the alternative macrocyclic compounds with molecular docking

It turned out that the flexible alkyl linker with the same size cycle failed to improve the inhibitory activity against CDK9. Therefore, the second optimisation idea was to adopt an alternative macrocycle. Molecular docking was employed in this part to predict the affinity of different ligands with CDK9.

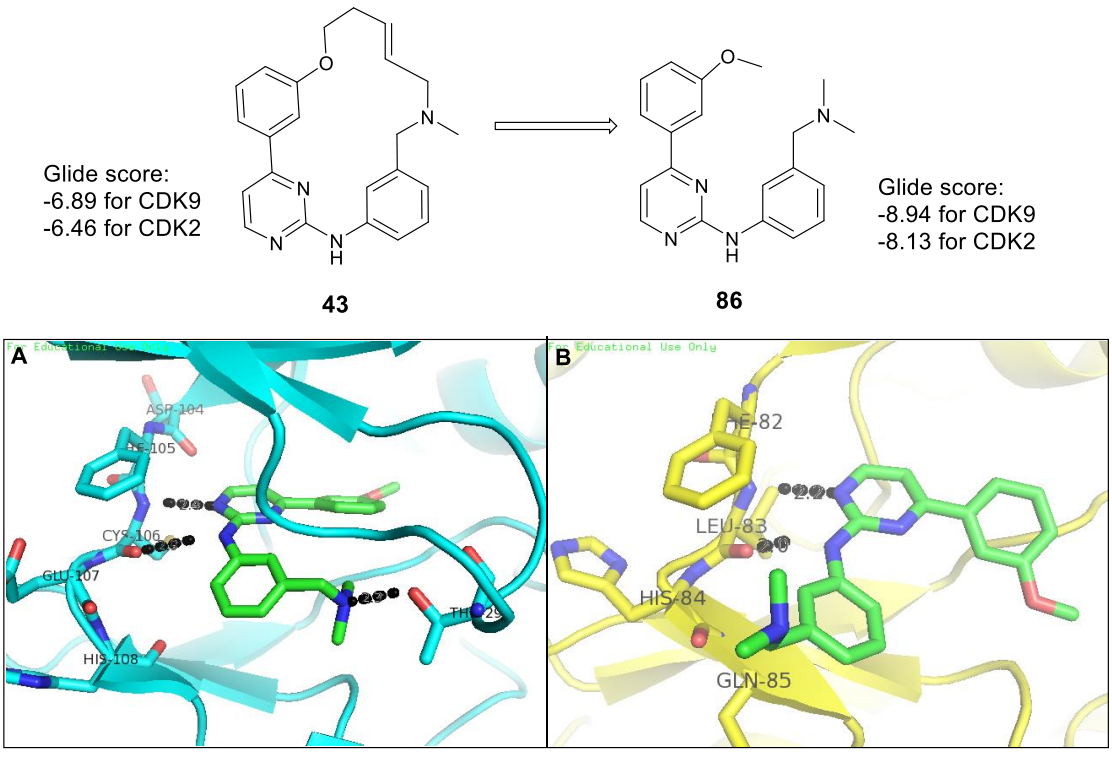

Figure 5.1 Chemical structure of compound **86** and docking pose of ligand **86** binding with (A) CDK9 (PDB code 4BCG) and (B) CDK2 (PDB code 4BCP)

Firstly, we broke the cycle of compound **43** and docked the opening structure compound **86** into the ATP binding site of CDK9 and CDK2 (**Figure 5.1**). The Glide score for compound **86** binding with CDK9 is raised to -9, and a tight binding pose of compound **86** with hinge region is shown in (A). However, the Glide score for compound **86** with CDK2 is also raised to -8. As is shown in (B), ligand **86** adopts an out-conformation and forms two hydrogen bonds with hinge region. Therefore, the structure must be cyclised to improve the selectivity for CDK9 over CDK2.

Following this idea, 39 compounds were designed and docked into CDK9, CDK2, aurora-A and aurora-B. The result shows only three compounds **87**, **88** and **89** exhibited good Glide scores for CDK9 and poor scores for the other three kinases.

Table 5.2 The Glide score (kcal/mol) of three designed compounds **87**, **88**, **89** and compound **43** as the control.

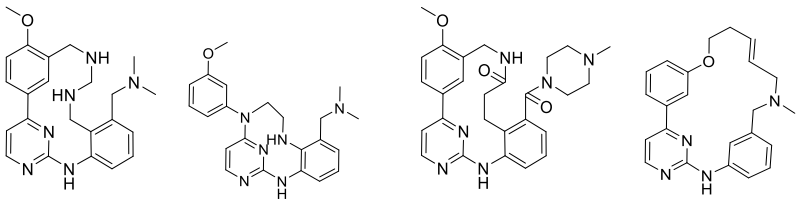

87 **88** **89** **43**

	Glide score	**Glide score**	**Glide score**	**Glide score**
Aurora-A	-5.09	-6.21	-4.72	-5.58
Aurora-B	-6.59	-6.59	-6.84	-4.10
CDK2/cyclin A	-6.20	-6.48	-4.83	-6.46
CDK9/cyclin T1	-9.23	-9.57	-8.80	-6.89

The Glide scores for three designed compounds **87**, **88**, and **89** against CDK9 are raised to -8.8, -9.2 and -9.6. Meanwhile, compounds **87** and **88** show the same level of selectivity for CDK9 over CDK2, aurora-A and aurora-B. Compound **89** with a bulky

N-methyl piperazine terminal group achieves a better selectivity against CDK9 over CDK2 and aurora-A than compounds **87** and **88**. Therefore, it is necessary to synthesise compound **89** and conduct a kinase assay.

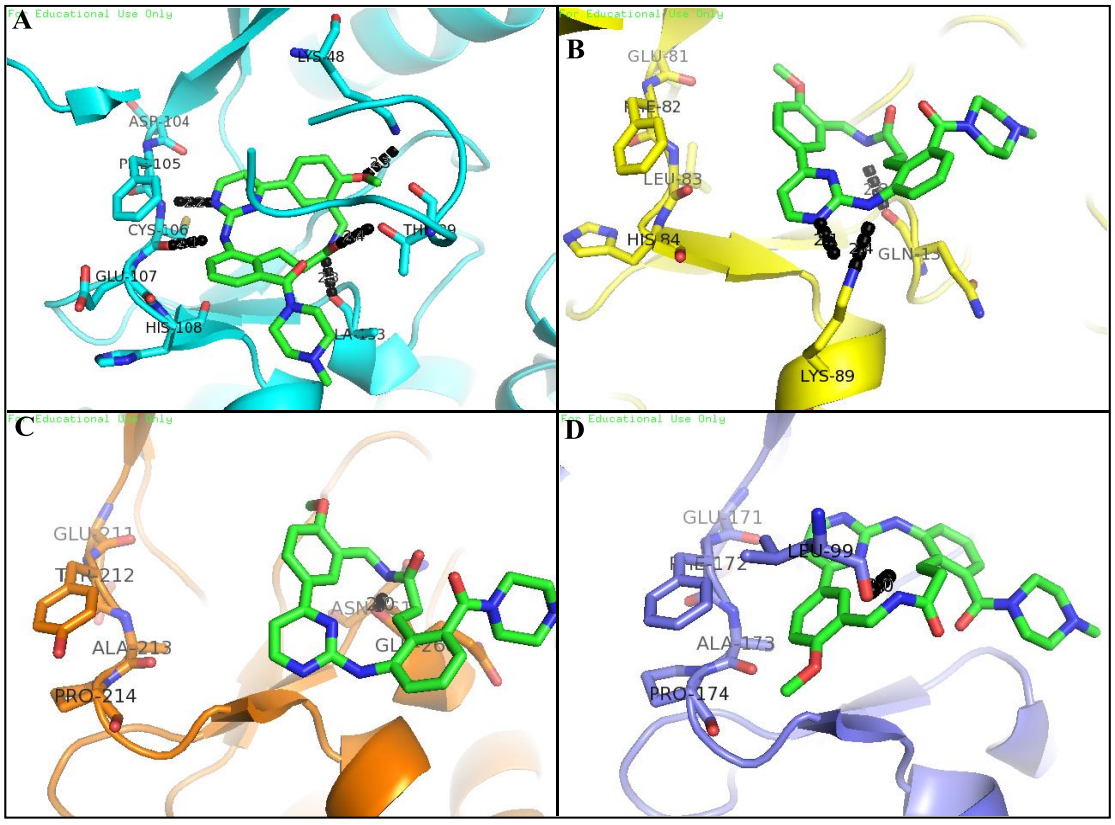

Figure 5.2: Docking pose of compound **89** with four different proteins, (A) CDK9 (PDB cdoe 4BCG), (B) CDK2 (PDB code 4BCP), (C) Aurora-A (PDB code 3UO5), (D) Aurora-B (PDB code 2BFY).

In **Figure 5.2**, the key residues of the hinge region are displayed in various color sticks (sky blue for CDK9, yellow for CDK2, brown for aurora-A, and dark blue for aurora-B), and compound **89** is shown in green. The docking pose in (A) shows that compound **89** has a tight binding with hinge region and three hydrogen bonds formed with residues Lys48 and Ala133 (shown in black dash). The NH of the amide liker also forms a hydrogen bond with Thr29 of glycine rich loop, which contributes to the low

Glide score -8.8. Compound **89** in (B), (C), (D) are away from the hinge region and only several hydrogen bonds are formed with the residues nearby (shown in black dash). It is consistent with their Glide scores (-4.83, -4.72, -6.84).

5.2.2 Initial synthesis of compound 89

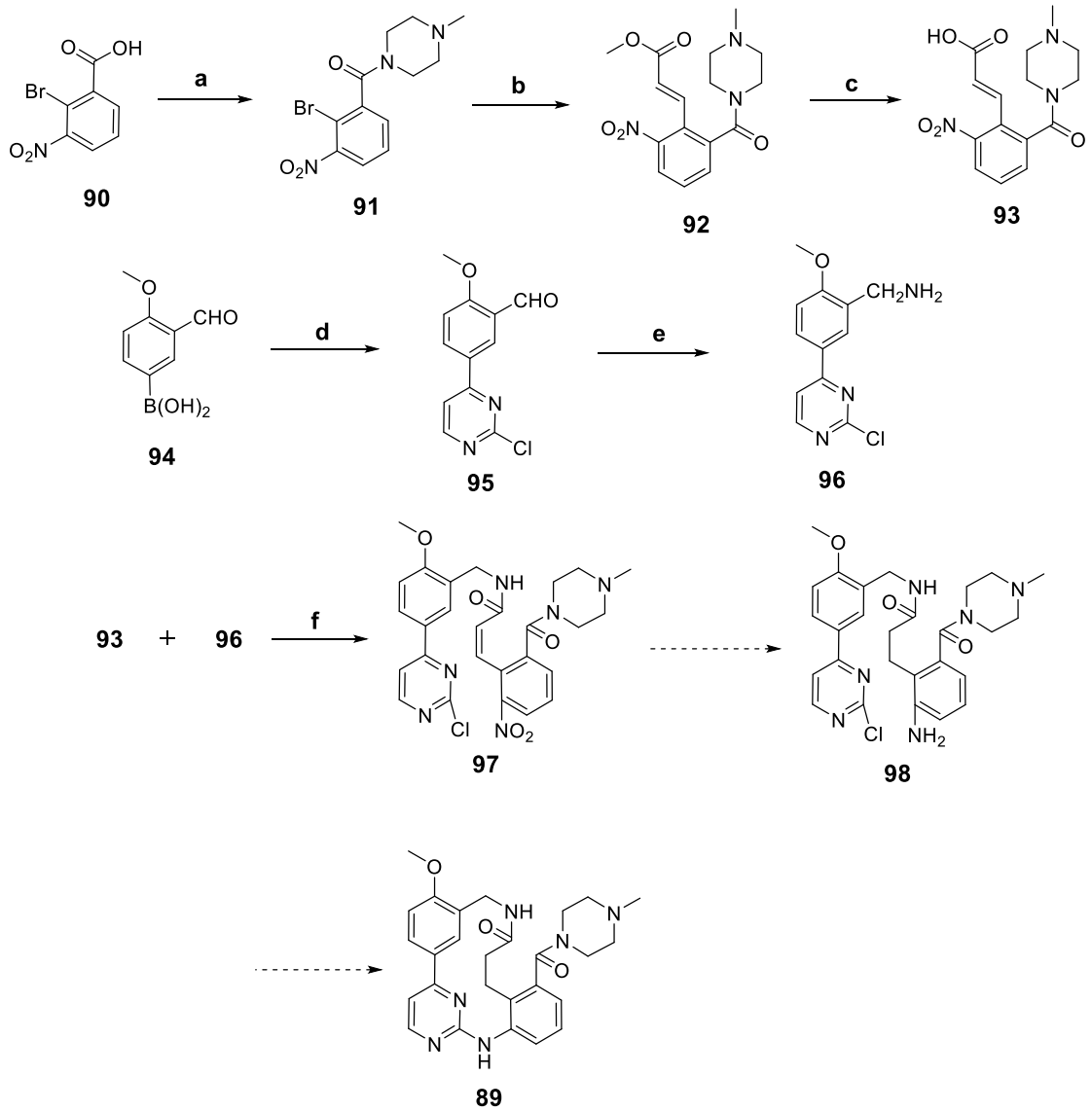

Scheme 5.1 Designed synthetic route for compound **89**. Reagents and conditions: (a) $P(OEt)_3$, I_2, TEA, methylpiperazine, CH_2Cl_2, RT, 2 h, 71%; (b) Methylacrylate, $Pd(OAc)_2$, PPh_3, K_2CO_3, DMF, 110 °C, 64%; (c) 10% NaOH, EtOH, 99%; (d) **46**,

Na_2CO_3, $Pd(PPh_3)_4$, 80 ºC, 53%; (e) NH_4OAc, NH_4OH, $NaBH_3CN$, THF, reflux, overnight, 36%; (f) HATU, TEA, DMF, 50 ºC, 12 h, 30%;

2-Bromo-3-nitrobenzoic acid was treated with methylpiperazine to afford amide intermediate **91**, followed by Heck reaction at 2-bromo position. The resulting compound **92** was hydrolysed to acrylic acid **93**. 3-Formyl-4-methoxyphenyl boronic acid was coupled with 2,4-dichloropyrimidine to give the intermediate **95**, benzaldehyde of which was then converted to phenylmethanamine by reductive amination to afford **96**. Amidation of compound **93** and **96** was achieved by heating at 50 ºC with HATU and triethylamine to furnish compound **97**. The rest of the synthesis has not been finished by the end of the project.

5.3 Conclusion

Because the most selective compound **79** shows 5-fold reduced inhibitory activity than lead compound **2** against CDK9, two strategies were employed to improve the activity against CDK9. According to the kinase assay result, the flexible alkyl linker of compound **85** which was synthesised from the alkene linker of compound **43** raised the selectivity for CDK9 over CDK2 to 50-fold, but it failed to increase the inhibitory activity against CDK9. Therefore, guided by molecular docking, synthesis of the alternative macrocyclic pyrimidine compound was adopted as the second strategy. Compound **89** shows a good Glide score -8.8 against CDK9 and -4.72, -6.84, -4.83 against Aurora-A, Aurora-B and CDK2, which is the most attractive compound so far, but this still needs to be confirmed by the kinase assay.

Chapter Six: Conclusion and Future work

6.1 Conclusion

The project aimed to develop highly selective CDK9 inhibitors based on the lead compound **5** shown in **Figure 6.1**. Because of the highly conserved ATP binding site, synthesis of a highly selective CDK9 inhibitor is still a big challenge. Through comparison of the cocrystal structures of lead compound **5** bound to CDK2 and CDK9, two alternative conformations, "inward" and "outward", can be adopted in CDK2/cyclin A, and only "inward" conformation is adopted by CDK9. Therefore, the hypothesis of a macrocycle to lock the compounds into "in-conformation" was proposed to improve the selectivity for CDK9.

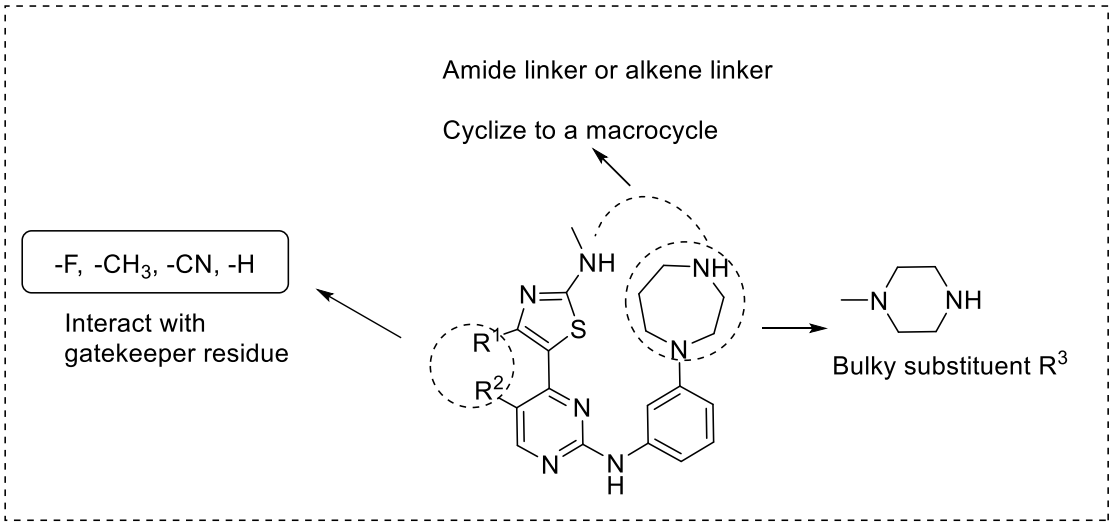

Figure 6.1 The design strategies for macrocyclic compounds.

Compounds **43** and **44** (**Table 6.1**), synthesised through RCM reactions, were selective for CDK9 over CDK2 and ARKs. Extensive structural modification identified

optimal R_1 and R_2 substituents for the lead compound. The combination of the hypothesis of a macrocycle and the optimal substituents produced a synergistic effect to afford the most selective compound **79** (**Table 6.1**).

Table 6.1 The K_i test result of key compounds **43**, **44**, **79** and lead compound **5** as the control.

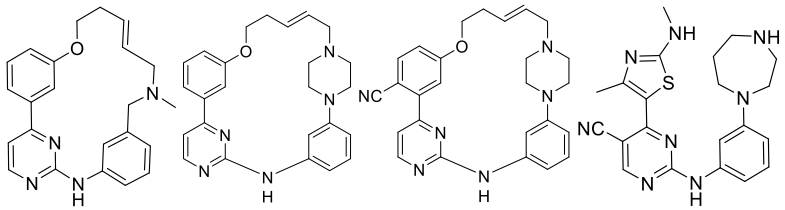

Kinases	Kinase inhibtion K_i (nM)[a]			
	43	**44**	**79**	**5**
Aurora-A	4455	284	2728	61
Aurora-B	2340	219	2899	54
CDK2/cyclin A	19	346	1821	568
CDK9/cyclin T1	1	18	36	7

[a]The data given are mean values derived from two replicates. Apparent inhibition constants (K_i) were calculated from IC_{50} values and the appropriate K_M (ATP) values for each kinase.

Three series of macrocyclic compounds were designed and synthesised, and kinase assay results of the key compounds are shown in **Table 6.1**. The first series of macrocyclic compounds were synthesised through a two-step amide coupling. The kinase assay result showed no inhibition against CDK9 by these compounds, which can be explained by molecular docking study: the structures of these compounds were too big to fit the ATP binding pocket. Therefore, in Chapter 3, model compound **43** was introduced to the structure optimisation to accomplish the RCM reaction. Compound **44**

was found to be a selective CDK9 inhibitor over CDK2 and Aurora kinases, but it exhibited less activity against CDK9. Extensive substituents modification of compound **44** afforded compound **79** as the most selective CDK9 inhibitor. It showed 60-fold selectivity for CDK9 over CDK2 and 90-fold selectivity for CDK9 over Aurora-A and Aurora-B. A further diversity kinase profile screening demonstrated the high selectivity of compound **79**, and only tyrosine-protein kinase Lyn(h) appeared as an off-target hit.

The alternative macrocycle pyrimidine compounds were virtual designed and optimised in a molecular docking view, affording an attractive compound **89**.

Table 6.2 The Glide score (kcal/mol) of the designed compound **89** and compound **43** as the control.

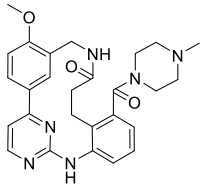

89

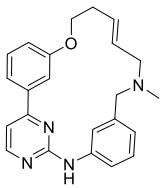

43

Kinase	Glide score	Glide score
Aurora-A	-4.72	-5.58
Aurora-B	-6.84	-4.10
CDK2/cyclin A	-4.83	-6.46
CDK9/cyclin T1	-8.80	-6.89

Compound **89** exhibits a potent Glide score of -8.8 against CDK9, and it achieves better selectivity against CDK9 over CDK2 and aurora-A than the model compound **43** (**Table 6.2**). Although compound **79** is less active than lead compound **5** against CDK9, it is the most selective CDK9 inhibitor (over CDK2 and Aurora kinases) among all the designed compounds. It provides a valuable chemical tool to yield a better

understanding of the role of CDK9 in cancer-relevant pathways.

Table 6.3 The physical properties of all synthesised macrocyclic compounds.

Compounds	Molar Mass (g/mol)	cLogP	H-bond acceptor	H-bond donor	PSA (Å,)
17a	463.18	2.33	7	1	92.97
17b	477.19	2.07	7	1	92.97
17c	491.21	2.63	7	1	92.97
43	372.20	5.27	5	1	49.22
44	413.22	5.28	6	1	52.46
60	431.21	5.47	6	1	52.46
65	427.24	5.78	6	1	52.46
72	438.22	4.82	7	1	76.25
79	438.22	4.96	7	1	76.25
84	427.24	5.77	6	1	52.46
85	374,21	5.55	5	1	49.22

To determine whether a compound is “druglike” or bioavailable, a common used method is to check the compliance of Lipinski’s rule of five. All the macrocyclic compounds in this project show < 500 molar mass, < 5 H-bond donors and <10 H-bond acceptors. Except compounds **17a-c**, **72**, and **79**, the other compounds all exhibits a cLogP > 5 and PSA < 75, which are associated with an increased risk of adverse events.[195] The most selective compound 68 shows a cLogP of 4.96, which is the baseline of Lipinski’ rule. Therefore, the hydrophilicity of compound **79** should be improved in

the future.

6.2 Future work

Complex of compound **79** and CDK9/cyclinT is undergoing X-ray crystallisation experiment; *in vitro* biochemical assay and cellular assays will also be carried out in the future.

According to the diversity kinase panel screening, compound **79** has shown a good selectivity profile for CDK9 over most of the other kinases in the human genome except tyrosine-protein kinase Lyn(h). Further confirmation of the inhibition activity of **79** against Lyn(h) is required. Compound **89** is the most potent and selective compound among all the virtual designed compounds guided by molecular docking studies. It will be synthesised and its activity in the kinase screen will be assessed in the future.

Chapter Seven: Materials, methods, experimental section

7.1 Chemistry

Chemical reagents and solvents were obtained from Sigma-Aldrich, VWR International Ltd., Fisher Scientific UK Ltd., and Scientific Glass Laboratories Limited. Anhydrous solvents such as DMF, THF, and DCM were used when necessary. ^{1}H-NMR and ^{13}C-NMR spectra were obtained using Bruker AV400, AV(III)5000 Ultrashield™ spectrometer at 400 MHz and 100 MHz respectively. All the NMR spectra were processed by Bruker TOPSPIN 2.1 and MestReNova 11.0 programme. Chemical shifts are given in parts per million (ppm) and expressed as δ values relative to tetramethylsilane as an internal standard. Coupling constants (J) are quoted to the nearest 0.1 Hz. The following abbreviations are used: s, singlet; d, doublet; t, triplet; q, quartet; m, multiplet and br, broad.

Mass spectra were obtained using a Waters 2759 spectrometer with positive electrospray ionisation (ESI^{+}). High resolution mass spectra (HRMS) were obtained on a Bruker™ microTOF, an orthogonal Time of Flight instrument with electrospray ionisation (ESI, both positive and negative ion) sources as indicated.

Flash chromatography was performed using either glass column packed with silica gel (200-400 mesh, Aldrich Chemical) or pre-packed silica gel cartridges (FlashMaster

systems, Biotage).

Analytical HPLC was performed on a Shimadzu UFLCXR system coupled to an Applied Biosystems API2000 (a mass spectrometer). Purity was calculated by integrating the area under the curve and is quoted at 254 nm for all compounds. Retention times are quoted in minutes. The following method using gradients of solvent A (0.1% Formic Acid in water) plus solvent B (0.1% Formic Acid in MeCN) were employed:

Method	Column	Temp (°C)	Acid	Time (min)	Organic Solvent%	Flow Rate (mL min^{-1})	Detection (nm)
A	Phenomenex Gemini-NX3 m-110A C18 50 x 2 mm	Ambient	0.1% Formic	0 1 3 5 5.5 6.5	5 5 98 98 5 5	0.5	220/254
B	Phenomenex Gemini-NX3 m-110A C18 50 x 2 mm	Ambient	0.1% Formic	0 1 1.5 9.5 11.5 12 13	5 5 10 98 98 5 5	0.5	220/254
C	Phenomenex Luna 3 m (PFP2) 110A 50 x 2 mm	Ambient	0.1% Formic	0 1 1.5 9.5 11.5 12 13	5 5 10 98 98 5 5	0.5	220/254

*LC-MS method

Melting points (m.p.) were determined with an electrothermal melting point apparatus.

Chemical names were generated from ChemBioDraw 13.0 and ChemBioDraw 14.0.

7.2 Experiment data

7.2.1 General synthetic procedure (1) for nitrobenzene derivatives (compounds 29, 11)

To a round-bottommed flask was added 1-fluoro-3-nitrobenzene and piperazine in DMSO, and the reaction was heated at 100 ºC for 24 h. Once TLC showed the reaction was finished, the reaction mixture was poured onto ice and stirred for another 30 min. The orange precipitate was collected through Buchner funnel.

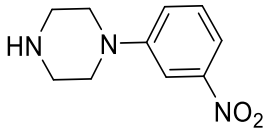

1-(3-Nitrophenyl) piperazine (29)[168]

The title compound was synthesised following general procedure (1) using 1-fluoro-3-nitrobenzene **10** (141mg, 1.0 mmol, 1 eq) and piperazine (430 mg, 5.0 mmol, 5 eq) in 10 mL DMSO to afford an orange solid. (145 mg, 70%). ^{1}H-NMR ($CDCl_3$): δ 7.73 (t, 1H, *J* = 2.0 Hz, Ph-H), 7.67 (dd, 1H, *J* = 2.8, 8.0 Hz, Ph-H), 7.39 (t, 1H, *J* = 8.0 Hz, Ph-H), 7.20 (dd, 1H, *J* = 2.8, 8.0 Hz, Ph-H), 3.26 (br t, 4H, *J* = 5.2 Hz, 2×CH_2), 3.07 (br t, 4H, *J* = 5.2 Hz, 2×CH_2). MS (ESI$^+$): *m/z* $[M + H]^+$ calcd for $C_{10}H_{14}N_3O_2$, 208.10, found 208.06.

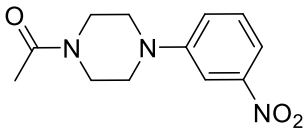

1-(4-(3-Nitrophenyl)-piperazine-1-yl)ethanone (11)[168]

The title compound was synthesised following general procedure (1) using **10** (141 mg, 1.0 mmol, 1 eq) and 1-acetylpiperazine (640 mg, 5.0 mmol, 5 eq) in 10 mL DMSO to yield an orange solid (175 mg, 70%). ^{1}H-NMR (DMSO-d_6): δ 7.65 (t, 1H, J = 2.2 Hz, Ph-H), 7.61 (ddd, 1H, J = 0.7, 2.0, 8.0 Hz, Ph-H), 7.50 (t, 1H, J = 8.0 Hz, Ph-H), 7.40 (ddd, 1H, J = 0.7, 2.5, 8.3 Hz, Ph-H), 3.60 (br t, 4H, J = 4.4 Hz, 2×CH_2), 3.31 (br t, 2H, J = 5.2 Hz, CH_2), 3.24 (br t, 2H, J = 5.2 Hz, CH_2), 2.05 (s, 3H, CH_3). MS (ESI^+): *m/z* $[M + H]^+$ calcd for $C_{12}H_{16}N_3O_3$, 250.12, found 250.13.

7.2.2 General synthetic procedures (2) for *N*- and *O*- substituted derivatives (compounds 30, 48, 63, 67, 81, 76, 59, 41)

To a mixture of the following compounds (**29**, **47**, **62**, **66**, **80**, **75**, **58**, **40**) and allyl bromide (or 4-bromo-1-butene) in DMF at RT was added potassium carbonate, and the resulting mixture was stirred at 90 ºC overnight. The mixture was cooled to RT and quenched with water. The reaction mixture was extracted with CH_2Cl_2 twice, and the combined organic extracts were concentrated and purified by flash column chromatography on silica gel, with (EtOAc/PE) as eluting solvent. The pure fractions were collected and evaporated to afford the target compound.

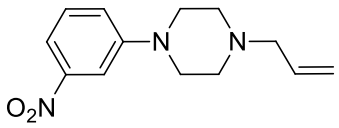

Allyl-4-(3-nitrophenyl) piperazine guanidine (30)

The title compound was synthesised following general procedure (2) using **29** (207

mg, 1.0 mmol, 1 eq), allyl bromide (180 mg, 1.5 mmol, 1.5 eq) and potassium carbonate (276 mg, 2 mmol, 2 eq) in 10 mL DMF to furnish a yellow solid (149 mg, 60%). ^{1}H-NMR ($CDCl_3$): δ 7.73 (t, 1H, *J* = 2.3 Hz, Ph-H), 7.66 (dd, 1H, *J* = 2.1, 8.1 Hz, Ph-H), 7.39 (t, 1H, *J* = 8.3 Hz, Ph-H), 7.20 (dd, 1H, *J* = 2.5, 8.4 Hz, Ph-H), 5.91 (ddt, 1H, *J* = 6.6, 10.2, 17.0 Hz, CH), 5.21-5.24 (m, 2H, 2×CH), 3.32 (br t, 4H, *J* = 5.1 Hz, 2×CH_2), 3.09 (dt, 2H, *J* = 1.2, 6.6 Hz, CH_2), 2.64 (br t, 4H, *J* = 5.1 Hz, 2×CH_2). MS (ESI^+): *m/z* $[M + H]^+$ calcd for $C_{13}H_{18}N_3O_2$, 248.14, found 248.14.

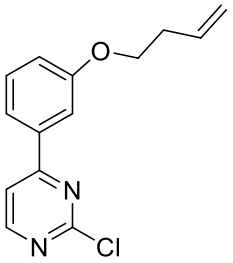

4-(3-(But-3-en-1-yloxy) phenyl)-2-chloropyrimidine (48)[184]

The title compound was synthesised following general procedure (2) using 3-(2-chloropyrimidin-4-yl)phenol **47** (412 mg, 2 mmol, 1 eq), 4-bromo-1-butene (405 mg, 3 mmol, 1.5 eq) and aqueous sodium carbonate (975 mg, 3 mmol, 1.5 eq) in DMF (10 mL) to yield a white solid (256 mg, 49 %). RP-HPLC t_R = 3.55 min (Method 1, 70+ %), *m/z* $[M+H]^+$ calcd for $C_{14}H_{14}N_2ClO$, 261.1, found 261.2.

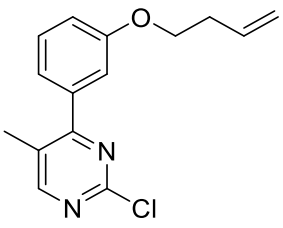

4-(3-(But-3-en-1-yloxy)phenyl)-2-chloro-5-methylpyrimidine (63)[184]

The title compound was synthesised following general procedure (2) using 3-(2-

chloro-5-methylpyrimidin-4-yl)phenol **62** (620 mg, 2.82 mmol, 1 eq), 4-bromo-1-butene (429 µL, 4.23 mmol, 1.5 eq) and cesium carbonate (1373 mg, 4.23 mmol, 1.5 eq) in DMF (10 mL) to yield a brown solid (539 mg, 70 %). ^{1}H-NMR ($CDCl_3$) δ 8.48 (d, 1H, *J* = 0.7 Hz, Ph-H), 7.43-7.36 (m, 2H, Ph-H), 7.16 (s, 2H, Ph-2H), 7.05-7.00 (m, 1H, Ph-H), 5.92 (ddt, 1H, *J* = 17.0, 10.3, 6.7 Hz, CH), 5.21-5.11 (m, 2H, 2×CH), 4.07 (t, 2H, *J* = 6.7 Hz, CH_2), 2.60-2.54 (m, 2H, CH_2), 2.38 (s, 3H, CH_3). RP-HPLC t_R = 3.13 min (Method 1, 95+ %) *m/z* $[M + H]^+$ calcd $C_{15}H_{16}N_2OCl$, 275.1, found 275.1.

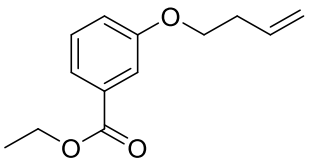

Ethyl-3-(but-3-en-1-yloxy)benzoate (67)[196]

The title compound was synthesised following general procedure (2) using 3-hydroxybenzoate **66** (680 mg, 5 mmol, 1 eq), 4-bromo-1-butene (755 µL, 7.5 mmol, 1.5 eq) and caesium carbonate (2438 mg, 7.5 mmol, 1.5 eq) in DMF (10 mL) to yield brown solid (995 mg, 90 %). ^{1}H-NMR ($CDCl_3$) δ 7.70 (dt, 1H, *J* = 7.6, 1.3 Hz, Ph-H), 7.61 (dd,1H, *J* = 2.7, 1.5 Hz, Ph-H), 7.36 (t, 1H, *J* = 8.0 Hz, Ph-H), 7.14 (ddd, 1H, *J* = 8.3, 2.7, 1.0 Hz, Ph-H), 5.85-5.95 (m, 1H, CH), 5.15-5.21 (dm, 1H, CH), 5.10-5.11 (dm, 1H, CH), 4.11 (q, 2H, *J* = 7.1 Hz, CH_2), 4.06 (t, 2H, *J* = 8.4 Hz, CH_2), 2.53-2.58 (m, 2H, CH_2), 1.25 (t, 3H, *J* = 7.1 Hz, CH_3).

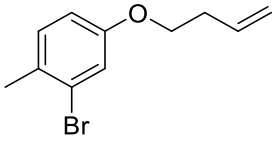

2-Bromo-4-(but-3-en-1-yloxy)-1-methylbenzene (81)

The title compound was synthesised following general procedure (2) using 3-bromo-4-methyl-phenyl **80** (372 mg, 2 mmol, 1 eq), 4-bromo-1-butene (304 µL, 3 mmol, 1.5 eq) and caesium carbonate (975 mg, 3 mmol, 1.5 eq) in DMF (10 mL) to yield a pale yellow solid (434 mg, 90 %). ^{1}H-NMR ($CDCl_3$) δ 7.18-7.12 (m, 2H, 2×Ph-H), 6.81 (dd, 1H, *J* = 8.4, 2.6 Hz, Ph-H), 5.94 (ddt, 1H, *J* = 17.2, 10.4, 6.7 Hz, Ph-H), 5.22 (ddt, 2H, *J* = 1.6, 3.6, 17.2 Hz, CH), 5.16 (ddt, 1H, *J* = 1.5, 2.8, 10.4 Hz, CH), 4.01 (t, 2H, *J* = 6.7 Hz, CH_2), 2.57 (dddt, 2H, *J* = 13.4, 6.5, 1.3 Hz, CH_2), 2.37 (s, 3H, CH_3).

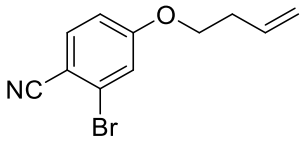

2-Bromo-4-(but-3-en-1-yloxy)benzonitrile (76)[197]

The title compound was synthesised following general procedure (2) using 2-bromo-4-hydroxybenzonitrile **75** (392 mg, 2 mmol, 1 eq), 4-bromo-1-butene (304 µL, 3 mmol, 1.5 eq) and cesium carbonate (975 mg, 3 mmol, 1.5 eq) in DMF (10 mL) to yield pale orange solid (420 mg, 83%). ^{1}H-NMR ($CDCl_3$) δ 7.49 (d, 1H, *J* = 8.7 Hz, Ph-H), 7.13 (d, 1H, *J* = 2.4 Hz, Ph-H), 6.86 (dd, 1H, *J* = 8.8, 2.5 Hz, Ph-H), 5.82 (ddt, 1H, *J* = 17.0, 10.3, 6.7 Hz, CH), 5.23-4.97 (m, 2H, CH_2), 4.02 (t, 2H, *J* = 6.6 Hz, CH_2), 2.52 (dddt, 2H, J = 13.6, 6.6, 1.4 Hz, CH_2).

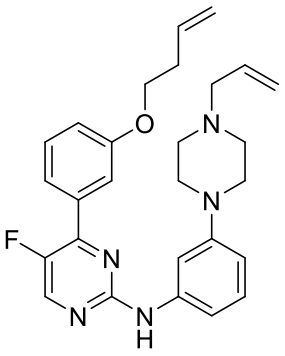

N-(3-(4-Allylpiperazin-1-yl)phenyl)-4-(3-(but-3-en-1-yloxy)phenyl)-5-fluoropyrimidin-2-amine (59)

The title compound was synthesised following general procedure (2) using 3-(2-((3-(4-allylpiperazin-1-yl)phenyl)amino)-5-fluoropyrimidin-4-yl)phenol **58** (606 mg, 1.5 mmol, 1 eq), 4-bromo-1-butene (228 μL, 2.25 mmol, 1.5 eq) and cesium carbonate (731 mg, 2.25 mmol, 1.5 eq) in DMF (10 mL) to yield white solid (481 mg, 70 %). ^{1}H-NMR ($CDCl_3$) δ 8.28 (d, 1H, *J* = 3.1 Hz, Ph-H), 8.00-7.94 (m, 1H, Ph-H), 7.64 (t, 1H, *J* = 2.3 Hz, Ph-H), 7.36 (t, 1H, *J* = 7.9 Hz, Ph-H), 7.29 (d, 1H, *J* = 16.3 Hz, Ph-H), 7.12 (dd, 1H, *J* = 7.8, 2.0 Hz, Ph-H), 7.03 (ddd, 1H, *J* = 8.3, 2.8, 1.0 Hz, Ph-H), 6.94 (d, 1H, *J* = 3.3 Hz, Ph-H), 6.74 (dd, 1H, *J* = 8.3, 2.3 Hz, Ph-H), 6.02-5.88 (m, 2H, 2×CH), 5.30-5.12 (m, 4H, 2×CH_2), 4.13 (t, 2H, *J* = 6.8 Hz, CH_2), 3.37-3.30 (m, 4H, 2×CH_2), 3.11 (dt, 2H, *J* = 6.6, 1.4 Hz, CH_2), 2.69-2.64 (m, 4H, 2×CH_2), 2.60 (dddt, 2H, *J* = 13.6, 6.8, 1.4 Hz, CH_2). ^{13}C NMR ($CDCl_3$) δ 159.2, 152.1, 149.66, 146.2, 143.6, 139.8, 139.6, 138.9, 134.8, 134.5, 129.5, 129.3, 120.7, 118.3, 117.1, 116.9, 113.9, 111.4, 111.2, 107.8, 67.3, 61.8, 53.1, 48.9, 33.7. RP-HPLC t_R = 2.37 min (Method 1, 95+ %) *m/z* $[M + H]^+$, calcd $C_{27}H_{30}N_5OF$, 460.3, found 460.3.

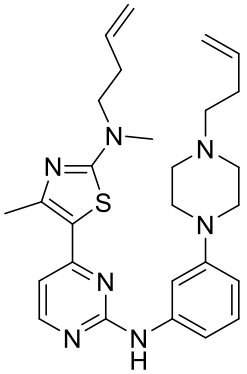

N-(But-3-en-1-yl)-5-(2-((3-(4-(but-3-en-1-yl)piperazin-1-yl)phenyl)amino)-pyrimidin-4-yl)-*N*,4-dimethylthiazol-2-amine (41)

The title compound was synthesised following general procedure (2) using **40** (109 mg, 0.25 mmol, 1 eq) and 4-bromo-1-butene (52 mg, 0.375 mmol, 1.5 eq) in 5 mL DMF to yield the yellow solid (68 mg, 56%). ^{1}H-NMR ($CDCl_3$): δ 8.25 (d, 1H, *J* = 5.4 Hz, PH-H), 7.89 (s, 1H, NH), 7.32 (s, 1H, Ph-H), 7.15 (t, 1H, J = 8.0, Ph-H), 7.04 (dd, 1H, *J* = 1.2, 7.9 Hz, Ph-H), 6.76 (dd, 1H, *J* = 1.3, 3.5 Hz, Ph-H), 6.56 (d, 1H, *J* = 8.0 Hz, PH-H), 5.72-5.84 (m, 2H, 2×CH), 4.97-5.23 (m, 4H, 2×CH_2), 3.52 (t, 2H, *J* = 5.8 Hz, CH_2), 3.21 (br s, 4H, 2×CH_2), 3.06 (s, 3H, CH_3), 2.56 (br s, 4H, 2×CH_2), 2.51 (s, 3H, CH_3), 2.41 (dd, 2H, *J* = 7.5, 16.70 Hz, 2×CH_2), 2.24 (dd, 2H, *J* = 6.5, 13.8 Hz, CH_2). ^{13}C-NMR ($CDCl_3$): δ 19.0, 19.1, 31.4, 31.5, 36.4, 38.2, 49.2, 52.4, 53.2, 53.5, 57.9, 107.4, 110.2, 110.9, 115.7, 117.4, 119.7, 129.2, 134.8, 136.5, 140.8, 151.9, 152.9, 157.2, 159.6, 159.8, 162.5, 169.7. RP-HPLC t_R = 3.52 min (Method 2, 95+ %) *m/z* $[M + H]^+$ calcd $C_{27}H_{36}N_7S$, 490.2, found 490.2.

7.2.3 Synthetic procedure for *N*-methyl-*N*-(3-nitrobenzyl)-prop-2-en-1-amine (50)

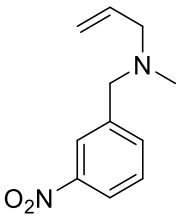

To a solution of 3-nitrobenzaldehyde **49** (151 mg, 1 mmol, 1eq) in CH_2Cl_2 was added

N-methyl allyl amine (85 mg, 1.2 mmol, 1.2 eq). The reaction mixture was stirred for 2 h, and $Na(OAc)_3BH$ (216 mg, 2 mmol, 2 eq) was added portionwise over 5 mins. The mixture was stirred at RT overnight and then quenched with saturated NH_4Cl. The product was extracted with CH_2Cl_2 and the combined organic extracts were washed with brine. The crude mixture was concentrated and purified by column chromatography (EtOAc/Hexane) to furnish a white solid (146 mg, 71 %). ^{1}H-NMR ($CDCl_3$): δ 8.21 (s, 1H, Ph-H), 8.11 (ddd, 1H, *J* = 8.1, 2.4, 1.1 Hz, Ph-H), 7.68 (dt, 1H, *J* = 7.8, 1.4 Hz, Ph-H), 7.49 (t, 1H, *J* = 7.9 Hz, Ph-H), 5.91 (ddt, 1H, *J* = 17.1, 10.2, 6.4 Hz, CH), 5.30-5.17 (m, 2H, CH_2), 3.59 (s, 2H, CH_2), 3.06 (d, 2H, *J* = 6.4 Hz, CH_2), 2.21 (s, 3H, CH_3). ^{13}C-NMR ($CDCl_3$): δ 42.1, 60.6, 117.9, 122.1, 123.6. 129.1, 134.9, 135.4, 141.7, 148.4. MS (ESI^+): *m/z* $[M + H]^+$ calcd for $C_{11}H_{15}N_2O_2$, 206.11, found 206.51.

7.2.4 Synthetic procedure for 3-(3-(but-3-en-1-yloxy)phenyl)-3-oxopropanenitrile (68)

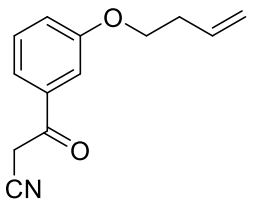

To a solution of acetonitrile (128 μL, 2.45 mmol, 1 eq) in 6 mL of anhydrous THF was added potassium butoxide (552 mg, 4.9 mmol, 2 eq). After stirring for 1 h, ethyl 3-(but-3-en-1-yloxy)benzoate **67** (539 mg, 2.45 mmol, 1 eq) was added to the solution. The reaction was stirred at RT for 2 h. After TLC indicated the completion of **67**, the mixture was acidified with diluted HCl solution and extracted with $CHCl_3$ (3×50 mL).

The resulting crude was then concentrated and purified by column chromatography (PE/EtOAc) to furnish a pale brown solid (223 mg, 45%). ^{1}H-NMR ($CDCl_3$) δ 7.43-7.33 (m, 3H, 3×Ph-H), 7.14 (ddd, 1H, *J* = 8.0, 2.7, 1.2 Hz, Ph-H), 5.87 (ddt, *J* = 17.0, 10.3, 6.7 Hz, CH_2), 5.15 (ddt, 1H, *J* = 17.2, 3.3, 1.2 Hz, CH), 5.09 (ddt, 1H, *J* =10.2, 2.8, 1.2 Hz, CH), 4.11 (s, 2H, CH_2), 4.02 (t, 2H, *J* = 6.7 Hz, CH_2), 2.52 (dddt, 2H, *J* = 13.3, 6.6, 1.3 Hz, CH_2).

7.2.5 General synthetic procedure (3) for aniline derivatives (compounds 12, 99)

A solution of the nitrophenyl-derivative in aqueous methanol was degassed three times and palladium on carbon (10%) was added. The flask was flushed three times with hydrogen, and the reaction was stirred under a hydrogen balloon for 24 h. The reaction mixture was filtered through Celite and concentrated to yield a grey solid.

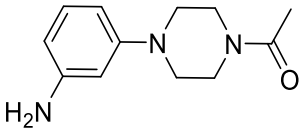

1-(4-(3-Aminophenyl) piperazine-1-yl)ethan-1-one (12)[168]

The title compound was synthesised following general procedure (3) using 1-(4-(3-nitrophenyl)piperazin-1-yl)ethan-1-one **11** (2.49 g, 10 mmol, 1eq) and 10% palladium on carbon (250 mg) in 50 mL methanol and water to afford a grey solid **7** (2.09 g, 95%). ^{1}H-NMR (DMSO-d_6): δ 6.87 (t, 1H, *J* = 7.9 Hz, Ph-H), 6.17 (br d, 1H, *J* = 1.8 Hz, Ph-H), 6.15 (dd, 1H, *J* = 1.6 , 8.1 Hz, Ph-H), 6.08 (dd, 1H, *J* = 1.1, 7.7 Hz, Ph-H), 4.89 (br

s, 2H, NH_2), 3.52-3.57 (br m, 4H, 2×CH_2), 3.05 (br t, 2H, J = 4.8 Hz, CH_2), 2.98 (br t, 2H, J = 5.0 Hz, CH_2), 2.04 (s, 3H, CH_3).

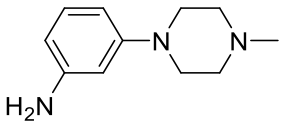

3-(4-Methylpiperazin-1-yl)aniline (99)[168]

The title compound was synthesised following general procedure (3) using 1-methyl-4-(3-nitrophenyl)piperazine (2330 mg, 11 mmol, 1eq) and 10% palladium on carbon (230 mg) in 50 mL methanol and water to afford a grey solid **99** (1.91 g, 83%). ^{1}H-NMR (DMSO-d_6) δ 6.83 (t, 1H, J = 7.9 Hz, Ph-H), 6.14 (t, 1H, J = 2.2 Hz, Ph-H), 6.11 (dd, 1H, J = 7.8, 2.3 Hz, Ph-H), 6.02 (dd, 1H, J = 7.6, 1.8 Hz, Ph-H), 4.82 (s, 2H, NH_2), 3.05-2.97 (m, 4H, 2×CH_2), 2.41 (dd, 4H, J = 6.2, 3.8 Hz, 2×CH_2), 2.20 (s, 3H, CH_3).

7.2.6 Synthetic procedure for 3-(4-allylpiperazine-1-yl) aniline (31)[198]

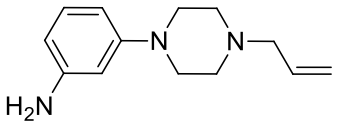

To a solution of **30** (2.47 g, 10 mmol, 1 eq) in methanol and water was added tin chloride dehydrate (6.75 g, 30 mmol, 3eq), and the reaction mixture was stirred at RT for 12 h. After completion of the reaction, the solvent from the reaction mixture was removed under reduced pressure, and the residue was taken into aqueous sodium carbonate and dichloromethane. The reaction mixture was filtered through filter paper. The organic layer was separated out from the filtrate, and the aqueous layer was extracted with dichloromethane. The combined organic extracts were dried with sodium

sulfate and concentrated under reduced pressure to afford a grey solid (2158 mg, 99%). ^{1}H-NMR ($CDCl_3$): δ 7. 07 (t, 1H, *J* = 8.1 Hz, Ph-H), 6.39 (dd, 1H, *J* = 8.1, 2.4 Hz, Ph-H), 6.28 (t, 1H, *J* = 2.3 Hz, Ph-H), 6.23 (dd, 1H, *J* = 7.8, 2.1 Hz, Ph-H), 5.93 (ddt, 1H, *J* = 16.9, 10.1, 6.6 Hz, CH), 5.34-5.18 (m, 2H, CH_2), 3.63 (br s, 2H, NH2), 2.61 (br t, 4H, J = 5.1 Hz, 2×CH2), 3.07(d, 2H, J = 6.6 Hz, CH2), 3.21 (br t, 4H, J = 4.8 Hz, 2×CH2). HR-MS (ESI$^+$): *m/z* $[M + H]^+$ calcd for $C_{27}H_{36}N_7S$, 218.1657, found 218.1649. RP-HPLC t_R = 0.32 min (Method 1, 95+ %), *m/z* $[M + H]^+$ calcd for $C_{27}H_{36}N_7S$, 218.2, found 218.3.

7.2.7 General synthetic procedure (4) for guanidine derivatives (compounds 13, 32)

Cyanamide and TMSCl were added sequentially to a solution of different amines in acetonitrile and the reaction was heated under reflux overnight. The reaction mixture was concentrated and purified by column chromatography (gradient DCM and MeOH as eluting solvent) to afford the desired compounds.

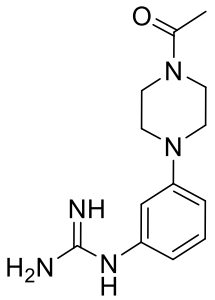

1-(3-Acetylpiperazin-1-yl)phenyl)guanidine (13)[168]

The title compound was synthesised following general procedure (4) using

cyanamide (284 mg, 2.0 mmol, 2 eq), TMSCl (109 mg, 1 mmol, 1 eq) and amine **12** (219 mg, 1.0 mmol, 1 eq) in acetonitrile to give a brown solid (176 mg, 71%). ^{1}H-NMR (DMSO-d_6): δ 7.02 (t, 1H, J = 8.0 Hz, Ph-H), 6.49 (dd, 1H, J = 1.6, 8.1 Hz, Ph-H), 6.39 (br s, 1H, Ph-H), 6.30 (d, 1H, J = 7.6 Hz, Ph-H), 5.34 (br s, 4H, 2×NH&NH_2), 3.59-3.51 (m, 4H, 2×CH_2), 3.09 (br t, 2H, J = 5.2 Hz, CH_2), 3.03 (br t, 2H, J = 5.2 Hz, CH_2), 2.04 (s, 3H, CH_3). RP-HPLC t_R = 0.43 min (Method 1, 95+ %), *m/z* $[M + H]^+$ calcd for $C_{13}H_{20}N_5O$, 262.3, found 262.3.

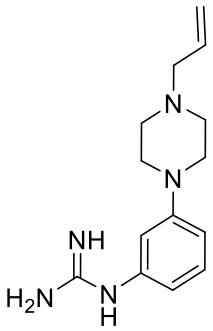

1-(3-(4-Allylpiperazin-1-yl)phenyl)guanidine (32)

The title compound was synthesised following general procedure (4) using **31** (217 mg, 1.0 mmol, 1 eq), cyanamide (284 mg, 2.0 mmol, 2 eq) and TMSCl (109 mg, 1 mmol, 1 eq) in 10 mL acetonitrile to yield the grey solid (130 mg, 60%). ^{1}H-NMR ($CDCl_3$): δ 7.17 (t, 1H, J = 8.1 Hz, Ph-H), 6.67 (dd, 1H, J = 8.4 Hz, Ph-H), 6.58 (br t, 1H, J = 2.0 Hz, Ph-H), 6.50 (dd, 1H, J = 1.1, 7.7 Hz, Ph-H), 5.88 (ddt, 1H, J = 16.8, 10.1, 6.6 Hz, CH), 5.27-5.17 (m, 2H, CH_2), 4.58 (br s, 4H, 2×NH&NH_2), 3.17 (br t, 4H, J = 6.8 Hz, 2×CH_2), 3.04 (d, 2H, J = 6.6 Hz, CH_2), 2.57 (br t, 4H, J = 6.8 Hz, 2×CH_2). MS (ESI^+): *m/z* $[M + H]^+$ calcd for $C_{14}H_{22}N_5$, 260.18, found 260.18.

7.2.8 General synthetic procedure (5) for thiazole derivatives (compounds 7, 26)

To a solution of 3-chloropentane-2, 4-dione in methanol was added thiourea derivatives and pyridine. The reaction was stirring at RT for 4 h. After concentrated, the precipitate was washed with saturated $NaHCO_3$ solution and concentrated to offer the desired compounds.

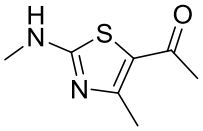

1-(4-Methyl-2-(methylamino) thiazol-5-yl) ethanone (7)[168]

The title compound was synthesised following general procedure (5) using 3-chloropentane-2, 4-dione **6** (13.4 g, 100 mmol, 1 eq), 1-methylthiourea (9.0 g, 100 mmol, 1 eq), (1.1 eq) and pyridine (8.1 mL, 100 mmol, 1 eq) to offer the target white solid (15.3 g, 90%). ^{1}H-NMR (DMSO-d_6): δ 8.37 (s, 1H, NH), 2.84 (s, 3H, CH_3), 2.44 (s, 3H, CH_3), 2.34 (s, 3H, CH_3). MS (ESI^+): m/z $[M + H]^+$ calcd for $C_7H_{12}N_2OS$, 171.06, found 171.06.

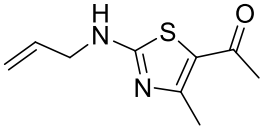

1-(2-(Allylamino)-4-methylthiazol-5-yl)ethanone (26)[69]

The title compound was synthesised following general procedure (5) using 1-allylthiourea (1.16 g, 10 mmol, 1 eq), 3-chloropentane-2,4-dione **6** (1.34 g, 10 mmol, 1 eq) and pyridine (0.81 mL, 10 mmol, 1 eq) in 30 mL methanol to yield white solid (1764

mg, 90%). ^{1}H-NMR (DMSO-d_6): δ 7.35 (br s 1H, NH), 5.85-5.94 (m, 1H, CH), 5.35 (ddt, 1H, J = 1.7, 3.5, 17.1, CH), 5.26 (ddt, 1H, J = 1.3, 3.3, 10.2 Hz, CH), 3.92 (d, 2H, J = 5.4 Hz, CH_2), 2.54 (s, 3H, CH_3), 2.43 (s, 3H, CH_3). ^{13}C-NMR ($CDCl_3$) δ 188.3, 169.2, 143.2, 128.6, 121.4, 120.9, 49.6, 29.0, 14.9.

7.2.9 General synthetic procedure (6) for Boc-protection of amine derivatives (compounds 27, 8)

To a solution of thiazole derivatives in DCM were added 4-dimethyl-aminopyridine and di-tertbutyl-dicarbonate, and the reaction was stirred for 2 h at room temperature. The resulting reaction mixture was washed with diluted HCl solution and washed with saturated $NaHCO_3$ solution, brine. The organic extract was concentrated to dryness to yield the desired compounds.

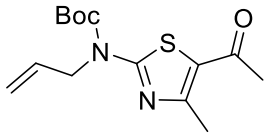

tert-Butyl-(5-acetyl-4-methylthiazol-2-yl)-allylcarbamate (27)

The title compound was synthesised following general procedure (6) using **26** (196 mg, 1 mmol, 1 eq), 4-dimethyl-aminopyridine (122 mg, 1 mmol, 1 eq) and di-tertbutyl-dicarbonate (436 mg, 2 mmol, 2 eq) in DCM to furnish a white solid (280 mg, 95%). ^{1}H-NMR (DMSO-d_6): δ 5.86-5.96 (m, 1H, CH), 5.16 (dd, 1H, J = 1.3, 10.3, CH), 5.08 (dd, 1H, J = 1.5, 17.2 Hz, CH), 4.65 (br d, 2H, J = 5.2 Hz, CH_2), 2.55 (s, 3H, CH_3), 2.47 (s, 3H, CH_3), 1.52 (s, 9H, 3×CH_3). ^{13}C-NMR (DMSO-d_6) δ 190.8, 161.4, 155.7, 152.9,

132.4, 125.8, 117.2, 84.0, 48.9, 30.5, 28.1, 18.5.

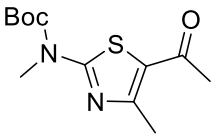

tert-Butyl (5-acetyl-4-methylthiazol-2-yl)(methyl)carbamate (8)[168]

The title compound was synthesised following general procedure (6) using **7** (170 mg, 1 mmol, 1 eq), di-tert-butyl dicarbonate (436 mg, 2 mmol, 2 eq) and DMAP (122 mg, 1 mmol, 1 eq) in 10 mL dichloromethane to yield white solid (255 mg, 95%). ^{1}H-NMR ($CDCl_3$): δ 2.83 (s. 3H, CH_3), 2.65 (s, 3H, CH_3), 2.48 (s, 3H, CH_3), 1.45 (s, 9H, 3×CH_3). ^{13}C NMR ($CDCl_3$) δ 191.3, 177.8, 161.2, 154.7, 125.7, 40.2, 36.5, 30.5, 27.9, 18.4.

7.2.10 General synthetic procedure (7) for enaminones derivatives (compounds 9, 38, 88)

The thiazole derivatives were treated with dimethoxymethyl-dimethylamine (DMF-DMA). After heating at 120 °C for 6 h, the mixture was evaporated to dryness. Target compounds were obtained after crystallisation from EtOAc/PE to desired compounds.

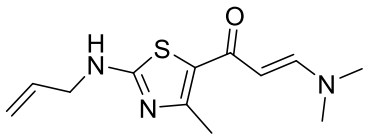

(*E*)-1-(2-(Allylamino)-4-methylthiazol-5-yl)-3-(dimethylamino)prop-2-en-1-one (100)[69]

The title compound was synthesised following general procedure (7) using 1-(2-

(allylamino)-4-methylthiazol-5-yl)ethan-1-one (182 mg, 1 mmol, 1 eq) in dimethoxymethyl-dimethylamine (DMF-DMA, 5 mL) to yield yellow solid (148 mg, 62%). ^{1}H-NMR ($CHCl_3$): δ 7.67 (d, 1H, *J* = 12.2 Hz, CH), 6.94(s, 1H, NH), 5.86-5.95 (m, 1H, CH), 5.28-5.35 (m, 2H, CH_2), 5.22 (dd, 1H, *J* = 1.1, 5.2 Hz, CH), 3.89 (br d, 2H, *J* = 5.1 Hz, CH_2), 3.00 (br s, 6H, 2×CH_3), 2.56 (s, 3H, CH_3).

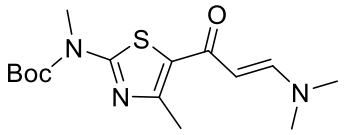

tert-Butyl-(5-(3-(dimethylamino) acryloyl)-4-methylthiazol-2-yl) (methyl)-carbamate (9)[168]

The title compound was synthesised following general procedure (7) using **8** (270 mg, 1 mmol, 1 eq) in DMF-DMA (5 mL) to yield yellow solid (211 mg, 65%). ^{1}H-NMR (DMSO-d_6): δ 7.63 (d, 1H, *J* = 12.2 Hz, CH), 5.33 (d, 1H, *J* = 12.2 Hz, CH), 3.44 (s, 3H, CH_3), 3.13 (br s, 3H, CH_3), 2.86 (br s, 3H, CH_3), 2.53 (s, 3H, CH_3), 1.53 (s, 9H, 3×CH_3).

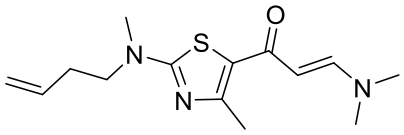

1-(2-(But-3-en-1-yl(methyl)-amino)-4-methylthiazol-5-yl)-3-(dimethyl-amino)prop-2-en-1-one (38)

The title compound was synthesised following general procedure (7) using **37** (224 mg, 1 mmol, 1 eq) in DMF-DMA (5 mL) to yield pale yellow solid (140 mg, 50%). ^{1}H-NMR ($CDCl_3$): δ 7.55 (d, 1H, *J* = 12.2 Hz, CH), 5.66-5.76 (m, 1H, CH), 5.22 (d, 1H, *J*

= 12.2 Hz, CH), 4.95-5.04 (m, 2H, CH_2), 3.44 (t, 2H, *J* = 7.1 Hz, CH_2), 3.00 (s, 3H, CH_3), 2.87 (br s, 6H, 2×CH_3), 2.50 (s, 3H, CH_3), 2.32 (dt, 2H, *J* = 14.5, 7.2 Hz, CH_2). MS (ESI^+): m/z $[M + H]^+$ calcd for $C_{14}H_{22}N_3OS$, 280.15, found 280.18.

7.2.11 Synthetic procedure for methyl 3-(2-(4-methyl-piperazine-1-carbonyl)-6-nitrophenyl)acrylate (92)

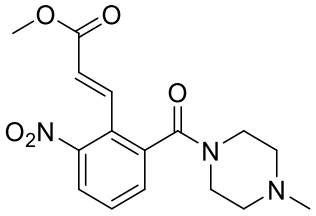

An oven dried rounded flask was charged with $Pd(OAc)_2$, PPh_3, K_2CO_3, **91** and methyl acrylate. DMF as the solvent was added in the flask and the mixture was heated at 100 ºC until TLC analysis indicated full consumption of the starting material. The reaction mixture was diluted with EtOAc and the organic layer washed with NH_4Cl, water, and brine. The concentrated organic extract was then purified by flash column chromatography (gradient DCM and MeOH as the eluting solvent) to afford the desired product. ^{1}H-NMR ($CDCl_3$) δ 7.99 (dd, 1H, *J* = 6.7, 2.8 Hz, CH), 7.79 (d, 1H, *J* = 16.1 Hz, Ph-H), 7.54-7.50 (m, 2H, Ph-2H), 6.13 (d, 1H, *J* = 16.1 Hz, CH), 3.32 (s, 3H, CH_3), 3.10 (t, 2H, *J* = 5.1 Hz, CH_2), 2.87-2.71 (m, 2H, CH_2), 2.33 (d, 4H, *J* = 57.9 Hz, 2×CH_2), 2.21 (s, 3H, CH_3).

7.2.12 Synthetic procedure for (5-(2-chloro-pyrimidin-4-yl)-2 methoxyphenyl)methanamine (96)

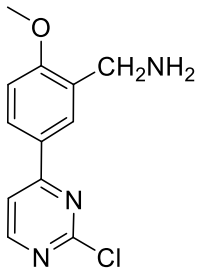

To a solution of **95** (248 mg, 1 mmol, 1 eq) in a saturated solution of NH_4OAc in EtOH (5 mL) were added $NaCNBH_3$ (192 mg, 3 mmol, 3 eq) and 30% aq NH3 (3 mL). The mixture was stirred at reflux for 18 h, cooled to room temperature, and concentrated under reduced pressure. The resulting reaction crude was then purified by flash column chromatography (PE and EtOAc) to afford the desired product (90 mg, 36%). ^{1}H NMR (DMSO-d_6) δ 8.78 (d, J = 5.2 Hz, Ph-H), 8.36 (d, J = 2.4 Hz, Ph-H), 8.25 (dd, J = 8.7, 2.4 Hz, Ph-H), 8.12 (d, J = 5.4 Hz, Ph-H), 7.26-7.23 (m, Ph-H), 4.02 (d, J = 1.3 Hz, CH_2), 3.93 (s, 3H, CH_3). ^{13}C-NMR ($CDCl_3$) δ 166.6, 161.8, 160.5, 159.5, 130.0, 128.7, 127.7, 127.4, 114.3, 110.6, 61.4, 55.7.

7.2.13 Synthetic procedure for phenyl borate derivatives

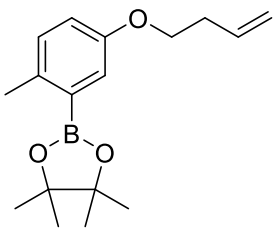

2-(5-(But-3-en-1-yloxy)-2-methylphenyl)-4,4,5,5-tetramethyl-1,3,2-

dioxaborolane (82)

Bis(pinacolato)diboran (128 mg, 2.2 mmol, 2 eq), Pd(dppf)Cl_2 (20 mg, 0.1 mmol, 0.05 eq), KOAc (134 mg, 6 mmol, 3 eq) were placed in a flask under argon. Then 2-bromo-4-(but-3-en-1-yloxy)-1-methylbenzene **81** (480 mg, 2 mmol, 1 eq) and dioxane (20 mL) were added. The reaction mixture was stirred under argon at 90°C overnight. The reaction mixture was filtered through a pad of Celite and washed with EtOAc. The solvent was evaporated to dryness to give the oil which was purified on a silica gel column to give the cream solid (230 mg, 40%). ^{1}H-NMR ($CDCl_3$) δ 7.37 (d, 1H, *J* = 2.9 Hz, Ph-H), 7.13 (d, 1H, *J* = 8.3 Hz, Ph-H), 6.93 (dd, 1H, *J* = 8.3, 2.9 Hz, Ph-H), 5.97 (ddt, 1H, *J* = 17.1, 10.3, 6.7 Hz, CH), 5.22 (ddt, 1H, *J* = 17.2, 3.4, 1.6 Hz, CH), 5.15 (ddt, 1H, *J* = 10.3, 3.0, 1.2 Hz, CH), 4.07 (t, 2H, *J* = 6.7 Hz, CH_2), 2.58 (dddt, 2H, *J* = 13.4, 6.7, 1.4 Hz, CH_2), 2.53 (s, 3H, CH_3), 1.39 (s, 12H, 4×CH_3).

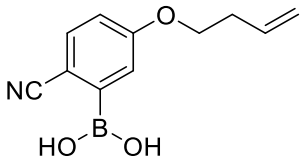

(5-(But-3-en-1-yloxy)-2-cyanophenyl)boronic acid (77)

n-BuLi (1.2 mL, 2 mmol, 2 eq) was added dropwise to a solution of compound 2-bromo-4-(but-3-en-1-yloxy)benzonitrile **76** (254 mg, 1 mmol, 1 eq) in anhydrous THF (5 mL) at -78°C. The mixture was stirred at this temperature for 30 min, then triisopropyl borate (350 ul, 1.5 mmol, 1.5 eq) was added and the mixture was stirred for 16 h while allowing the temperature to rise to 20°C. The HCl (24 mL, 2 M) was added, the organic layer separated, the aqueous layer extracted with diethyl ether (50 mL) three times, the

combined organic layer dried over $MgSO_4$, and concentrated under reduce pressure. The product was obtained as white solid by flash column chromatography (98 mg, 45%). ^{1}H NMR (Methanol-d_4) δ 7.66 (d, 1H, J = 8.6 Hz, Ph-H), 7.17 (s, 1H, Ph-H), 7.06 (dd, 1H, J = 8.6, 2.7 Hz, Ph-H), 6.02-5.90 (m, 1H, CH), 5.25-5.08 (m, 2H, CH_2), 4.13 (t, 2H, J = 6.6 Hz, CH_2), 2.57 (ddd, 2H, J = 6.6, 3.5, 2.0 Hz, CH_2). ^{13}C NMR (Methanol-d_4) δ 163.8, 161.5, 134.3, 134.2, 125.1, 116.1, 116.1, 114.8, 113.7, 67.2, 33.3.

7.2.14 General synthetic procedure (8) for Suzuki coupling (compounds 47, 62, 78, 95)

To a degassed solution of pyrimidine derivatives and phenylboronic acid in 1, 4-dioxane was added sequentially, potassium fluoride dihydrate and $Pd(PPh_3)_4$. The resulting mixture was stirred at 100 ºC overnight, cooled to room temperature and quenched with saturated NH_4Cl solution. The crude mixture was extracted with CH_2Cl_2 thrice, washed with brine, dried over Na_2SO_4. The concentrated organic extract was then purified by flash column chromatography (EtOAc/ Hexane) to furnish the desired product.

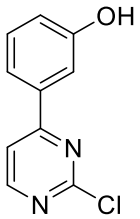

3-(2-Chloropyrimidin-4-yl) phenol (47)[184]

The title compound was synthesised following general procedure (8) using 2, 4-

dichloropyrimidine **46** (1480 mg, 10 mmol, 1 eq), 3-hydroxyphenylboronic acid (1650 mg, 12 mmol, 1.2 eq), potassium fluoride dihydrate (4240 mg, 40 mmol, 4 eq) and $Pd(PPh_3)_4$ (577.5 mg, 0.5 mmol, 0.05 eq) to furnish the white solid (1483 mg, 72%). ^{1}H-NMR ($CDCl_3$): δ 7.89 (d, 1H, *J* = 5.5 Hz, Ph-H), 7.26(s, 1H, Ph-H), 7.63 (t, 1H, *J* = 1.9 Hz, Ph-H), 7.65 (d, 1H, *J* = 5.2 Hz, Ph-H), 7.94 (t, 1H, *J* = 2.0 Hz, Ph-H), 7.98 (dd, 1H, *J* = 1.1, 1.6 Hz, Ph-H). RP-HPLC t_R = 2.44 min (Method 1, 95+ %), *m/z* $[M + H]^+$ calcd for $C_{27}H_{36}N_7S$, 207.1, found 207.1.

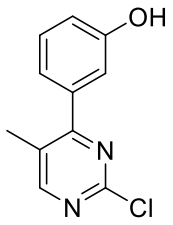

3-(2-Chloro-5-methylpyrimidin-4-yl)phenol (62)[184, 199]

The title compound was synthesised following general procedure (8) using 2,4-dichloro-5-methylpyrimidine **61** (160 mg, 1 mmol, 1 eq), 3-hydroxyphenyl-boronic acid (166 mg, 1.2 mmol, 1.2eq), potassium fluoride dihydrate (424 mg, 4 mmol, 4 eq) and $Pd(PPh_3)_4$ (100 mg, 0.1 mmol, 0.1 eq) in 1,4-dioxane (5 mL) to yield white solid (88 mg, 40%). RP-HPLC t_R = 2.57 min (Method 1, 95+ %), *m/z* $[M + H]^+$, calcd for $C_{11}H_{10}N_2OCl$, 221.0, found 221.0.

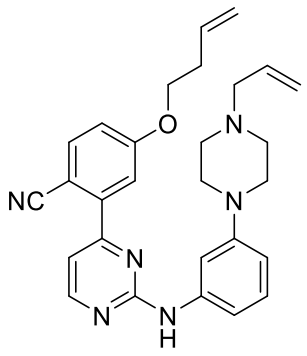

2-(2-((3-(4-Allylpiperazin-1-yl)phenyl)amino)pyrimidin-4-yl)-4-(but-3-en-1-yloxy)benzonitrile (78)

The title compound was synthesised following general procedure (8) using **73** (60 mg, 0.18 mmol, 1 eq), (5-(but-3-en-1-yloxy)-2-cyanophenyl)boronic acid **77** (45 mg, 0.21 mmol, 1.1 eq), sodium carbonate (40 mg, 0.36 mmol, 2 eq) and $Pd(PPh_3)_4$ (25 mg, 0.02 mmol, 0.1 eq) in toluene and ethane (1:1, 10 mL) to yield yellow solid (34 mg, 40%). ^{1}H-NMR ($CDCl_3$) δ 8.57 (d, 1H, *J* = 5.1 Hz, Ph-H), 7.75 (d, 1H, *J* = 8.6 Hz, Ph-H), 7.46 (d, 1H, *J* = 2.6 Hz, Ph-H), 7.42 (t, 1H, *J* = 2.2 Hz, Ph-H), 7.38 (s, 1H, NH), 7.27-7.21 (m, 2H, Ph-2H), 7.14 (dd, 1H, *J* = 7.8, 1.9 Hz, Ph-H), 7.06 (dd, 1H, *J* = 8.6, 2.6 Hz, Ph-H), 6.67 (dd, 1H, *J* = 8.1, 2.3 Hz, Ph-H), 5.99-5.85 (m, 2H, 2×CH), 5.29-5.14 (m, 4H, 2×CH_2), 4.14 (t, 2H, *J* = 6.7 Hz, CH_2), 3.31-3.25 (m, 4H, 2×CH_2), 3.09 (dt, 2H, *J* = 6.6, 1.3 Hz, CH_2), 2.67-2.58 (m, 6H, 3×CH_2). ^{13}C NMR ($CDCl_3$) δ 162.8, 162.2, 160.3, 159.1, 152.1, 143.2, 140.1, 136.2, 134.8, 133.6, 129.4, 118.7, 118.3, 117.7, 116.0, 115.9, 111.0, 110.8, 110.7, 107.4, 102.5, 67.8, 61.8, 53.1, 49.0, 33.3. RP-HPLC t_R = 2.40 min (Method 1, 95+ %), *m/z* $[M + H]^+$ calcd for $C_{28}H_{30}N_6O$, 467.3, found 467.4.

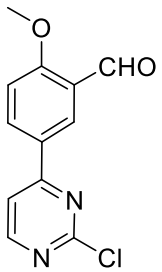

5-(2-Chloropyrimidin-4-yl)-2-methoxybenzaldehyde (95)[199]

The title compound was synthesised following general procedure (8) using phenylboronic acid **94** (360 mg, 2.0 mmol, 1 eq), 2,4-dichloropyrimidine (300 mg, 2

mmol, 1 eq), aqueous Na_2CO_3 (5 mL) and $Pd(PPh_3)_4$ (100 mg, 0.1 mmol, 0.05 eq) in toluene and ethane (1:1, 10 mL) to yield pale yellow solid (220 mg, 44%). ^{1}H-NMR ($CDCl_3$) δ 10.49 (s, 1H, CHO-H), 8.61 (d, 1H, *J* = 5.3 Hz, Ph-H), 8.48-8.44 (m, 2H, 2×Ph-H), 7.66 (d, 1H, *J* = 5.3 Hz, Ph-H), 7.14 (d, 1H, *J* = 9.2 Hz, Ph-H), 4.03 (s, 3H, CH_3).

7.2.15 Synthetic procedure for *N*-(3-(4-allylpiperazin-1-yl)phenyl)-4-(5-(but-3-en-1-yloxy)-2-methyl-phenyl)pyrimidin-2-amine (83)

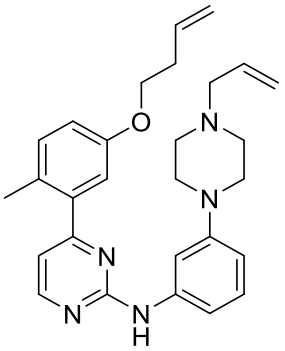

Dicyclohexyl(2,6-dimethoxy-[1,1-biphenyl]-2-yl)phosphine(SPhos) (22 mg, 0.05 mmol, 0.25 eq) and tris(dibenzylideneacetone)dipalladium(0) (20 mg, 0.02 mmol, 0.1 eq) were combined in a pressure vessel. To this was added dry 1,4-dioxane (1 mL), and the mixture was stirred for 20 min. In a separate flask were dissolved **73** (70 mg, 0.21 mmol, 1 eq) and 2-(5-(but-3-en-1-yloxy)-2-methylphenyl)-4,4,5,5-tetramethyl-1,3,2-dioxaborolane **82** (66 mg, 0.23 mmol, 1.1 eq) in dioxane (1 mL). The starting materials were then added to the preformed catalyst, followed by potassium phoshate tribasic (4 mL). The vessel was sealed and heated with microwave irradiation to 150 ºC for 20 min. The reaction was concentrated and purified by column chromatography (DCM/MeOH)

to afford pale yellow solid (52 mg, 55%). ^{1}H-NMR ($CDCl_3$) δ 8.47 (d, 1H, *J* = 5.0 Hz, Ph-H), 7.89 (ddd, 1H, *J* = 11.0, 7.8, 1.5 Hz, Ph-H), 7.53 (ddt, 1H, *J* = 8.9, 7.4, 1.6 Hz, Ph-H), 7.46 (s, 1H, NH), 7.33 (t, 1H, *J* = 8.4 Hz, Ph-H), 7.21 (dd, 1H, *J* = 8.2, 3.4 Hz, Ph-H), 7.11 (dd, 1H, *J* = 7.9, 2.0 Hz, Ph-H), 7.06 (d, 1H, *J* = 2.7 Hz, Ph-H), 6.92 (dd, 1H, *J* = 8.4, 2.7 Hz, Ph-H), 6.85 (d, 1H, *J* = 5.0 Hz, Ph-H), 5.99-5.87 (m, 2H, 2×CH), 5.25-5.09 (m, 4H, 2×CH_2), 4.06 (t, 2H, *J* = 6.7 Hz, CH_2), 3.29-3.23 (m, 4H, 2×CH_2), 3.09 (dt, 2H, *J* = 6.6, 1.3 Hz, CH_2), 2.63 (t, 4H, *J* = 5.0 Hz, 2×CH_2), 2.57 (qt, 2H, *J* = 6.8, 1.4 Hz, CH_2), 2.38 (s, 3H, CH_3). ^{13}C NMR ($CDCl_3$) δ 167.9, 159.9, 157.8, 157.1, 152.0, 140.4, 134.4, 132.0, 129.4, 129.2, 127.8, 118.2, 117.0, 115.6, 115.3, 112.4, 110.7, 110.3, 107.0, 103.4, 67.4, 61.8, 55.6, 53.4, 53.1, 49.0, 33.7, 19.6. RP-HPLC t_R = 2.42 min (Method 1, 90+ %), m/z $[M + H]^+$, calcd for $C_{28}H_{33}N_5O$, 456.3, found 456.5.

7.2.16 General synthetic procedure (9) for 2, 4-di-substituted pyrimidine derivatives (compounds 73, 57)

2,4-Dichloroethane derivative was stirred in *t*-BuOH and 1, 2-dichloroethane at 0 ºC and 1.0 M $ZnCl_2$ solution in diethyl ether was added cautiously over 20 minutes. The reaction was left stirring at 0 ºC for 30 mins. A solution of amine in *t*-BuOH and 1,2-dichloroethane (1:1) was added drop-wise over 15 mins at 0 ºC followed by a solution of trimethylamine in *t*-BuOH and 1,2-dichloroethane (1:1) and the reaction was warm at RT for 18 h. The resulting mixture was quenched with water and extracted with CH_2Cl_2 thrice. Then the combined organic extracts were washed with saturated $NaHCO_3$

followed by brine, dried over Na_2SO_4, and concentrated under reduced pressure to furnish the oil, which was purified by column chromatography (gradient DCM and MeOH as the eluting solvent) to afford the desired product.

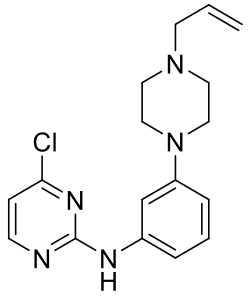

N-(3-(4-Allylpiperazin-1-yl)phenyl)-4-chloropyrimidin-2-amine (62)

The title compound was synthesised following general procedure (9) using 2,4-dichloroethane **46** (30 mg, 0.2 mmol, 1 eq), 1.0 M $ZnCl_2$ solution in diethyl ether (200 µL), **31** (43 mg, 0.2 mmol, 1 eq) and trimethylamine (100 µL) in t-BuOH and 1,2-dichloroethane (1:1, 4 mL) to afford yellow solid (23 mg, 35%). ^{1}H-NMR ($CDCl_3$) δ 8.26 (d, 1H, *J* = 5.2 Hz, Ph-H), 7.45 (s, 1H, Ph-H), 7.29 (t, 1H, *J* = 2.3 Hz, Ph-H), 7.21 (t, 1H, *J* = 8.1 Hz, Ph-H), 7.00 (dd, 1H, *J* = 7.9, 2.0 Hz, Ph-H), 6.71 (d, 1H, *J* = 5.2 Hz, Ph-H), 6.65 (dd, 1H, *J* = 8.3, 2.3 Hz, Ph-H), 5.90 (ddt, 1H, *J* = 16.8, 10.1, 6.6 Hz, CH), 5.28-5.16 (m, 2H, CH_2), 3.28-3.21 (m, 4H, 2×CH_2), 3.06 (dd, 2H, *J* = 6.6, 1.5 Hz, CH_2), 2.65-2.58 (m, 4H, 2×CH_2). ^{13}C NMR ($CDCl_3$) δ 161.2, 159.9, 159.0, 152.1, 139.4, 134.9, 129.5, 118.2, 111.9, 111.2, 111.1, 107.5, 61.8, 53.0, 48.9. RP-HPLC t_R = 2.03 min (Method 1, 90+ %), *m/z* $[M + H]^+$, calcd for $C_{17}H_{21}N_5Cl$, 330.2, found 330.3.

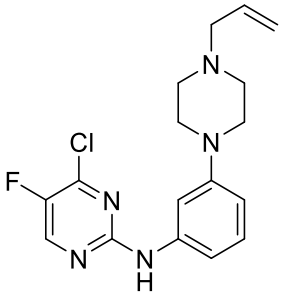

N-(3-(4-Allylpiperazin-1-yl)phenyl)-4-chloro-5-fluoropyrimidin-2-amine (57)

The title compound was synthesised following general procedure (9) using 2,4-dichloro-5-fluoropyrimidine **56** (148 mg, 1 mmol, 1 eq), 1.0 M $ZnCl_2$ solution in diethyl ether (1 mL), **31** (217 mg, 1 mmol, 1 eq) and triethylamine (0.5 mL) in butanol and 1,2-dichloroethane (10 mL) to afford pale yellow solid (270 mg, 78 %). ^{1}H-NMR ($CDCl_3$) δ 8.02 (d, 1H, *J* = 2.8 Hz, Ph-H), 7.34 (t, 1H, *J* = 2.3 Hz, Ph-H), 7.23 (t, 1H, *J* = 8.1 Hz, Ph-H), 7.04-6.98 (m, 2H, 2×Ph-H), 6.72 (dd, 1H, *J* = 8.3, 2.4 Hz, Ph-H), 5.90 (ddt, 1H, *J* = 16.8, 10.1, 6.6 Hz, CH), 5.27-5.16 (m, 2H, CH_2), 3.25 (dd, 4H, *J* = 6.2, 3.9 Hz, 2×CH_2), 3.06 (dd, 2H, *J* = 6.6, 1.5 Hz, CH_2), 2.65-2.57 (m, 4H, 2×CH_2). ^{13}C-NMR ($CDCl_3$) δ 152.0, 146.3, 143.8, 140.9, 140.7, 137.7, 134.8, 129.7, 118.3, 112.4, 111.5, 108.1, 61.8, 52.9, 48.8. RP-HPLC t_R = 1.92 min (Method 1, 90+ %), *m/z* $[M + H]^+$ calcd for $C_{17}H_{20}N_5ClF$, 348.1, found 348.1.

7.2.17 Synthetic procedure for *N*-(3-(4-allylpiperazin-1-yl)phenyl)-2-chloropyrimidin-4-amine (101)

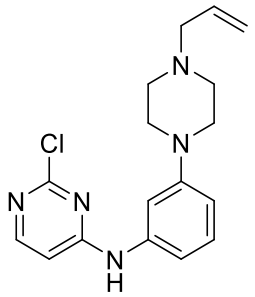

To a solution of 2, 4-dichloropyrimidine **46** (148 mg, 1 mmol, 1 eq) and triethylamine (284 mg, 2 mmol, 2 eq) in ethanol (10 mL) at 0 °C, **31** (217 mg, 1 mmol, 1 eq) was added. The reaction mixture was stirred at RT for 2 h. After completion of the reaction as observed by TLC, excess ethanol was evaporated and the reaction mixture was diluted with water. The solid thus obtained was filtered and washed with excess water. The crude product was purified by column chromatography using EtOAc/Hexane as eluent to afford yellow solid (230 mg, 70%). ^{1}H-NMR ($CDCl_3$) δ 8.05 (d, 1H, *J* = 5.9 Hz, Ph-H), 7.69 (d, 1H, *J* = 7.5 Hz, Ph-H), 7.24 (t, 1H, *J* = 8.9 Hz, Ph-H), 6.83 (s, 1H, NH), 6.80-6.68 (m, 2H, 2×Ph-H), 6.57 (d, 1H, *J* = 6.0 Hz, Ph-H), 5.92-5.83 (m, 1H, CH), 5.23-5.16 (m, 2H, CH_2), 3.20 (t, 4H, *J* = 4.9 Hz, 2×CH_2), 3.04 (d, 2H, *J* = 6.4 Hz, CH_2), 2.61-2.57 (m, 4H, 2×CH_2). RP-HPLC t_R = 1.94 min (Method 1, 95+ %), *m/z* $[M + H]^+$ calcd for $C_{17}H_{21}N_5Cl$, 330.2, found 330.3.

7.2.18 General synthetic procedure (10) for pyrimidine derivatives (compounds 53, 52, 64)

To a mixture of 2-chloro-pyrimidine derivatives, aniline derivatives in n-butanol at ambient temperature was added 4M HCl and the resulting mixture was stirred at 100 ºC overnight. The reaction mixture was cooled to 0 ºC and quenched with water. The product was extracted with CH_2Cl_2 thrice, and the combined organic extracts were washed with saturated $NaHCO_3$ followed by brine, dried over Na_2SO_4, and concentrated under reduced pressure to furnish the oil, which was purified by flash column chromatography to afford the desired product.

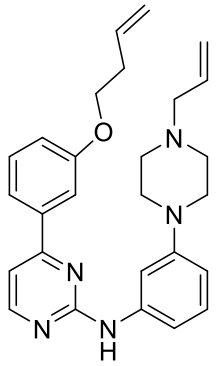

N-(3-(4-Allylpiperazin-1-yl)-phenyl)-4-(3-(but-3-en-1-yloxy)phenyl)-pyrimidin-2-amine (53)

The title compound was synthesised following general procedure (10) using **31** (100 mg, 0.41 mmol, 1 eq), **48** (133 mg, 0.62 mmol, 1.5 eq) and 4M HCl (2 mL) in n-butanol (6 mL) to afford pale brown solid (67 mg, 37%). ^{1}H-NMR ($CDCl_3$): δ 2.58 (dt, 2H, J = 1.3, 6.7 Hz, CH_2), 2.63 (br t, 4H, J = 5.2 Hz, 2×CH_2), 3.07 (d, 2H, J = 6.5 Hz, CH_2), 3.28 (br t, 4H, J = 4.9 Hz, 2×CH_2), 4.10 (t, 2H, J = 6.8 Hz, CH_2), 5.11-5.26 (m, 4H,

2×CH_2), 5.88-5.96 (m, 2H, 2×CH), 6.63 (dd, 1H, *J* = 1.8, 8.3 Hz, Ph-H), 7.03 (ddd, 1H, *J* = 0.8, 2.5, 8.2 Hz, PH-H), 7.10 (dd, 1H, *J* = 1.3, 8.0 Hz, Ph-H), 7.12 (d, 1H, *J* = 5.2, Ph-H), 7.22 (t, 1H, *J* = 8.1Hz, Ph-H), 7.27 (s, 1H, NH), 7.38 (t, 1H, *J* = 8.0 Hz, Ph-H), 7.50 (t, 1H, *J* = 2.1 Hz, Ph-H), 7.64 (br d, 1H, *J* = 7.7 Hz, Ph-H), 7.66 (br t, 1H, *J* = 2.4 Hz, Ph-H), 8.45 (d, 1H, *J* = 5.2 Hz, Ph-H). RP-HPLC t_R = 2.38 min (Method 1, 95+ %), m/z $[M + H]^+$ calcd for $C_{27}H_{32}N_5O$, 442.2, found 442.2.

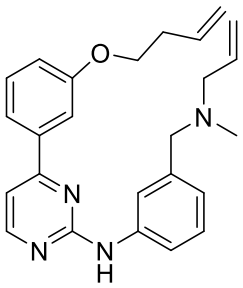

N-(3-((Allyl(methyl)amino)-methyl)phenyl)-4-(3-(but-3-en-1-yloxy)-phenyl)-pyrimidin-2-amine (52)

The title compound was synthesised following general procedure (10) using **48** (260 mg, 1 mmol, 1 eq), **51** (264 mg, 1.5 mmol, 1.5 eq) and 4 M HCl (4 mL) in 12 mL *n*-Butanol to afford a pale brown solid (84 mg, 21%). ^{1}H-NMR ($CDCl_3$): δ 2.26 (s, 3H, CH_3), 2.60 (q, 2H, *J* = 6.9 Hz, CH_2), 3.11 (d, 2H, *J* = 6.4 Hz, CH_2), 3.57 (s, 2H, CH_2), 4.11 (t, 2H, *J* = 6.6 Hz, CH_2), 5.12-5.25 (m, 4H, 2×CH_2), 5.89-6.00 (m, 2H, 2×CH), 7.04 (dd, 1H, *J* = 2.9, 8.0 Hz, Ph-H), 7.03 (ddd, 1H, *J* = 0.8, 2.5, 8.2 Hz, PH-H), 7.10 (dd, 1H, *J* = 1.3, 8.0 Hz, Ph-H), 7.14 (d, 1H, *J* = 5.2 Hz, Ph-H), 7.31 (t, 1H, *J* = 7.8 Hz, Ph-H), 7.39 (t, 1H, *J* = 8.0 Hz, Ph-H), 7.65 (br d, 2H, *J* = 7.1, 2×Ph-H), 7.68 (br t, 1H, *J* = 2.4 Hz, Ph-H), 7.71 (d, 1H, *J* = 7.7 Hz, Ph-H), 8.46 (d, 1H, *J* = 8.5 Hz, Ph-H). ^{13}C-NMR ($CDCl_3$): δ 14.2, 20.9, 33.6, 41.9, 60.4, 61.5, 67.3, 108.4, 113.0, 117.1, 117.2, 117.9,

118.1, 119.5, 119.9, 123.2, 128.7, 129.8, 134.3, 135.4, 138.5, 139.2, 139.8, 158.5, 159.4, 160.3, 164.7, 171.1. RP-HPLC t_R = 2.32 min (Method 1, 95+ %), *m/z* $[M + H]^+$ calcd for $C_{25}H_{29}N_4O$, 401.2, found 401.1.

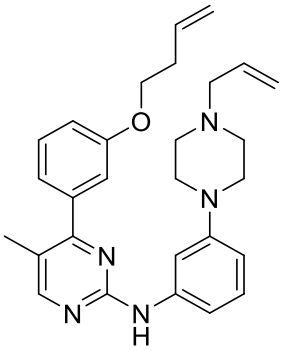

N-(3-(4-Allylpiperazin-1-yl)phenyl)-4-(3-(but-3-en-1-yloxy)phenyl)-5-methylpyrimidin-2-amine (64)

The title compound was synthesised following general procedure (10) using 4-(3-(but-3-en-1-yloxy)phenyl)-2-chloro-5-methylpyrimidine **63** (120 mg, 0.44 mmol, 1 eq), 3-(4-allylpiperazin-1-yl)aniline **31** (142 mg, 0.65 mmol, 1.5 eq) and 4 M HCl (6 mL) in 12 mL butanol to afford pale brown solid (70 mg, 35 %). ^{1}H-NMR ($CDCl_3$) δ 8.30 (s, 1H, Ph-H), 7.60 (s, 1H, NH), 7.37 (t, 1H, *J* = 8.0 Hz, Ph-H), 7.20 (dd, 1H, *J* = 2.7, 1.5 Hz, 1H), 7.18 (tt, 1H, *J* = 4.8, 2.1 Hz, 3H), 6.99 (ddd, 1H, *J* = 6.9, 2.7, 1.4 Hz, 2H), 6.56 (dd, 1H, *J* = 8.2, 2.4 Hz, 1H), 5.98-5.88 (m, 2H, 2×CH), 5.22-5.09 (m, 4H, 2×CH_2), 4.07 (t, 2H, *J* = 6.7 Hz, CH_2), 3.36 (br s, 4H, 2×CH_2), 2.79 (br s, 4H, 2×CH_2), 2.61-2.54 (m, 4H, 2×CH_2), 2.27 (s, 3H, CH_3). RP-HPLC t_R = 2.43 min (Method 1, 95+ %), *m/z* $[M + H]^+$ calcd for $C_{28}H_{34}N_5O$, 456.3, found 456.6.

7.2.19 General synthetic procedure (11) for pyrimidine derivatives (compounds 14, 33, 39, 55, 71)

The mixture of guanidine and enaminone in 2-methoxyethanol were heated under microwave condition at 140 °C for 60 mins. The reaction mixture was concentrated to dryness and purified by flash column chromatography to give the desired product.

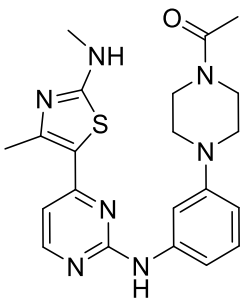

1-(4-(3-((4-(4-Methyl-2-(methylamino) thiazol-5-yl) pyrimidin-2-yl) amino) phenyl) piperazin-1-yl) ethanone (14)

The title compound was synthesised following general procedure (11) using guanidine **13** (522 mg, 2mmol, 1 eq) and enaminone **9** (450 mg, 2 mmol, 1 eq) in 2-methoxyethanol (3 mL) to give pale yellow solid (507 mg, 60%). ^{1}H-NMR (DMSO-d_6): δ 2.04 (s, 3H, CH_3), 2.43 (s, 3H, CH_3), 2.81 (s, 3H, CH_3), 3.10 (br t, 2H, J = 5.1 Hz, CH_2), 3.16 (br t, 2H, J = 6.8 Hz, CH_2), 3.59 (br q, 4H, J = 5.6 Hz, 2×CH_2), 5.22 (d, 1H, J = 11.8 Hz, NH), 6.56 (dd, 1H, J = 1.9, 6.2 Hz, Ph-H), 6.89 (d, 1H, J = 5.7 Hz, PH-H), 7.12 (t, 1H, J = 8.1, Ph-H), 7.23 (dd, 1H, J = 1.0, 7.1 Hz, Ph-H), 7.51 (d, 1H, J = 12.15 Hz, Ph-H), 8.32 (d, 1H, J = 5.2 Hz, Ph-H), 9.29 (s, 1H, NH). ^{13}C-NMR (DMSO-d_6): δ 18.5, 21.4, 31.1, 41.2, 45.9, 49.1, 49.6, 94.0, 107.1, 109.9, 111.0, 118.4, 121.9, 129.2, 141.8, 151.7, 152.8, 153.7, 157.9, 160.0, 168.9, 179.9. MS (ESI$^+$): *m/z* [M + H] + calcd

for $C_{21}H_{26}N_7OS$, 424.19, found 424.19. RP-HPLC t_R = 2.13 min (Method 1, 90+ %), *m/z* $[M + H]^+$ calcd for $C_{25}H_{29}N_4O$, 424.2, found 424.3.

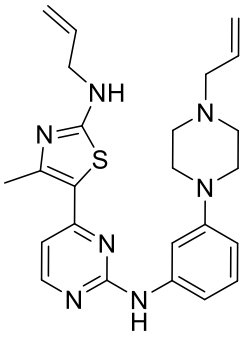

N-Allyl-5-(2-((3-(4-allylpiperazin-1-yl)phenyl)amino)pyrimidin-4-yl)-4-methylthiazol-2-amine (33)

The title compound was synthesised following general procedure (11) using **28** (518 mg, 2 mmol, 1 eq) and guanidine **32** (502 mg, 2 mmol, 1 eq) in DMA (3 mL) at 200 °C to yield yellow solid (384 mg, 45%). ^{1}H-NMR ($CDCl_3$): δ 2.53 (s, 3H, CH_3), 2.62 (br t, 4H, *J* = 4.8 Hz, 2×CH_2), 3.64 (d, 2H, *J* = 6.8 Hz, CH_2), 3.28 (br t, 4H, *J* = 4.8 Hz, 2×CH_2), 3.93 (br d, 2H, *J* = 5.5 Hz, CH_2), 5.26 (s, 1H, NH), 5.18-5.38 (m, 4H, 2×CH_2), 5.86-5.98 (m, 2H, 2×CH), 6.30 (dd, 1H, *J* = 1.9, 8.2 Hz, Ph-H), 6.82 (d, 1H, *J* = 5.5 Hz, PH-H), 7.05 (dd, 1H, *J* = 1.3, 7.9 Hz, Ph-H), 7.21 (t, 1H, *J* = 8.0, Ph-H), 7.37 (br t, 1H, *J* = 2.0, Ph-H), 7.60 (s, 1H, NH), 8.29 (d, 1H, *J* = 5.4 Hz, Ph-H). ^{13}C-NMR ($CDCl_3$): δ 18.7, 48.4, 49.2, 53.2, 61.8, 107.2, 107.3, 110.4, 111.1, 117.5, 118.2, 119.7, 129.2, 133.0, 134.9, 140.6, 151.8, 152.0, 157.3, 159.4, 159.7, 170.3. RP-HPLC t_R = 2.29 min (Method 1, 90+ %), *m/z* $[M + H]^+$ calcd for $C_{26}H_{29}N_5O$, 428.2, found 428.2.

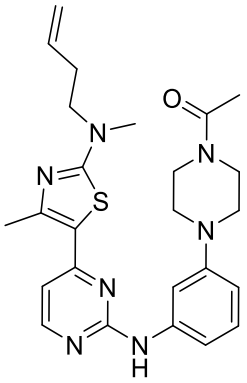

28

1-(4-(3-((4-(2-(But-3-en-1-yl(methyl-)amino)-4-methylthiazol-5-yl)-pyrimidin-2-yl)amino)phenyl)piperazin-1-yl)ethanone (39)

The title compound was synthesised following general procedure (11) using **38** (558 mg, 2 mmol, 1 eq) and guanidine **13** (574 mg, 2.2 mmol, 1.1 eq) in 2-methoxyethanol (15 mL) to yield pale brown solid (391 mg, 41%). ^{1}H-NMR ($CDCl_3$): δ 2.11 (s, 3H, CH_3), 2.41 (q, 2H, *J* = 7.2, 2H), 2.54 (s, 3H, CH_3), 3.10 (s, 3H, CH_3), 3.19 (br t, 4H, *J* = 4.9 Hz, 2×CH_2), 3.55 (br t, 4H, *J* = 4.9 Hz, 2×CH_2), 3.75 (t, 2H, *J* = 5.3 Hz, CH_2), 5.04-5.13 (m, 2H, CH_2), 5.74-5.84 (m, 1H, CH), 6.60 (dd, 1H, *J* = 3.9, 8.4 Hz, Ph-H), 6.81 (d, 1H, *J* = 5.6 Hz, PH-H), 7.05 (dd, 1H, *J* = 3.9, 8.1 Hz, Ph-H), 7.19 (t, 1H, *J* = 8.1, Ph-H), 7.42 (br t, 1H, *J* = 2.0, Ph-H), 7.74 (s, 1H, NH), 8.27 (d, 1H, *J* = 5.6 Hz, Ph-H). ^{13}C-NMR ($CDCl_3$): δ 19.0, 21.3, 31.5, 38.2, 41.4, 46.2, 49.4, 49.8, 52.4, 107.3, 107.5, 110.7, 111.6, 117.4, 119.5, 129.3, 134.8, 140.9, 151.6, 153.2, 157.2, 159.6, 159.7, 168.9, 169.6. RP-HPLC t_R = 2.52 min (Method 1, 80+ %), m/z $[M + H]^+$ calcd for $C_{25}H_{32}N_7OS$, 478.2, found 478.2.

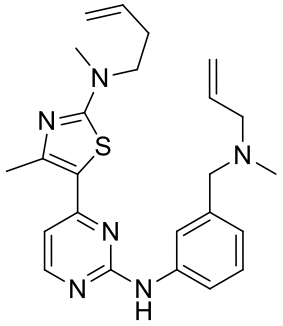

5-(2-((3-((Allyl(methyl)amino)methyl)-phenyl)amino)-pyrimidin-4-yl)-*N*-(but-3-en-1-yl)-*N*,4-dimethylthiazol-2-amine (55)

The title compound was synthesised following general procedure (11) using **38** (279 mg, 1 mmol, 1 eq) and guanidine **54** (218 mg, 1 mmol, 1 eq) in DMA (5 mL) at 200 ºC to yield yellow solid (170 mg, 40%). ^{1}H-NMR ($CDCl_3$): δ 2.21 (s, 3H, CH_3), 2.45 (q, 2H, *J* = 7.2, CH_2), 2.56 (s, 3H, CH_3), 3.05 (d, 2H, *J* = 6.4, CH_2), 3.14 (s, 3H, CH_3), 3.52 (s, 2H, CH_2), 3.58 (t, 2H, *J* = 7.5 Hz, CH_2), 5.07-5.22 (m, 4H, 2×CH_2), 5.78-5.96 (m, 2H, 2×CH), 6.82 (d, 1H, *J* = 5.6 Hz, Ph-H), 7.00 (d, 1H, *J* = 7.5 Hz, PH-H), 7.16 (s, 1H, Ph-H), 7.28 (t, 1H, *J* = 7.7 Hz, Ph-H), 7.57 (dd, 1H, *J* = 1.4, 8.0 Hz, Ph-H), 7.60 (s, 1H, NH), 8.27 (d, 1H, *J* = 5.5 Hz, Ph-H). RP-HPLC t_R = 2.14 min (Method 1, 95+ %), *m/z* $[M + H]^+$ calcd for $C_{24}H_{31}N_6S$, 435.2, found 435.2.

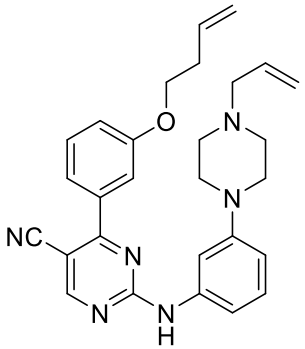

2-((3-(4-Allylpiperazin-1-yl)phenyl)amino)-4-(3-(but-3-en-1-yloxy)phenyl)-pyrimidine-5-carbonitrile (71)

The title compound was synthesised following general procedure (11) using enaminone **70** and guanidine **32** (280 mg, 1.1 mmol, 1 eq) in 2-methoxyethanol (2 mL) at 140 ºC to yield yellow solid (163 mg, 35%). ^{1}H-NMR ($CDCl_3$) δ 8.68 (s, 1H, NH), 7.66 (d, 1H, *J* = 7.8 Hz, Ph-H), 7.59 (d, 2H, *J* = 6.8 Hz, 2×Ph-H), 7.42 (t, 2H, *J* = 8.0 Hz, 2×Ph-H), 7.25 (d, 1H, *J* = 8.9 Hz, Ph-H), 7.10 (ddd, 1H, *J* = 8.2, 2.5, 0.9 Hz, Ph-H), 7.01 (dd, 1H, *J* = 7.9, 2.1 Hz, Ph-H), 6.71 (dd, 1H, *J* = 8.3, 2.3 Hz, Ph-H), 5.96-5.86 (m, 2H, 2×CH), 5.23-5.09 (m, 4H, 2×CH_2), 4.10 (t, 2H, *J* = 6.7 Hz, CH_2), 3.28-3.22 (m, 4H, 2×CH_2), 3.07 (dd, 2H, *J* = 6.6, 1.4 Hz, CH_2), 2.61 (dd, 4H, *J* = 5.9, 4.2 Hz, 2×CH_2), 2.58 (dt, 2H, *J* = 6.7, 1.5 Hz, CH_2). ^{13}C NMR ($CDCl_3$) δ 168.2, 163.3, 159.8, 159.2, 152.1, 138.7, 136.8, 134.7, 134.3, 129.9, 129.6, 121.1, 118.5, 118.4, 117.4, 117.3, 114.4, 111.8, 107.9, 95.9, 67.5, 61.8, 52.9, 48.9, 33.6. HPLC t_R = 2.46 min (Method 1, 95+ %), *m/z* $[M + H]^+$ calcd for $C_{28}H_{31}N_6O$, 467.3, found 467.3.

7.2.20 Synthetic procedure for 2-bromo-4-hydroxybenzonitrile (75)[200]

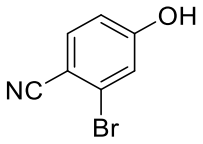

To a stirring solution of 2-bromo-4-fluoro-benzonitrile **74** (198 mg, 1 mmol, 1 eq) in DMF (5 mL) was added 2-(methylsulfonyl-ethanol) (186 mg, 1.5 mmol, 1.5 eq) and the solution cooled to 0 °C. Sodium hydride (120 mg, 3 mmol, 3 equiv.) was added and the reaction mixture allowed to be stirred at RT. The mixture was quenched with a 1 M HCl solution and partitioned between ethyl acetate and brine. The organic layer was

concentrated to dryness and the crude organics purified by flash column chromatography to afford pale orange solid (176 mg, 90%). ^{1}H NMR (DMSO-d_6) δ 11.10 (s, 1H, OH), 7.72 (d, 1H, J = 8.6 Hz, Ph-H), 7.18 (d, 1H, J = 2.3 Hz, Ph-H), 6.91 (dd, 1H, J = 8.6, 2.4 Hz, Ph-H).

7.2.21 General synthetic procedure (12) for acetamide derivatives (compounds 15 and 40)

A mixture of acetamide derivative and 2 M HCl in methanol was heated and refluxed overnight. Upon completion, the reaction mixture was neutralised by Na_2CO_3 solution and extracted with $CHCl_3$ to afford the desired product.

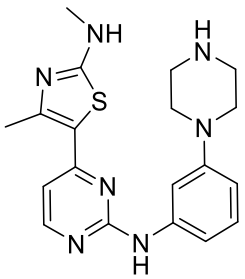

N, 4-Dimethyl-5-(2-((3-(piperazin-1-yl)phenyl)amino)-pyrimidin-4-yl)thiazol-2-amine (15)[168]

The title compound was synthesised following general procedure (13) using **14** (423 mg, 1 mmol) and 2 M HCl (4 mL) in methanol (10 mL) to afford a yellow solid (342 mg, 90%). ^{1}H-NMR (DMSO-d_6): δ 2.46 (s, 3H, CH_3), 2.86 (br d, 7H, CH_3 & 2×CH_2), 3.06 (br t, 4H, J = 4.5 Hz, 2×CH_2), 6.52 (d, 1H, J = 7.7 Hz, Ph-H), 6.88 (d, 1H, J = 5.5 Hz, Ph-H), 7.08 (t, 1H, J = 8.0, Ph-H), 7.19 (d, 1H, J = 8.2 Hz, Ph-H), 7.42 (s, 1H, Ph-H), 8.05 (br d, 1H, J = 4.5 Hz, NH), 8.31 (d, 1H, J = 5.4 Hz, Ph-H), 9.23 (s, 1H, NH).

^{13}C-NMR (DMSO-d_6): δ 19.1, 31.3, 45.9, 50.1, 106.6, 107.1, 109.4, 110.4, 118.4, 129.2, 141.7, 152.5, 152.7, 158.1, 159.0, 160.0, 169.8. MS (ESI$^+$): *m/z* [M + H]$^+$ calcd for $C_{19}H_{24}N_7S$ 382.18, found 382.13. RP-HPLC t_R = 1.79 min (Method 1, 95+ %), *m/z* [M + H]$^+$ calcd for $C_{19}H_{24}N_7S$, 382.2, found 382.2.

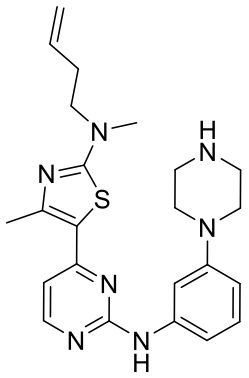

N-(But-3-en-1-yl)-N,4-dimethyl-5-(2-((3-(piperazin-1-yl)phenyl)-amino)-pyrimidin-4-yl)thiazol-2-amine (40)

The title compound was synthesised following general procedure (13) using **39** (2.05 g, 4.3 mmol) and 2 M HCl (10 mL) in methanol (30 mL) to afford a brown solid (1833 mg, 98 %). ^{13}C-NMR ($CDCl_3$): δ 18.9, 31.5, 38.2, 46.2, 50.5, 52.5, 107.1, 107.3, 111.0, 117.4, 119.6, 129.3, 134.8, 140.6, 152.5, 152.9, 157.2, 159.6, 159.7, 169.7. RP-HPLC t_R = 2.10 min (Method 1, 95+ %), *m/z* [M + H]$^+$ calcd for $C_{23}H_{30}N_7S$, 436.2, found 436.1.

7.2.22 General synthetic procedure (13) for amide coupling (compounds 16c, 16b, 16a)

To a solution of 2-chloro-4, 6-dimethoxy-1, 3, 5-triazine in CH_2Cl_2, *N*-methyl-morpholine was added at 0-5 °C under continuous stirring. A white suspension was

formed after 30-40 min and to this mixture carboxylic acid in CH_2Cl_2 (10 mL) was added resulting in the formation of a clear solution. After stirring the mixture for 1 h, amines were added at RT. After completion of the reaction, the mixture was washed with diluted HCl solution and the aqueous extract was concentrated to furnish the desired product.

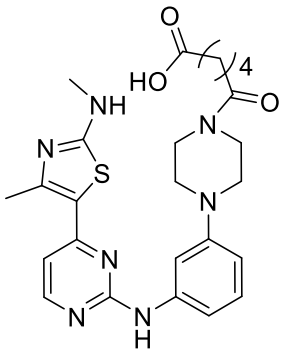

6-(4-(3-((4-(4-Methyl-2-(methylamino) thiazol-5-yl) pyrimidin-2-yl) amino) phenyl) piperazin-1-yl)-6-oxohexanoic acid (16c)

The title compound was synthesised following general procedure (13) using 2-chloro-4, 6-dimethoxy-1, 3, 5-triazine (88 mg, 0.5 mmol), *N*-methyl-morpholine (152 mg, 1.5 mmol), adipic acid (73 mg, 0.5 eq) and compound **15** (190 mg, 0.5 mmol) in CH_2Cl_2 (10 mL) to afford a pale green solid (249 mg, 98%). ^{1}H-NMR (DMSO-d_6): δ 1.75 (br s, 4H, J = 7.6, 2×CH_2), 2.42 (br d, 4H, J = 7.6, 2×CH_2), 2.50 (s, 3H, CH_3), 2.99 (s, 3H, CH_3), 3.24 (br s, 4H, 2×CH_2), 3.64 (br t, 2H, J = 3.2 Hz, CH_2), 3.79 (br t, 2H, J = 4.8 Hz, CH_2), 4.07 (s, 1H, NH), 6.30 (dd, 1H, J = 1.9, 8.1 Hz, Ph-H), 6.78 (d, 1H, J = 5.6 Hz, PH-H), 7.03 (dd, 1H, J = 1.4, 7.9 Hz, Ph-H), 7.23 (t, 1H, J = 8.0, Ph-H), 7.55 (br t, 1H, J = 1.6, Ph-H), 8.17 (d, 1H, J = 5.2 Hz, Ph-H), 8.67 (s, 1H, NH). MS (ESI$^+$): *m/z* $[M + H]^+$ calcd for $C_{25}H_{32}N_7O_3S$, 510.22, found 510.15.

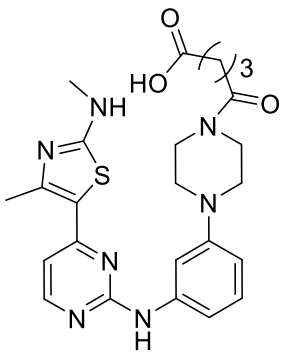

5-(4-(3-((4-(4-Methyl-2-(methylamino)thiazol-5-yl)pyrimidin-2-yl)amino)-phenyl)piperazin-1-yl)-5-oxopentanoic acid (16b)

The title compound was synthesised following general procedure (13) using **15** (380 mg, 1 mmol, 1 eq) and glutaric acid (132 mg, 1 mmol, 1 eq) to yield pale green solid (445 mg, 90%). MS (ESI^+): m/z $[M + H]^+$ calcd for $C_{24}H_{30}N_7O_3S$ 496.21, found 496.16. RP-HPLC t_R = 2.22 min (Method 1, 90 %), *m/z* $[M + H]^+$ calcd for $C_{24}H_{30}N_7O_3S$, 496.2, found 496.1.

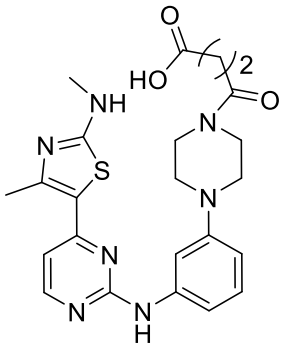

3-(4-(3-((4-(4-Methyl-2-(methylamino)thiazol-5-yl)pyrimidin-2-yl)amino)-phenyl)piperazin-1-yl)-3-oxopropanoic acid (16a)

The title compound was synthesised following general procedure (13) using **15** (380 mg, 1 mmol, 1 eq) and succinic acid (118 mg, 1 mmol, 1 eq) to yield pale green solid (457 mg, 95%). MS (ESI^+): m/z $[M + H]^+$ calcd for $C_{23}H_{28}N_7O_3S$ 482.19, found 482.12.

RP-HPLC t_R = 2.19 min (Method 1, 90 %), *m/z* $[M + H]^+$ calcd for $C_{23}H_{28}N_7O_3S$, 482.2, found 482.2.

7.2.23 General synthetic procedure (14) for macrocyclic compounds with amide linker (compounds 17a, 17b, 17c, 97)

To a round-bottomed flask was added following compounds (**96**, **16a**, **16b**, **16c**), HATU and TEA in DMF. The solution was heated to 50 ºC for 16 h. After completion of reaction, the reaction mixture was extracted with DCM and washed with brine thrice. The organic layers were combined and purified by flash column chromatography (gradient DCM and MeOH as the eluting solvent) to yield the desired product.

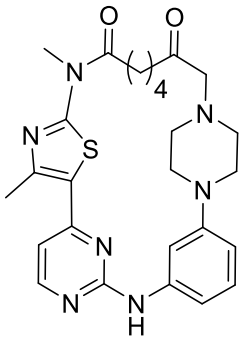

14, 12-Dimethyl-3, 12-diaza-1(5, 2)-thiazola-2(4, 2)-pyrimidina-5 (1, 4)-piperazina-4(1, 3)-benzenacyclododecaphane-6, 11- dione (17c)

The title compound was synthesised following general procedure (14) using **16c** (102 mg, 0.2 mmol), HATU (114 mg, 0.3 mmol) and TEA (20 mg, 0.2 mmol) in DMF to yield yellow solid (15 mg, 16%). mp: >300 ºC. ^{1}H-NMR ($CDCl_3$) δ 8.38 (d, 1H, *J* = 5.2 Hz, Ph-H), 8.12 (t, 1H, *J* = 2.2 Hz, Ph-H), 7.77 (s, 1H, NH), 7.18 (t, 1H, *J* = 8.1 Hz, Ph-H), 6.97 (d, 1H, *J* = 5.3 Hz, Ph-H), 6.71 (dd, 1H, *J* = 7.8, 2.3 Hz, Ph-H), 6.49 (dd, 1H,

J = 7.9, 2.0 Hz, Ph-H), 3.84 (t, 2H, *J* = 5.2 Hz, CH_2), 3.80 (t, 2H, *J* = 5.3 Hz, CH_2), 3.74 (s, 3H, CH_3), 3.52 (t, 2H, *J* = 5.2 Hz, CH_2), 3.32 (t, 2H, *J* = 5.2 Hz, CH_2), 2.78 (t, 2H, *J* = 5.2 Hz, CH_2), 2.62 (s, 3H, CH_3), 2.52 (t, 2H, *J* = 8.0 Hz, CH_2), 1.89 (t, 2H, *J* = 7.8 Hz, CH_2), 1.78 (t, 2H, *J* = 7.8 Hz, CH_2). ^{13}C-NMR ($CDCl_3$): δ 32.5, 49.3, 50.6, 57.9, 67.6, 106.9, 108.7, 109.0, 109.2, 113.2, 115.8, 119.8, 125.8, 129.1, 129.7, 133.1, 139.5, 140.8, 152.3, 158.4, 160.0, 160.4, 165.1. HR-MS (ESI^+): *m/z* $[M + H]^+$ calcd for $C_{25}H_{30}N_7O_2S$ 492.2182, found 492.2172. RP-HPLC t_R = 5.08 min (Method 2, 95+ %), *m/z* $[M + H]^+$ calcd for $C_{25}H_{30}N_7O_2S$, 492.2, found 492.3. RP-HPLC t_R = 6.00 min (Method 3, 95 %), *m/z* $[M + H]^+$ calcd for $C_{25}H_{30}N_7O_2S$, 492.2, found 492.3.

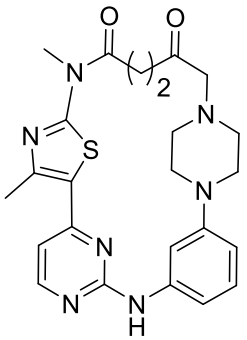

14,10-Dimethyl-3,10-diaza-1(5,2)-thiazola-2(4,2)-pyrimidina-5(1,4)-piperazina-4(1,3)-benzenacyclodecaphane-6,9-dione (17a)

The title compound was synthesised following general procedure (14) using **16a** (480 mg, 1 mmol, 1 eq), HATU (380 mg, 1 mmol, 1 eq) and TEA (1 mL, 2 mmol, 2 eq) in DMF to yield pale yellow solid (28 mg, 6%). mp: >300 °C. ^{1}H-NMR (DMSO-d_6): δ 9.30 (s, 1H, NH), 8.45 (d, 1H, *J* = 5.2, Ph-H), 7.92 (t, 1H, *J* = 2.1 Hz, Ph-H), 7.15 (t, 1H, *J* = 8.0 Hz, PH-H), 7.10 (d, 1H, *J* = 5.3 Hz, Ph-H), 6.76-6.81 (m, 2H, *J* = 1.0, 2×Ph-H), 3.79-3.95 (br s, 2H, CH_2), 3.57-3.76 (br s, 5H, CH_3&CH_2), 3.44-3.52 (br s,

2H, CH_2), 3.04-3.09 (br s, 2H, CH_2), 2.95 (t, 2H, J = 4.9 Hz, CH_2), 2.60 (s, 3H, CH_3), 2.55-2.72 (br s, 2H, CH_2). ^{13}C NMR (DMSO-d_6) δ 174.3, 171.5, 160.1, 159.9, 159.6, 158.5, 154.1, 147.7, 141.4, 128.7, 126.1, 117.6, 113.9, 110.3, 107.7, 52.9, 49.2, 47.4, 43.1, 33.9, 31.3, 26.9, 18.6. HR-MS (ESI$^+$): *m/z* $[M + H]^+$ calcd for $C_{23}H_{26}N_7O_2S$ 464.1869, found 464.1862. RP-HPLC t_R = 3.94 min (Method 2, 95+ %), *m/z* $[M + H]^+$ calcd for $C_{23}H_{26}N_7O_2S$, 464.2, found 464.1. RP-HPLC t_R = 4.10 min (Method 3, 95 %), *m/z* $[M + H]^+$ calcd for $C_{23}H_{26}N_7O_2S$, 464.2, found 464.1.

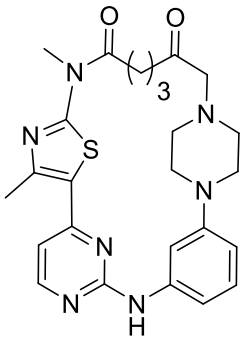

14,11-Dimethyl-3,11-diaza-1(5,2)-thiazola-2(4,2)-pyrimidina-5(1,4)-piperazina-4(1,3)-benzenacycloundecaphane-6,10-dione (17b)

The title compound was synthesised following general procedure (14) using **17b** (495 mg, 1 mmol, 1 eq), HATU (380 mg, 1 mmol, 1 eq) and Et_3N (1 mL, 2 mmol, 2 eq) in DMF to yield pale yellow solid (48 mg, 10%). mp: >300 ^{o}C. ^{1}H-NMR (DMSO-d_6): δ 9.57 (s, 1H, NH), 8.46 (d, 1H, J = 5.3, Ph-H), 7.95 (s, 1H, Ph-H), 7.13 (t, 1H, J = 7.9 Hz, PH-H), 7.09 (d, 1H, J = 5.3 Hz, Ph-H), 6.77 (dd, 1H, J = 1.5, 8.3 Hz, Ph-H), 6.68 (dd, 1H, J = 1.0, 7.9 Hz, Ph-H), 3.65 (s, 5H, CH_3&CH_2), 3.40-3.44 (m, 2H, CH_2), 3.11 (t, 2H, J = 4.7 Hz, CH_2), 2.85 (br t, 2H, J = 4.1 Hz, CH_2), 2.60 (s, 3H, CH_3), 2.31-2.42 (br, 4H, 2×CH_2), 1.98-2.06 (br, 2H, CH_2). ^{13}C NMR (DMSO-d_6) δ 173.2, 170.3, 159.9,

159.8, 159.6, 158.6, 153.3, 147.7, 141.4, 132.1, 128.7, 126.4, 114.8, 112.1, 108.2, 107.6, 51.5, 48.6, 46.4, 41.8, 33.8, 33.1, 31.5, 18.6, 11.23. HR-MS (ESI^+): *m/z* $[M + H]^+$ calcd for $C_{24}H_{28}N_7O_2S$ 478.2025, found 478.2042. RP-HPLC t_R = 4.41 min (Method 2, 95+ %), *m/z* $[M + H]^+$ calcd for $C_{24}H_{28}N_7O_2S$, 478.2, found 478.2. RP-HPLC t_R = 4.46 min (Method 3, 95 %), *m/z* $[M + H]^+$ calcd for $C_{24}H_{28}N_7O_2S$, 478.2, found 478.2.

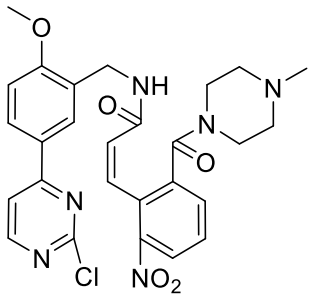

N-(5-(2-Chloropyrimidin-4-yl)-2-methoxybenzyl)-3-(2-(4-methyl-piperazine-1-carbonyl)-6-nitrophenyl)acrylamide (97)

The title compound was synthesised following general procedure (14) using **96** (249 mg, 1 mmol, 1 eq), **93** (320 mg, 1 mmol, 1 eq), HATU (380 mg, 1 mmol, 1 eq) and Et_3N (0.5 mL, 2 mmol, 2 eq) in DMF to yield a yellow solid (48 mg, 10%). ^{1}H-NMR ($CDCl_3$) δ 8.68 (dd, 1H, *J* = 4.5, 1.4 Hz, Ph-H), 8.47 (dd, 1H, *J* = 8.4, 1.4 Hz, Ph-H), 8.41 (d, *J* = 5.2 Hz, CH), 8.02-8.00 (m, 1H, Ph-H), 7.81 (d, 1H, *J* = 2.3 Hz, Ph-H), 7.74 (dd, 1H, *J* = 8.6, 2.4 Hz, Ph-H), 7.54-7.51 (m, 2H, 2×Ph-H), 7.47-7.44 (m, 1H, Ph-H), 6.84 (d, 1H, *J* = 8.8 Hz, Ph-H), 6.26 (d, 1H, *J* = 15.8 Hz, CH), 4.46 (d, 2H, *J* = 6.0 Hz, CH_2), 3.86 (s, CH_3), 3.03-3.09 (m, 4H, 2×CH_2), 2.17-2.27 (m, 4H, 2×CH_2), 2.09 (s, 3H, CH_3). ^{13}C NMR ($CDCl_3$) δ 167.1 , 164.4, 160.7, 160.1, 151.7, 148.2, 140.6, 137.7, 134.5, 133.7, 131.7, 128.7, 128.6, 128.4, 126.8, 125.9, 125.2, 120.9, 113.7, 110.7, 55.7, 46.4, 45.6,

41.5, 39.0, 37.4, 35.8. RP-HPLC t_R = 2.21 min (Method 3, 95 %), *m/z* $[M + H]^+$ calcd for $C_{27}H_{28}N_6O_5Cl$, 551.1, found 551.1.

7.2.24 Synthetic procedure for (2-bromo-3-nitrophenyl)(4-methylpiperazin-1-yl)methanone (91)[201]

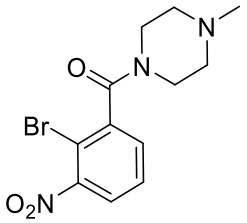

A solution of $P(OEt)_3$ (332 mg, 2.0 mmol, 1 eq) in CH_2Cl_2 (5 mL) was added successively I_2 (508 mg, 2.0 mmol, 1 eq), 2-bromo-3-nitrobenzonic acid **90** (490 mg, 2.0 mmol, 1 eq) and Et_3N (1 mL) at 0 ºC and then stirred at RT for 30 mins. After addition of methylpiperazine (240 mg, 2.4 mmol, 1.2 eq), the reaction mixture was allowed to be stirred for another 12 h. The resulting reaction mixture was diluted with CH_2Cl_2 (60 mL) and washed with aqueous NH_4Cl, 5% NaOH and brine, and evaporated to afford a white solid. (465 mg, 71%). ^{1}H-NMR ($CDCl_3$) δ 7.56 (dd, 1H, *J* = 8.0, 1.6 Hz, Ph-H), 7.35 (t, 1H, *J* = 7.8 Hz, Ph-H), 7.24 (dd, 1H, *J* = 8.0, 1.6 Hz, Ph-H), 3.64-3.51 (m, 2H, CH_2), 3.02 (m, 2H, CH_2), 2.34-2.09 (m, 4H, 2×CH_2), 2.07 (s, 3H).

7.2.25 General synthetic procedure (15) for macrocyclic compounds with alkene linker (compounds 43, 44, 60, 65, 72, 79, 84)

Solution of diene derivative in dichloromethane was taken in a flask equipped with a reflux condenser and nitrogen inlet. The solution was degassed with nitrogen for 1 h and

then Grubbs II catalyst and 4 M HCl in dioxane was added. The mixture was warmed at 50 ºC overnight under nitrogen while monitoring by TLC. After completion of the reaction, DCM was evaporated under reduced pressure and then purified by column (DCM/MeOH) to furnish the desired product.

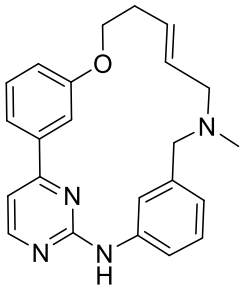

(*E*)-6-Methyl-12-oxa-3,6-diaza-2(4,2)-pyrimidina-1,4(1,3)-dibenzen-acyclodo-decaphan-8-ene (43)

The title compound was synthesised following general procedure (15) using **52** (100 mg, 0.23 mmol, 10 mM, 1 eq), Grubbs II (20 mg, 0.023 mmol, 0.1 eq) and 4 M HCl in dioxane (1.25 mL, 0.22 M) in dichloromethane (23 mL) to furnish a brown solid (34 mg, 40%). mp: 128-129 ºC. ^{1}H-NMR (DMSO-d_6): δ 8.93 (s, 1H, NH), 8.46 (d, 1H, J = 5.2 Hz, Ph-H), 8.03 (s, 1H, Ph-H), 7.55 (d, 1H, J = 7.1 Hz, Ph-H), 7.37-7.49 (m, 2H, 2×Ph-H), 7.29-7.32 (m, 2H, 2×Ph-H), 7.15 (dd, 1H, J = 2.3, 8.0 Hz, Ph-H), 7.09 (dd, 1H, J = 1.5, 8.0 Hz, Ph-H), 7.03 (d, 1H, J = 7.5 Hz, Ph-H), 5.93 (dt, 1H, J = 15.4, 6.4 Hz, CH), 5.76 (dt, 1H, J = 15.4, 7.2 Hz, CH), 4.22 (t, 2H, J = 5.1 Hz, CH_2), 3.81 (s, 2H, CH_2), 3.41 (d, 2H, J = 7.2 Hz, CH_2), 2.56 (q, 2H, J = 5.6 Hz, CH_2), 2.28 (s, 3H, CH_3). ^{13}C-NMR (DMSO-d_6): δ 31.7, 39.1, 59.2, 59.8, 65.1, 107.4, 114.3, 116.9, 118.2, 118.8, 120.3, 122.9, 124.5, 128.4, 129.3, 129.7, 135.2, 138.4, 140.9, 158.9, 159.1, 160.0, 163.6. HR-MS (ESI$^+$): m/z [M + H]$^+$ calcd for $C_{23}H_{25}N_4O$ 373.2028, found 373.2031. RP-

HPLC t_R = 3.48 min (Method 2, 95+ %), *m/z* $[M + H]^+$ calcd for $C_{23}H_{25}N_4O$, 373.2, found 373.3. RP-HPLC t_R = 4.09 min (Method 3, 95 %), *m/z* $[M + H]^+$ calcd for $C_{23}H_{25}N_4O$, 373.2, found 373.2.

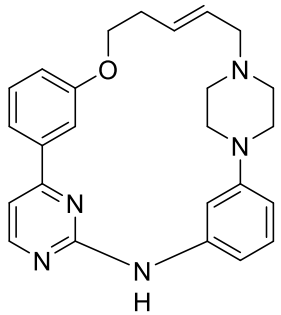

11-Oxa-3-aza-2(4,2)-pyrimidina-5(1,4)-piperazina-1,4(1,3)-dibenzena-cycloundecaphan-7-ene (44)

The title compound was synthesised following general procedure (15) using **53** (100 mg, 0.23 mmol, 10 mM, 1 eq), Grubbs II (20 mg, 0.023 mmol, 0.1 eq) and 4 M HCl in dioxane (1.25 mL, 0.22 M) in 23 mL dichloromethane at 50 °C to afford pale yellow solid (15 mg, 15 %), mp: 96-98 °C. ^{1}H-NMR ($CDCl_3$): δ 8.62 (t, 1H, *J* = 2.2 Hz, Ph-H), 8.41 (d, 1H, *J* = 5.2, Ph-H), 7.86 (br t, 1H, *J* = 1.5 Hz, Ph-H), 7.41-7.42 (m, 2H, 2×PH-H), 7.27 (s, 1H, Ph-H), 7.14 (t, 1H, *J* = 5.13 Hz, 2×PH-H), 7.01-7.04 (m, 1H, Ph-H), 6.53 (dd, 1H, *J* = 2.1, 7.6 Hz, Ph-H), 6.36 (dd, 1H, *J* = 1.5, 7.9 Hz, Ph-H), 5.65-5.81 (m, 2H, 2×CH), 4.08 (t, 2H, *J* = 5.3 Hz, CH_2), 3.33 (br t, 4H, *J* = 4.9 Hz, 2×CH_2), 3.25 (d, 2H, *J* = 6.5 Hz, CH_2), 2.79 (br t, 4H, *J* = 5.2 Hz, 2×CH_2), 2.59 (q, 2H, *J* = 5.6 Hz, CH_2). ^{13}C-NMR ($CDCl_3$): δ 32.5, 49.3, 50.6, 57.9, 67.6, 106.9, 108.7, 109.0, 109.2, 113.2, 115.8, 119.8, 125.8, 129.1, 129.7, 133.1, 139.5, 140.8, 152.3, 158.4, 160.0, 160.4, 165.1. HR-MS (ESI^+): *m/z* $[M + H]^+$ calcd for $C_{25}H_{28}N_5O$, 414.2294, found 414.2279. RP-

HPLC t_R = 3.78 min (Method 2, 95+ %), *m/z* $[M + H]^+$ calcd for $C_{25}H_{28}N_5O$, 414.2, found 414.2. RP-HPLC t_R = 4.38 min (Method 3, 95 %), *m/z* $[M + H]^+$ calcd for $C_{25}H_{28}N_5O$, 414.2, found 414.2.

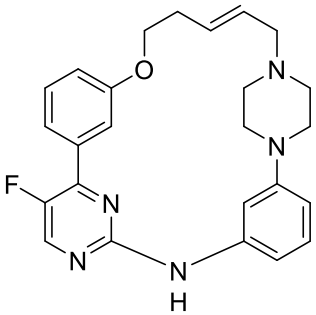

2-Fluoro-11-oxa-3-aza-2(4,2)-pyrimidina-5(1,4)-piperazina-1,4(1,3)-dibenzenacycloundecaphan-7-ene (60)

The title compound was synthesised following general procedure (15) using **59** (10 mg, 0.023 mmol, 10 mM, 1 eq), Grubbs II (2 mg, 0.0023 mmol, 0.1 eq) and 4 M HCl in dioxane (0.125 mL, 0.22 M) in 2 mL dichloromethane at 50 ºC to afford dark yellow solid (3 mg, 30%), mp: 82-83 ºC. ^{1}H-NMR ($CDCl_3$) δ 8.59 (s, 1H, NH), 8.27 (d, 1H, *J* = 2.9 Hz, Ph-H), 8.02 (d, 1H, *J* = 8.0 Hz, Ph-H), 7.84 (t, 1H, *J* = 2.2 Hz, Ph-H), 7.40 (t, 1H, *J* = 8.1 Hz, Ph-H), 7.19 (t, 1H, *J* = 8.0 Hz, Ph-H), 6.99 (dd, 1H, *J* = 8.3, 2.6 Hz, Ph-H), 6.90 (d, 1H, *J* = 3.8 Hz, Ph-H), 6.57 (dd, 1H, *J* = 8.3, 2.3 Hz, Ph-H), 6.41 dd, 1H, *J* = 7.9, 2.1 Hz, Ph-H), 5.68-5.80 (m, 2H, 2×CH), 4.08 (t, 2H, *J* = 5.4 Hz, CH_2), 3.48 (s, 2H, CH_2), 3.36-3.40 (m, 4H, 2×CH_2), 2.98-2.75 (m, 4H, 2×CH2), 2.61 (q, 2H, *J* = 5.3 Hz, CH_2). ^{13}C-NMR ($CDCl_3$) δ 159.5, 151.8, 149.9, 146.3, 143.7, 139.5, 139.4, 139.3, 139.2, 129.5, 129.5, 121.2, 116.3, 112.7, 109.7, 109.6, 108.3, 67.0, 67.0, 57.9, 50.3, 48.8, 32.7, 21.1. HR-MS (ESI^+): *m/z* $[M + H]^+$ calcd for $C_{25}H_{27}N_5OF$ 432.2200, found

432.2186. RP-HPLC t_R = 3.83 min (Method 2, 95+ %), *m/z* $[M + H]^+$ calcd for $C_{25}H_{27}N_5OF$, 432.2, found 432.2. RP-HPLC t_R = 4.47 min (Method 3, 95 %), *m/z* $[M + H]^+$ calcd for $C_{25}H_{27}N_5OF$, 432.2, found 432.2.

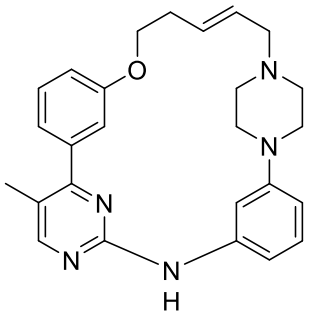

(*E*)-2-Methyl-11-oxa-3-aza-2(4,2)-pyrimidina-5(1,4)-piperazina-1,4(1,3)-dibenzenacycloundecaphan-7-ene (65)

The title compound was synthesised following general procedure (15) using **64** (10 mg, 0.023 mmol, 10 mM, 1 eq), Grubbs II (2 mg, 0.0023 mmol, 0.1 eq) and 4 M HCl in dioxane (0.125 mL, 0.22 M) in 2 mL dichloromethane at 50 ºC to afford brown solid (2.5 mg, 25%), mp: 130-132 ºC. ^{1}H-NMR ($CDCl_3$) δ 8.59 (t, 1H, *J* = 2.2 Hz, Ph-H), 8.28 (s, 1H, Ph-H), 7.36 (t, 1H, *J* = 8.0 Hz, Ph-H), 7.31 (dd,1H, *J* = 2.5, 1.6 Hz, Ph-H), 7.21 (s, 1H, NH), 7.13 (t, 1H, *J* = 8.1 Hz, Ph-H), 7.07 (dt, 1H, *J* = 7.9, 1.0 Hz, Ph-H), 6.95 (dd, 1H, *J* = 8.1, 2.6 Hz, Ph-H), 6.54 (dd, 1H, *J* = 8.1, 2.4 Hz, Ph-H), 6.34 (dd, 1H, *J* = 7.8, 2.0 Hz, Ph-H), 5.95 (dt, 1H, *J* = 15.4, 7.2 Hz, CH), 5.63 (dt, 1H, *J* = 15.4, 6.0 Hz, CH), 4.10 (t, 2H, *J* = 5.4 Hz, CH_2), 3.30 (t, 4H, *J* = 4.9 Hz, 2×CH_2), 3.16 (d, 2H, *J* = 6.1 Hz, CH_2), 2.71 (t, 4H, *J* = 4.9 Hz, 2×CH_2), 2.56 (q, 2H, *J* = 5.9 Hz, CH_2), 2.23 (s, 3H, CH_3). ^{13}C NMR ($CDCl_3$) δ 165.2, 160.0, 159.7, 158.6, 151.8, 141.4, 140.5, 129.1, 128.7, 121.5, 118.6, 117.2, 112.1, 109.4, 108.6, 105.9, 68.7, 57.8, 53.5, 50.8, 50.7, 48.7,

31.9, 16.5. HR-MS (ESI$^+$): *m/z* [M + H]$^+$ calcd for $C_{26}H_{30}N_5O$ 428.2450, found 428.2444. RP-HPLC t_R = 3.77 min (Method 2, 95+ %), *m/z* [M + H]$^+$ calcd for $C_{26}H_{30}N_5O$, 428.2, found 428.3. RP-HPLC t_R = 4.40 min (Method 3, 95 %), *m/z* [M + H]$^+$ calcd for $C_{26}H_{30}N_5O$, 428.2, found 428.3.

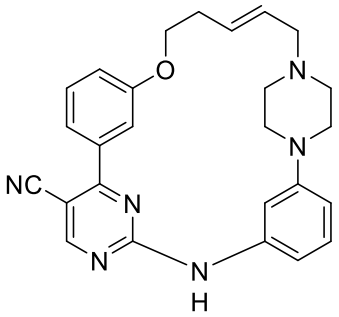

(*E*)-11-Oxa-3-aza-2(4,2)-pyrimidina-5(1,4)-piperazina-1,4(1,3)-dibenzen-acycloundecaphan-7-ene-25-carbonitrile (72)

The title compound was synthesised following general procedure (15) using **71** (20 mg, 0.046 mmol, 10 mM, 1 eq), Grubbs II (4 mg, 0.0046 mmol, 0.1 eq) and 4 M HCl in dioxane (0.25 mL, 0.22 M) in 4 mL dichloromethane at 50 ºC to afford brown solid (4 mg, 20%), mp: 114-115 ºC. ^{1}H-NMR ($CDCl_3$) δ 8.66 (s, 1H, Ph-H), 8.44 (s, 1H, Ph-H), 7.68 (d, 1H, *J* = 7.8 Hz, Ph-H), 7.59 (s, 1H, NH), 7.52-7.48 (m, 2H, 2×Ph-H), 7.21 (t, 1H, *J* = 8.0 Hz, Ph-H), 7.12 (dd, 1H, *J* = 8.4, 2.7 Hz, Ph-H), 6.62 (dd, 1H, *J* = 2.0, 8.0 Hz, Ph-H), 6.47 (d, 1H, *J* = 7.9 Hz, Ph-H), 5.96 (dt, 1H, *J* = 15.4, 6.4 Hz, CH), 5.70 (dt, 1H, *J* = 15.4, 6.2 Hz, CH), 4.13 (t, 2H, *J* = 5.5 Hz, CH_2), 3.42 (br s, 6H, 3×CH_2), 2.95 (br s, 4H, 2×CH_2), 2.63 (q, 2H, *J* = 6.3 Hz, CH_2). HR-MS (ESI$^+$): *m/z* [M + H]$^+$ calcd for $C_{26}H_{27}N_6O$ 439.2246, found 439.2245. RP-HPLC t_R = 3.73 min (Method 2, 95+ %), *m/z* [M + H]$^+$ calcd for $C_{26}H_{27}N_6O$, 439.2, found 439.4. RP-HPLC t_R = 4.20 min

(Method 3, 95 %), *m/z* $[M + H]^+$ calcd for $C_{26}H_{27}N_6O$, 439.2, found 439.4.

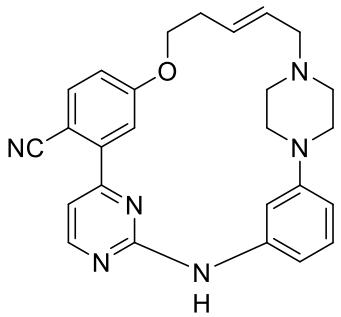

(*E*)-11-Oxa-3-aza-2(4,2)-pyrimidina-5(1,4)-piperazina-1,4(1,3)-dibenzena-cycloundecaphan-7-ene-16-carbonitrile (79)

The title compound was synthesised following general procedure (15) using **78** (100 mg, 0.23 mmol, 10 mM, 1 eq), Grubbs II (20 mg, 0.023 mmol, 0.1 eq) and 4 M HCl in dioxane (1.25 mL, 0.22 M) in 20 mL dichloromethane at 50 °C to afford dark yellow (37 mg, 37%), Decomp. 110-113 °C. ^{1}H-NMR ($CDCl_3$) δ 8.55-8.48 (m, 2H, 2×Ph-H), 7.77 (d, 1H, *J* = 8.6 Hz, Ph-H), 7.62-7.54 (m, 2H, NH&Ph-H), 7.30 (d, 1H, *J* = 5.0 Hz, Ph-H), 7.16 (t, 1H, *J* = 8.0 Hz, Ph-H), 7.02 (dd, 1H, *J* = 8.7, 2.7 Hz, Ph-H), 6.57 (dd, 1H, *J* = 8.1, 2.5 Hz, Ph-H), 6.40 (dd, 1H, *J* = 7.9, 2.0 Hz, Ph-H), 5.91 (dt, 1H, *J* = 15.4, 7.2 Hz, CH), 5.65 (dt, 1H, *J* = 15.4, 7.2 Hz, CH), 4.13 (t, 2H, *J* = 5.5 Hz, CH_2), 3.29 (t, 4H, *J* = 4.9 Hz, 2×CH_2), 3.20 (d, 2H, *J* = 5.9 Hz, CH_2), 2.73 (t, 4H, *J* = 4.9 Hz, 2×CH_2), 2.59 (q, 2H, *J* = 6.0 Hz, CH_2). ^{13}C NMR ($CDCl_3$) δ 162.7, 162.3, 160.5, 158.9, 152.2, 143.8, 140.7, 136.6, 129.2, 126.4, 118.7, 118.5, 112.5, 112.1, 109.9, 109.3, 106.6, 102.8, 69.1, 57.5, 50.7, 49.1, 31.6. HR-MS (ESI^+): *m/z* $[M + H]^+$ calcd for $C_{26}H_{27}N_6O$ 439.2246, found 439.2241. RP-HPLC t_R = 3.61 min (Method 2, 95+ %), *m/z* $[M + H]^+$calcd for $C_{26}H_{27}N_6$, 439.2, found 439.4. RP-HPLC t_R = 4.21 min (Method 3, 95 %), *m/z* [M +

H]$^+$calcd for $C_{26}H_{27}N_6O$, 439.2, found 439.4.

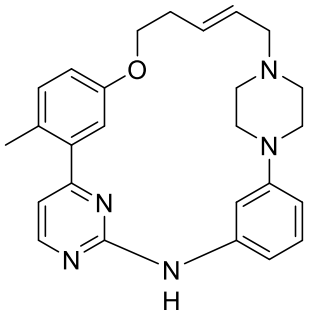

(*E*)-16-Methyl-11-oxa-3-aza-2(4,2)-pyrimidina-5(1,4)-piperazina-1,4(1,3)-dibenzenacycloundecaphan-7-ene (84)

The title compound was synthesised following general procedure (15) using **83** (100 mg, 0.23 mmol, 10 mM, 1 eq), Grubbs II (20 mg, 0.023 mmol, 0.1 eq) and 4 M HCl in dioxane (1.25 mL, 0.22 M) in 20 mL dichloromethane at 50 ºC to afford brown solid (49 mg, 50%), Decomp. 125-127 ºC. ^{1}H-NMR ($CDCl_3$) δ 8.61 (s, 1H, Ph-H), 8.39 (d, 1H, *J* = 5.0 Hz, Ph-H), 7.47 (s, 1H, NH), 7.24 (d, 1H, *J* = 2.7 Hz, Ph-H), 7.21 (d, 1H, *J* = 8.4 Hz, Ph-H), 7.14 (t, 1H, *J* = 8.0 Hz, Ph-H), 6.87 (dd, 1H, *J* = 8.3, 2.9 Hz, Ph-H), 6.82 (d, 1H, *J* = 5.0 Hz, Ph-H), 6.55 (dd, 1H, *J* = 8.3, 2.3 Hz, Ph-H), 6.37 (dd, 1H, *J* = 7.9, 2.1 Hz, Ph-H), 5.94 (dt, 1H, *J* = 15.4, 7.2 Hz, CH), 5.61 (dt, 1H, *J* = 15.4, 6.2 Hz, CH), 4.06 (t, 2H, *J* = 5.5 Hz, CH_2), 3.33 (t, 4H, *J* = 4.7 Hz, 2×CH_2), 3.16 (d, 2H, *J* = 6.0 Hz, CH_2), 2.74-2.69 (m, 4H, 2×CH_2), 2.53 (q, 2H, *J* = 6.1 Hz, CH_2), 2.33 (s, 3H, CH_3). ^{13}C NMR ($CDCl_3$) δ 166.6, 160.5, 157.5, 157.3, 151.7, 141.1, 140.3, 131.9, 129.2, 127.4, 117.6, 113.2, 112.6, 109.7, 108.8, 106.3, 68.8, 57.9, 50.7, 50.6, 48.6, 31.9, 19.9, 11.0. HR-MS (ESI$^+$): *m/z* [M + H]$^+$ calcd for $C_{26}H_{30}N_5O$ 428.2450, found 428.2440. RP-HPLC t_R = 3.64 min (Method 2, 95+ %), *m/z* [M + H]$^+$ calcd for $C_{26}H_{30}N_5O$, 428.2,

found 428.3. RP-HPLC t_R = 4.34 min (Method 3, 95 %), *m/z* $[M + H]^+$ calcd for $C_{26}H_{30}N_5O$, 428.2, found 428.3.

7.2.26 Synthetic procedure for 6-methyl-12-oxa-3,6-diaza-2(4,2)-pyrimidina-1,4(1,3)-dibenzenacyclodo-decaphane (86)

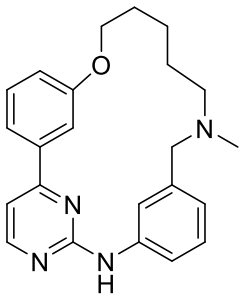

A solution of **43** (100 mg, 0.27 mmol, 1 eq) in THF/tert-butanol (1:1, 10 mL) was treated with palladium hydroxide (40 mg, 0.27 mmol, 1 eq) and the mixture was saturated under a hydrogen balloon. The reaction was stirred at RT overnight. The reaction mixture was filtered on Celite filter and washed with dichloromethane. The resulting crude was concentrated and purified by column (gradient DCM/MeOH) to afford the title compound as a pale orange solid (25 mg, 25%). Decomp. 118-120 ºC. ^{1}H-NMR ($CDCl_3$) δ 8.82 (s, 1H, Ph-H), 8.43 (d, 1H, *J* = 5.2 Hz, Ph-H), 8.06 (s, 1H, NH), 7.43 (d, 1H, *J* = 8.0 Hz, Ph-H), 7.38 (t, 1H, *J* = 7.7 Hz, Ph-H), 7.33 (br s, 1H, Ph-H), 7.22 (t, 1H, *J* = 7.7 Hz, Ph-H), 7.17 (d, 1H, *J* = 5.2 Hz, Ph-H), 7.06 (dd, 1H, *J* = 7.9, 2.8 Hz, Ph-H), 6.98 (br s, 1H, Ph-H), 6.82 (dd, 1H, *J* = 8.1, 2.3 Hz, Ph-H), 4.21 (t, 2H, *J* = 5.6 Hz, CH_2), 3.61 (br s, 2H, CH_2), 2.61 (br s, 2H, CH_2), 2.19 (s, 3H, CH_3), 1.94-1.84 (m, 4H, 2×CH_2), 1.63 (q, 2H, *J* = 6.7 Hz, CH_2). ^{13}C NMR ($CDCl_3$) δ 164.6, 160.2,

159.5, 158.6, 140.3, 138.7, 129.6, 128.3, 123.6, 119.2, 119.2, 117.7, 116.1, 116.0, 108.5, 69.5, 62.4, 57.8, 41.5, 27.2, 26.7, 24.9. HR-MS (ESI^+): *m/z* $[M + H]^+$ calcd for $C_{25}H_{28}N_5O$ 375.2185, found 375.2186.

7.3 Molecular docking

Schrodinger Glide and PyMOL were used in molecular docking.

Glide is designed for ligand screening based on the binding mode and affinity with a given protein receptor. Glide is characteristic by a systematic search of the conformational, orientational, and positional space of a ligand in the binding mode. The docking mode prediction of Glide is more robust than the reported docking methods, such as GOLD, FlexX.[202]

PyMOL is used to view, share, and analyse the molecular docking data. In addition to being lightweight and fast, PyMOL can create images of peerless visualization quality, while offering the flexibility of Python-based development and scalability.

All the ligand structures were formed by Glide-ligand preparation, converting 2D (. mol format) to 3D ligand(.sdf format), with all other settings on default. PDB files of protein receptors, 4BCG, 4BCP, 3UO5 and 2BFY were generated using the Glide-protein preparation wizard, with default settings. Then receptor grid generation was obtained through a series of procedures involving identifying the ligand, defining the size of docking box and setting up the constraints of H-bond, with other setting on default. Hydrogen bond constraints between the ligand and residue Cys106 (in CDK9) were enforced. Dockings were performed using Glide-ligand docking programme, including the setting of SP standard precision, flexible ligand sampling and 5 poses per ligand imported. All other setting in the docking were on default. The docking results were

viewed and analysed using PyMOL software.

PDB files of protein receptors were downloaded from protein data bank, code 4BCG for CDK9; 4BCP for CDK2; 3UO5 for Aurora-A, 2BFY for Aurora-B.

7.4 Kinase assays

Kinase assays were carried out by Eurofins Kinase Screening & Profiling service using the radiometric assay.[203, 204] Half-maximal inhibition (IC_{50}) values were calculated from 10-point dose-response curves and were mean values derived from two replicates. The apparent inhibition constants (K_i) were calculated from the IC_{50} values and appropriate K_m (ATP) values using the Cheng-Prusoff equation.

References

1. Cancer statistics in the UK in 2014; Available from: http://publications.cancerresearchuk.org/cancerstats

2. Cooper, G. M. "The development and Causes of Cancer". In: The cell: A Molecular Approach. **2009**, 725-734.

3. Doucas, H.; Berry, D. P. Basic principles of the molecular biology of cancer I. *Surgery (Oxford)* **2006**, 24, 43-47.

4. Hejmadi, M. Introduction-to-Cancer Biology. **2009**.

5. Does, A.; Johnson, N. A.; Thiel, T. Cell Biology and Cancer in "Rediscovering Biology: Molecular to Global Perspectives". **2003**.

6. Flalkow. Clonal Origin of Human Tumors. **1976**, 458, 283-321.

7. Greaves, M.; Maley, C. C. Clonal evolution in cancer. *Nature* **2012**, 481, 306-13.

8. Stratton, M. R. Exploring the genomes of cancer cells: progress and promise. *Science* **2011**, 331, 1553-8.

9. About Cancer. Available from http://www.cancerresearchuk.org/about-cancer

10. Weinberg, R. A. The biology of cancer. **2013**.

11. Baba, A. I.; Catoi, C. Tumor Cell Morphology In: Comparative Oncology. **2007**.

12. Benign Tumor. (n.d.). *Medical Dictionary for the Health Professions and Nursing* **2012**, Retrieved September 19 2017 from http://medical-dictionary.thefreedictionary.com/benign+tumor.

13. Types of cancer, (2014) Available from: http://www.cancerresearchuk.org/about-cancer/what-is-cancer/how-cancer-starts/types-of-cancer

14. Tumor Grader, (2013) Available from: https://www.cancer.gov/about-cancer/diagnosis-staging/prognosis/tumor-grade-fact-sheet

15. Hanahan, D.; Weinberg, R. A. Hallmarks of cancer: the next generation. *Cell* **2011**, 144, 646-74.

16. Cheng, N.; Chytil, A.; Shyr, Y.; Joly, A.; Moses, H. L. Transforming Growth Factor-β Signaling–Deficient Fibroblasts Enhance Hepatocyte Growth Factor Signaling in Mammary Carcinoma Cells to Promote Scattering and Invasion. *Molecular Cancer Research* **2008**, 6, 1521-1533.

17. Evan, G.; Littlewood, T. A Matter of Life and Cell Death. *Science* **1998**, 281, 1317-1322.

18. McClintock, B. The Production of Homozygous Deficient Tissues with Mutant Characteristics by means of the Aberrant Mitotic Behavior of Ring-Shaped Chromosomes. *Genetics* **1938**, 23, 315-376.

19. van Steensel, B.; Smogorzewska, A.; de Lange, T. TRF2 Protects Human Telomeres from End-to-End Fusions. *Cell* **1998**, 92, 401-413.

20. Gilson, E.; Geli, V. How telomeres are replicated. *Nat Rev Mol Cell Biol* **2007**, 8, 825-838.

21. Meyerson, M. Role of Telomerase in Normal and Cancer Cells. *Journal of Clinical Oncology* **2000**, 18, 2626-2634.

22. Ribatti, D.; Vacca, A.; Dammacco, F. The Role of the Vascular Phase in Solid Tumor Growth: A Historical Review. *Neoplasia* **1999**, 1, 293-302.

23. Baeriswyl, V.; Christofori, G. The angiogenic switch in carcinogenesis. *Seminars in Cancer Biology* **2009**, 19, 329-337.

24. Radisky, D. C. Epithelial-mesenchymal transition. *Journal of Cell Science* **2005**, 118, 4325-4326.

25. Berx, G.; van Roy, F. Involvement of Members of the Cadherin Superfamily in Cancer. *Cold Spring Harbor Perspectives in Biology* **2009**, 1, a003129.

26. Cavallaro, U.; Christofori, G. Cell adhesion and signalling by cadherins and Ig-CAMs in cancer. *Nature reviews. Cancer* **2004**, 4, 118-132.

27. Warburg, O.; Wind, F.; Negelein, E. The Metabolism of Tumors In The Body. *The Journal of General Physiology* **1927**, 8, 519-530.

28. Weinhouse, S.; Warburg, O.; Burk, D.; Schade, A. L. On Respiratory Impairment in Cancer Cells. *Science* **1956**, 124, 267-272.

29. Roder, F. An Analysis of Warburg's View on the Origin of Cancer Cells. *Philosophy of Science* **1956**, 23, 343-347.

30. DeBerardinis, R. J.; Lum, J. J.; Hatzivassiliou, G.; Thompson, C. B. The Biology of Cancer: Metabolic Reprogramming Fuels Cell Growth and Proliferation. *Cell Metabolism* **2008**, 7, 11-20.

31. Jones, R. G.; Thompson, C. B. Tumor Suppressors and Cell Metabolism: aRecipe for Cancer Growth. *Genes & development* **2009**, 23, 537-48.

32. Hanahan, D. W., R. A. The Hallmarks of Cancer. *Cell* **2000**, 100, 57-70.

33. DeNardo, D. G.; Andreu, P.; Coussens, L. M. Interactions between lymphocytes and myeloid cells regulate pro- versus anti-tumor immunity. *Cancer and Metastasis Reviews* **2010**, 29, 309-316.

34. Qian, B. Z.; Pollard, J. W. Macrophage Diversity Enhances Tumor Progression and Metastasis. *Cell* **2010**, 141, 39-51.

35. Colotta, F.; Allavena, P.; Sica, A.; Garlanda, C.; Mantovani, A. Cancer-related inflammation, the seventh hallmark of cancer: links to genetic instability. *Carcinogenesis* **2009**, 30, 1073-1081.

36. Grivennikov, S. I.; Greten, F. R.; Karin, M. Immunity, Inflammation, and Cancer. *Cell* **2010**, 140, 883-899.

37. Bettayeb, K.; Baunbæk, D.; Delehouze, C.; Loaëc, N.; Hole, A. J.; Baumli, S.; Endicott, J. A.; Douc-Rasy, S.; Bénard, J.; Oumata, N.; Galons, H.; Meijer, L. CDK Inhibitors Roscovitine and CR8 Trigger Mcl-1 Down-Regulation and Apoptotic Cell Death in Neuroblastoma Cells. *Genes & Cancer* **2010**, 1, 369-380.

38. Bertilaccio, M. T.; Scielzo, C.; Muzio, M.; Caligaris-Cappio, F. An overview of chronic lymphocytic leukaemia biology. *Best practice & research. Clinical haematology* **2010**, 23, 21-32.

39. Singer, C.; Goldstone, T. Chronic Lymphocytic Leukaemia. *Clinical Medicine* **2001**, 1, 350-353.

40. Rozman, C.; Montserrat, E. Chronic lymphocytic leukemia. *The New England*

Journal of Medicine **1995**, 333, 1052-1057.

41. Jurlander, J. The Cellular Biology of B-cell Chronic Lymphocytic Leukemia. *Critical Reviews in Oncology/Hematology* **1998**, 27, 29-52.

42. Hamblin, T. J.; Oscier, D. G. Chronic lymphocytic leukaemia: the nature of the leukaemic cell. *Blood reviews/Haematological oncology* **1997**, 11, 119-128.

43. Ichim, G.; Tait, S. W. A fate worse than death: apoptosis as an oncogenic process. *Nature reviews. Cancer* **2016**, 16, 539-48.

44. Delbridge, A. R. D.; Grabow, S.; Strasser, A.; Vaux, D. L. Thirty Years of BCL-2:Translating Cell Death Discoveries into Novel Cancer Therapies. *Nature reviews. Cancer* **2016**, 16, 99-109.

45. Letai, A. G. Diagnosing and Exploiting Cancer's Addiction to Blocks in Apoptosis. *Nature reviews. Cancer* **2008**, 8, 121-132.

46. Nagata, S. Apoptosis and autoimmune diseases. *Annals of the New York Academy of Sciences* **2010**, 1209, 10-16.

47. Ouyang, L.; Shi, Z.; Zhao, S.; Wang, F. T.; Zhou, T. T.; Liu, B.; Bao, J. K. Programmed cell death pathways in cancer: a review of apoptosis, autophagy and programmed necrosis. *Cell Proliferation* **2012**, 45, 487-498.

48. Tait, S. W.; Green, D. R. Mitochondria and cell death: outer membrane permeabilization and beyond. *Nat Rev Mol Cell Biol* **2010**, 11, 621-32.

49. Kerr, J. F. R.; Wyllie, A. H.; Currie, A. R. Apoptosis: A Basic Biological Phenomenon with Wide-ranging Implications in Tissue Kinetics. *British Journal of*

Cancer **1972**, 26, 239-257.

50. Cory, S.; Adams, J. M. The Bcl2 family: regulators of the cellular life-or-death switch. *Nature reviews. Cancer* **2002**, 2, 647-656.

51. Lessene, G.; Czabotar, P. E.; Colman, P. M. BCL-2 family antagonists for cancer therapy. *Nat Rev Drug Discov* **2008**, 7, 989-1000.

52. Packham, G.; Stevenson, F. K. Bodyguards and assassins: Bcl-2 family proteins and apoptosis control in chronic lymphocytic leukaemia. *Immunology* **2005**, 114, 441-449.

53. Chen, L. S.; Balakrishnan, K.; Gandhi, V. Inflammation and survival pathways: Chronic lymphocytic leukemia as a model system. *Biochemical Pharmacology* **2010**, 80, 1936-1945.

54. Burger, J. A.; Ghia, P.; Rosenwald, A.; Caligaris-Cappio, F. The microenvironment in mature B-cell malignancies: a target for new treatment strategies. *Blood* **2009**, 114, 3367-75.

55. Pleyer, L.; Egle, A.; Hartmann, T. N.; Greil, R. Molecular and cellular mechanisms of CLL: novel therapeutic approaches. *Nat Rev Clin Oncol* **2009**, 6, 405-418.

56. Jean-Pierre, K.; Catherine, K.; Claire, Q.; Viviana, R.; Christian, B. Re-Establishment of a Normal Apoptotic Process as a Therapeutic Approach in B-CLL. *Current Drug Targets - Cardiovascular & Hematological Disorders* **2003**, 3, 261-286.

57. Reed, J. C. Apoptosis-targeted therapies for cancer. *Cancer Cell* **2003**, 3, 17-22.

58. Loeder, S.; Zenz, T.; Schnaiter, A.; Mertens, D.; Winkler, D.; Döhner, H.; Debatin, K.-M.; Stilgenbauer, S.; Fulda, S. A Novel Paradigm to Trigger Apoptosis in Chronic

Lymphocytic Leukemia. *Cancer research* **2009**, 69, 8977-8986.

59. Pepper, C.; Lin, T. T.; Pratt, G.; Hewamana, S.; Brennan, P.; Hiller, L.; Hills, R.; Ward, R.; Starczynski, J.; Austen, B.; Hooper, L.; Stankovic, T.; Fegan, C. Mcl-1 expression has in vitro and in vivo significance in chronic lymphocytic leukemia and is associated with other poor prognostic markers. *Blood* **2008**, 112, 3807-3817.

60. Awan, F. T.; Kay, N. E.; Davis, M. E.; Wu, W.; Geyer, S. M.; Leung, N.; Jelinek, D. F.; Tschumper, R. C.; Secreto, C. R.; Lin, T. S.; Grever, M. R.; Shanafelt, T. D.; Zent, C. S.; Call, T. G.; Heerema, N. A.; Lozanski, G.; Byrd, J. C.; Lucas, D. M. Mcl-1 expression predicts progression-free survival in chronic lymphocytic leukemia patients treated with pentostatin, cyclophosphamide, and rituximab. *Blood* **2009**, 113, 535-537.

61. Hussain, S.-R. A.; Cheney, C. M.; Johnson, A. J.; Lin, T. S.; Grever, M. R.; Caligiuri, M. A.; Lucas, D. M.; Byrd, J. C. Mcl-1 Is a Relevant Therapeutic Target in Acute and Chronic Lymphoid Malignancies: Down-Regulation Enhances Rituximab-Mediated Apoptosis and Complement-Dependent Cytotoxicity. *Clinical Cancer Research* **2007**, 13, 2144-2150.

62. Johnson, L. N.; Lowe, E. D.; Noble, M. E. M.; Owen, D. J. The structural basis for substrate recognition and control by protein kinases 1. *FEBS Letters* **1998**, 430, 1-11.

63. Protein kinase in Wilipedia 2017, Available from: https://en.wikipedia.org/wiki/Protein_kinase

64. Taylor, S. S.; Knighton, D. R.; Zheng, J.; Sowadski, J. M.; Gibbs, C. S.; Zoller, M. J. A template for the protein kinase family. *Trends in Biochemical Sciences* **1993**, 18,

84-89.

65. Bossemeyer, D. The glycine-rich sequence of protein kinases: a multifunctional element. *Trends in Biochemical Sciences* **1994**, 19, 201-205.

66. Hemmer, W.; McGlone, M.; Tsigelny, I.; Taylor, S. S. Role of the Glycine Triad in the ATP-binding Site of cAMP dependent protein kinase. *The Journal of Biological Chemistry* **1997**, 272, 16946-16954.

67. Zhang, J.; Yang, P. L.; Gray, N. S. Targeting cancer with small molecule kinase inhibitors. *Nature reviews. Cancer* **2009**, 9, 28-39.

68. Norman, R. A.; Toader, D.; Ferguson, A. D. Structural approaches to obtain kinase selectivity. *Trends in Pharmacological Sciences* **2012**, 33, 273-278.

69. Wang, S.; Meades, C.; Wood, G.; Osnowski, A.; Anderson, S.; Yuill, R.; Thomas, M.; Mezna, M.; Jackson, W.; Midgley, C.; Griffiths, G.; Fleming, I.; Green, S.; McNae, I.; Wu, S.-Y.; McInnes, C.; Zheleva, D.; Walkinshaw, M. D.; Fischer, P. M. 2-Anilino-4-(thiazol-5-yl)pyrimidine CDK Inhibitors: Synthesis, SAR Analysis, X-ray Crystallography, and Biological Activity. *Journal of medicinal chemistry* **2004**, 47, 1662-1675.

70. Huse, M.; Kuriyan, J. The Conformational Plasticity of Protein Kinases. *Cell* **2002**, 109, 275-282.

71. Nolen, B.; Taylor, S.; Ghosh, G. Regulation of Protein Kinases. *Molecular cell* **2004**, 15, 661-675.

72. Endicott, J. A.; Noble, M. E.; Johnson, L. N. The structural basis for control of

eukaryotic protein kinases. *Annual review of biochemistry* **2012**, 81, 587-613.

73. Noble, M. E. M.; Endicott, J. A.; Johnson, L. N. Protein Kinase Inhibitors: Insights into Drug Design from Structure. *Science* **2004**, 303, 1800-1805.

74. Jura, N.; Zhang, X.; Endres, Nicholas F.; Seeliger, Markus A.; Schindler, T.; Kuriyan, J. Catalytic Control in the EGF Receptor and Its Connection to General Kinase Regulatory Mechanisms. *Molecular cell* **2011**, 42, 9-22.

75. Malumbres, M.; Harlow, E.; Hunt, T.; Hunter, T.; Lahti, J. M.; Manning, G.; Morgan, D. O.; Tsai, L.-H.; Wolgemuth, D. J. Cyclin-dependent kinases: a family portrait. *Nat Cell Biol* **2009**, 11, 1275-1276.

76. Sherr, C. J. Cancer Cell Cycles. *Science* **1996**, 274, 1672-1677.

77. Morgan, D. O. Cyclin-Dependent Kinases: Engines, Clocks, and Microprocessors. *Annual Review of Cell and Developmental Biology* **1997**, 13, 261-291.

78. Rudolph, J. Inhibiting transient protein-protein interactions: lessons from the Cdc25 protein tyrosine phosphatases. *Nature reviews. Cancer* **2007**, 7, 202-11.

79. Bruyère, C.; Meijer, L. Targeting cyclin-dependent kinases in anti-neoplastic therapy. *Current Opinion in Cell Biology* **2013**, 25, 772-779.

80. Romano, G. Deregulations in the Cyclin-Dependent Kinase-9-Related Pathway in Cancer: Implications for Drug Discovery and Development. *ISRN Oncology* **2013**, 2013, 305371.

81. Rickert, P.; Corden, J. L.; LEES, E. Cyclin C/CDK8 and cyclin H/CDK7/p36 are biochemically distinct CTD kinases. *1999* **1999**, 18, 1093-1102.

82. Fujinaga, K.; Irwin, D.; Huang, Y.; Taube, R.; Kurosu, T.; Peterlin, B. M. Dynamics of Human Immunodeficiency Virus Transcription: P-TEFb Phosphorylates RD and Dissociates Negative Effectors from the Transactivation Response Element. *Molecular and Cellular Biology* **2004**, 24, 787-795.

83. Yamada, T.; Yamaguchi, Y.; Inukai, N.; Okamoto, S.; Mura, T.; Handa, H. P-TEFb-Mediated Phosphorylation of hSpt5 C-Terminal Repeats Is Critical for Processive Transcription Elongation. *Molecular cell* **2006**, 21, 227-237.

84. Hengartner, C. J.; Myer, V. E.; Liao, S.-M.; Wilson, C. J.; Koh, S. S.; Young, R. A. Temporal Regulation of RNA Polymerase II by Srb10 and Kin28 Cyclin-Dependent Kinases. *Molecular cell* **1998**, 2, 43-53.

85. Bagella, L.; Stiegler, P.; De Luca, A.; Siracusa, L. D.; Giordano, A. Genomic organization, promoter analysis, and chromosomal mapping of the mouse gene encoding Cdk9. *Journal of Cellular Biochemistry* **2000**, 78, 170-178.

86. Bagella, L.; MacLachlan, T. K.; Buono, R. J.; Pisano, M. M.; Giordano, A.; De Luca, A. Cloning of murine CDK9/PITALRE and its tissue-specific expression in development. *Journal of Cellular Physiology* **1998**, 177, 206-213.

87. Falco, G. D.; Neri, L. M.; Falco, M. D.; Luca, A. D.; Leoncini, L.; Bellan, C.; Giordano, A. Cdk9, a Member of the Cdc2-Like Family of Kinases, Binds to gp130, the Receptor of the IL-6 Family of Cytokines. *Oncogene* **2002**, 21, 7464-7470.

88. Graña, X.; De Luca, A.; Sang, N.; Fu, Y.; Claudio, P. P.; Rosenblatt, J.; Morgan, D. O.; Giordano, A. PITALRE, a Nuclear CDC2-Related Protein Kinase that

Phosphorylates the Retinoblastoma Protein in vitro. *Proceedings of the National Academy of Sciences of the United States of America* **1994**, 91, 3834-3838.

89. Keeffe, B. O.; Fong, Y.; Chen, D.; Zhou, S.; Zhou, Q. Requirement for a Kinase-specific Chaperone Pathway in the production of a Cdk9/Cyclin T1 Heterodimer Responsible for P-TEFb-mediated Tat Stimulation of HIV-1 Transcription. *The Journal of Biological Chemistry* **2000**, 275, 279-287.

90. Lin, X.; Taube, R.; Fujinaga, K.; Peterlin, B. M. P-TEFb containing cyclin K and Cdk9 can activate transcription via RNA. *J Biol Chem* **2002**, 277, 16873-8.

91. Price, D. H. P-TEFb, a Cyclin-Dependent Kinase Controlling Elongation by RNA Polymerase II. *Molecular and Cellular Biology* **2000**, 20, 2629-2634.

92. Romano, G.; Kasten, M.; De Falco, G.; Micheli, P.; Khalili, K.; Giordano, A. Regulatory functions of Cdk9 and of cyclin T1 in HIV Tat transactivation pathway gene expression. *Journal of Cellular Biochemistry* **1999**, 75, 357-368.

93. Zhou, Q.; Yik, J. H. N. The Yin and Yang of P-TEFb Regulation: Implications for Human Immunodeficiency Virus Gene Expression and Global Control of Cell Growth and Differentiation. *Microbiology and Molecular Biology Reviews* **2006**, 70, 646-659.

94. Lam, L. T.; Pickeral, O. K.; Peng, A. C.; Rosenwald, A.; Hurt, E. M.; Giltnane, J. M.; Averett, L. M.; Zhao, H.; Davis, R. E.; Sathyamoorthy, M.; Wahl, L. M.; Harris, E. D.; Mikovits, J. A.; Monks, A. P.; Hollingshead, M. G.; Sausville, E. A.; Staudt, L. M. Genomic-scale measurement of mRNA turnover and the mechanisms of action of the anti-cancer drug flavopiridol. *Genome Biology* **2001**, 2, research0041.1-

research0041.11.

95. Hahntow, I. N.; Schneller, F.; Oelsner, M.; Weick, K.; Ringshausen, I.; Fend, F.; Peschel, C.; Decker, T. Cyclin-dependent kinase inhibitor Roscovitine induces apoptosis in chronic lymphocytic leukemia cells. *Leukemia* **2004**, 18, 747-755.

96. Chen, R.; Wierda, W. G.; Chubb, S.; Hawtin, R. E.; Fox, J. A.; Keating, M. J.; Gandhi, V.; Plunkett, W. Mechanism of action of SNS-032, a novel cyclin-dependent kinase inhibitor, in chronic lymphocytic leukemia. *Blood* **2009**, 113, 4637-4645.

97. Chen, R.; Keating, M. J.; Gandhi, V.; Plunkett, W. Transcription inhibition by flavopiridol: mechanism of chronic lymphocytic leukemia cell death. *Blood* **2005**, 106, 2513-2519.

98. Shapiro, G. I. Cyclin-Dependent Kinase Pathways As Targets for Cancer Treatment. *Journal of Clinical Oncology* **2006**, 24, 1770-1783.

99. Whittaker, S. R.; Walton, M. I.; Garrett, M. D.; Workman, P. The Cyclin-dependent Kinase Inhibitor CYC202 (R-Roscovitine) Inhibits Retinoblastoma Protein Phosphorylation, Causes Loss of Cyclin D1, and Activates the Mitogen-activated Protein Kinase Pathway. *Cancer research* **2004**, 64, 262-272.

100. Carlson, B.; Lahusen, T.; Singh, S.; Loaiza-Perez, A.; Worland, P. J.; Pestell, R.; Albanese, C.; Sausville, E. A.; Senderowicz, A. M. Down-Regulation of Cyclin D1 by Transcriptional Repression in MCF-7 Human Breast Carcinoma Cells Induced by Flavopiridol. *Cancer research* **1999**, 59, 4634-4641.

101. Gordon, V.; Bhadel, S.; Wunderlich, W.; Zhang, J.; Ficarro, S. B.; Mollah, S.

A.; Shabanowitz, J.; Hunt, D. F.; Xenarios, I.; Hahn, W. C.; Conaway, M.; Carey, M. F.; Gioeli, D. CDK9 Regulates AR Promoter Selectivity and Cell Growth through Serine 81 Phosphorylation. *Molecular Endocrinology* **2010**, 24, 2267-2280.

102. Chen, C. D.; Welsbie, D. S.; Tran, C.; Baek, S. H.; Chen, R.; Vessella, R.; Rosenfeld, M. G.; Sawyers, C. L. Molecular determinants of resistance to antiandrogen therapy. *Nat Med* **2004**, 10, 33-39.

103. Stockwin, L. H.; Yu, S. X.; Stotler, H.; Hollingshead, M. G.; Newton, D. L. ARC (NSC 188491) has identical activity to Sangivamycin (NSC 65346) including inhibition of both P-TEFb and PKC. *BMC Cancer* **2009**, 9, 63-63.

104. Liebl, J.; Weitensteiner, S. B.; Vereb, G.; Takács, L.; Fürst, R.; Vollmar, A. M.; Zahler, S. Cyclin-dependent Kinase 5 Regulates Endothelial Cell Migration and Angiogenesis. *The Journal of Biological Chemistry* **2010**, 285, 35932-35943.

105. Radhakrishnan, S. K.; Gartel, A. L. A Novel Transcriptional Inhibitor Induces Apoptosis in Tumor Cells and Exhibits Antiangiogenic Activity. *Cancer research* **2006**, 66, 3264-3270.

106. Melillo, G.; Sausville, E. A.; Cloud, K.; Lahusen, T.; Varesio, L.; Senderowicz, A. M. Flavopiridol, a Protein Kinase Inhibitor, Down-Regulates Hypoxic Induction of Vascular Endothelial Growth Factor Expression in Human Monocytes. *Cancer research* **1999**, 59, 5433-5437.

107. Ali, M. A.; Choy, H.; Habib, A. A.; Saha, D. SNS-032 Prevents Tumor Cell-Induced Angiogenesis By Inhibiting Vascular Endothelial Growth Factor. *Neoplasia*

(New York, N.Y.) **2007**, 9, 370-381.

108. Claudio, P. P.; Cui, J.; Ghafouri, M.; Mariano, C.; White, M. K.; Safak, M.; Sheffield, J. B.; Giordano, A.; Khalili, K.; Amini, S.; Sawaya, B. E. Cdk9 phosphorylates p53 on serine 392 independently of CKII. *Journal of Cellular Physiology* **2006**, 208, 602-612.

109. Radhakrishnan; K., S.; Gartel, A. L. CDK9 Phosphorylates p53 on Serine Residues 33, 315 and 392. *Cell Cycle* **2006**, 5, 519-521.

110. Fridman, J. S.; Lowe, S. W. Control of apoptosis by p53. *Oncogene* **2003**, 22, 9030-9040.

111. Teodoro, J. G.; Evans, S. K.; Green, M. R. Inhibition of tumor angiogenesis by p53: a new role for the guardian of the genome. *Journal of Molecular Medicine* **2007**, 85, 1175-1186.

112. Vousden, K. H.; Lu, X. Live or let die: the cell's response to p53. *Nature reviews. Cancer* **2002**, 2, 594-604.

113. Lu, W.; Chen, L.; Peng, Y.; Chen, J. Activation of p53 by Roscovitine-Mediated Suppression of MDM2 Expression. *Oncogene* **2001**, 20, 3206-3216.

114. Demidenko, Z. N.; Blagosklonny, M. V. Flavopiridol Induces p53 via Initial Inhibition of Mdm2 and p21 and, Independently of p53, Sensitizes Apoptosis-Reluctant Cells to Tumor Necrosis Factor. *Cancer research* **2004**, 64, 3653-3660.

115. Gartel, A. L. Transcriptional inhibitors, p53 and apoptosis. *Biochimica et Biophysica Acta (BBA) - Reviews on Cancer* **2008**, 1786, 83-86.

116.Lim, S.; Kaldis, P. Cdks, cyclins and CKIs: roles beyond cell cycle regulation. *Development* **2013**, 140, 3079-3093.

117.DePinto, W.; Chu, X.-J.; Yin, X.; Smith, M.; Packman, K.; Goelzer, P.; Lovey, A.; Chen, Y.; Qian, H.; Hamid, R.; Xiang, Q.; Tovar, C.; Blain, R.; Nevins, T.; Higgins, B.; Luistro, L.; Kolinsky, K.; Felix, B.; Hussain, S.; Heimbrook, D. In vitro and in vivo activity of R547: a potent and selective cyclin-dependent kinase inhibitor currently in phase I clinical trials. *Molecular Cancer Therapeutics* **2006**, 5, 2644-2658.

118.Misra, R. N.; Xiao, H.-y.; Kim, K. S.; Lu, S.; Han, W.-C.; Barbosa, S. A.; Hunt, J. T.; Rawlins, D. B.; Shan, W.; Ahmed, S. Z.; Qian, L.; Chen, B.-C.; Zhao, R.; Bednarz, M. S.; Kellar, K. A.; Mulheron, J. G.; Batorsky, R.; Roongta, U.; Kamath, A.; Marathe, P.; Ranadive, S. A.; Sack, J. S.; Tokarski, J. S.; Pavletich, N. P.; Lee, F. Y. F.; Webster, K. R.; Kimball, S. D. N-(Cycloalkylamino)acyl-2-aminothiazole Inhibitors of Cyclin-Dependent Kinase 2. N-[5-[[[5-(1,1-Dimethylethyl)-2-oxazolyl]methyl]thio]-2-thiazolyl]-4- piperidinecarboxamide (BMS-387032), a Highly Efficacious and Selective Antitumor Agent. *Journal of medicinal chemistry* **2004**, 47, 1719-1728.

119.McInnes, C. Progress in the evaluation of CDK inhibitors as anti-tumor agents. *Drug discovery today* **2008**, 13, 875-881.

120. Scholz, A.; Luecking, U.; Siemeister, G.; Lienau, P.; Boemer, U.; Ellinghaus, P.; Walter, A. O.; Valencia, R.; Ince, S.; von Nussbaum, F.; Mumberg, D.; Brands, M.; Ziegelbauer, K. Abstract DDT02-02: BAY 1143572: A first-in-class, highly selective, potent and orally available inhibitor of PTEFb/CDK9 currently in Phase I, inhibits MYC

and shows convincing anti-tumor activity in multiple xenograft models by the induction of apoptosis. *Cancer research* **2015**, 75, DDT02-02-DDT02-02.

121. Scholz, A.; Oellerich, T.; Hussain, A.; Lindner, S.; Luecking, U.; Walter, A. O.; Ellinghaus, P.; Valencia, R.; von Nussbaum, F.; Mumberg, D.; Brands, M.; Ince, S.; Serve, H.; Ziegelbauer, K. Abstract 3022: BAY 1143572, a first-in-class, highly selective, potent and orally available inhibitor of PTEFb/CDK9 currently in Phase I, shows convincing anti-tumor activity in preclinical models of acute myeloid leukemia (AML). *Cancer research* **2016**, 76, 3022-3022.

122. Narita, T.; Ishida, T.; Ito, A.; Masaki, A.; Kinoshita, S.; Suzuki, S.; Takino, H.; Yoshida, T.; Ri, M.; Kusumoto, S.; Komatsu, H.; Imada, K.; Tanaka, Y.; Takaori-Kondo, A.; Inagaki, H.; Scholz, A.; Lienau, P.; Kuroda, T.; Ueda, R.; Iida, S. Cyclin-dependent kinase 9 is a novel specific molecular target in adult T-cell leukemia/lymphoma. *Blood* **2017**, 130, 1114-1124.

123. Luecking, U.; Scholz, A.; Kosemund, D.; Bohlmann, R.; Briem, H.; Lienau, P.; Siemeister, G.; Terebesi, I.; Meyer, K.; Prelle, K.; Valencia, R.; Ince, S.; Nussbaum, F.; Mumberg, D.; Ziegelbauer, K.; Brands, M. *Abstract 984: Identification of potent and highly selective PTEFb inhibitor BAY 1251152 for the treatment of cancer: from p.o. to i.v. application via scaffold hops*. 2017; Vol. 77, p 984-984.

124. Chao, S.-H.; Fujinaga, K.; Marion, J. E.; Taube, R.; Sausville, E. A.; Senderowicz, A. M.; Peterlin, B. M.; Price, D. H. Flavopiridol Inhibits P-TEFb and Blocks HIV-1 Replication. *Journal of Biological Chemistry* **2000**, 275, 28345-28348.

125. Phelps, M. A.; Lin, T. S.; Johnson, A. J.; Hurh, E.; Rozewski, D. M.; Farley, K. L.; Wu, D.; Blum, K. A.; Fischer, B.; Mitchell, S. M.; Moran, M. E.; Brooker-McEldowney, M.; Heerema, N. A.; Jarjoura, D.; Schaaf, L. J.; Byrd, J. C.; Grever, M. R.; Dalton, J. T. Clinical response and pharmacokinetics from a phase 1 study of an active dosing schedule of flavopiridol in relapsed chronic lymphocytic leukemia. *Blood* **2009**, 113, 2637-2645.

126. Byrd, J. C.; Lin, T. S.; Dalton, J. T.; Wu, D.; Phelps, M. A.; Fischer, B.; Moran, M.; Blum, K. A.; Rovin, B.; Brooker-McEldowney, M.; Broering, S.; Schaaf, L. J.; Johnson, A. J.; Lucas, D. M.; Heerema, N. A.; Lozanski, G.; Young, D. C.; Suarez, J.-R.; Colevas, A. D.; Grever, M. R. Flavopiridol administered using a pharmacologically derived schedule is associated with marked clinical efficacy in refractory, genetically high-risk chronic lymphocytic leukemia. *Blood* **2007**, 109, 399-404.

127. Meijer, L.; Borgne, A.; Mulner, O.; Chong, J. P. J.; Blow, J. J.; Inagaki, N.; Inagaki, M.; Delcros, J.-G.; Moulinoux, J.-P. Biochemical and Cellular Effects of Roscovitine, a Potent and Selective Inhibitor of the Cyclin-Dependent Kinases cdc2, cdk2 and cdk5. *European Journal of Biochemistry* **1997**, 243, 527-536.

128. Siegel-Lakhai, W. S.; Rodenstein, D. O.; Beijnen, J. H.; Gianella-Borradori, A.; Schellens, J. H. M.; Talbot, D. C. Phase I study of seliciclib (CYC202 or R-roscovitine) in combination with gemcitabine (gem)/cisplatin (cis) in patients with advanced non-small cell lung cancer (NSCLC). *Journal of Clinical Oncology* **2005**, 23, 2060-2060.

129. Ortiz-Ferron, G.; Yerbes, R.; Eramo, A.; Lopez-Perez, A. I.; De Maria, R.;

Lopez-Rivas, A. Roscovitine sensitizes breast cancer cells to TRAIL-induced apoptosis through a pleiotropic mechanism. *Cell Res* **2008**, 18, 664-676.

130. Nutley, B. P.; Raynaud, F. I.; Wilson, S. C.; Fischer, P. M.; Hayes, A.; Goddard, P. M.; McClue, S. J.; Jarman, M.; Lane, D. P.; Workman, P. Metabolism and pharmacokinetics of the cyclin-dependent kinase inhibitor R-roscovitine in the mouse. *Molecular Cancer Therapeutics* **2005**, 4, 125-139.

131. McClue, S. J.; Stuart, I. Metabolism of the Trisubstituted Purine Cyclin-Dependent Kinase Inhibitor Seliciclib (R-Roscovitine) in Vitro and in Vivo. *Drug Metabolism and Disposition* **2008**, 36, 561-570.

132. Vita, M.; Abdel-Rehim, M.; Olofsson, S.; Hassan, Z.; Meurling, L.; Sidén, Å.; Sidén, M.; Pettersson, T.; Hassan, M. Tissue distribution, pharmacokinetics and identification of roscovitine metabolites in rat. *European Journal of Pharmaceutical Sciences* **2005**, 25, 91-103.

133. Bettayeb, K.; Oumata, N.; Echalier, A.; Ferandin, Y.; Endicott, J. A.; Galons, H.; Meijer, L. CR8, a potent and selective, roscovitine-derived inhibitor of cyclin-dependent kinases. *Oncogene* **2008**, 27, 5797-5807.

134. Cosimo, E.; McCaig, A. M.; Carter-Brzezinski, L. J. M.; Wheadon, H.; Leach, M. T.; Le Ster, K.; Berthou, C.; Durieu, E.; Oumata, N.; Galons, H.; Meijer, L.; Michie, A. M. Inhibition of NF-κB–Mediated Signaling by the Cyclin-Dependent Kinase Inhibitor CR8 Overcomes Prosurvival Stimuli to Induce Apoptosis in Chronic Lymphocytic Leukemia Cells. *Clinical Cancer Research* **2013**, 19, 2393-2405.

135. Klebl, B. M.; Choidas, A. CDK9/cyclin T1: a host cell target for antiretroviral therapy. *Future Virology* **2006**, 1, 317-330.

136. Shima, D.; Yugami, M.; Tatsuno, M.; Wada, T.; Yamaguchi, Y.; Handa, H. Mechanism of H-8 inhibition of Cyclin-dependent kinase 9: study using inhibitor-immobilized matrices. *Genes to Cells* **2003**, 8, 215-223.

137. Nuwayhid, S. J.; Hyde, J.; Aleshin, A.; Walker, D. H.; Arkin, M. R. SNS-032 is a potent and selective inhibitor of CDK2, 7 and 9 and induces cell death by inhibiting cell cycle progression and the expression of antiapoptotic proteins. *Cancer research* **2006**, 66, 491-491.

138. Tong, W.-G.; Chen, R.; Plunkett, W.; Siegel, D.; Sinha, R.; Harvey, R. D.; Badros, A. Z.; Popplewell, L.; Coutre, S.; Fox, J. A.; Mahadocon, K.; Chen, T.; Kegley, P.; Hoch, U.; Wierda, W. G. Phase I and Pharmacologic Study of SNS-032, a Potent and Selective Cdk2, 7, and 9 Inhibitor, in Patients With Advanced Chronic Lymphocytic Leukemia and Multiple Myeloma. *Journal of Clinical Oncology* **2010**, 28, 3015-3022.

139. Byth, K. F.; Thomas, A.; Hughes, G.; Forder, C.; McGregor, A.; Geh, C.; Oakes, S.; Green, C.; Walker, M.; Newcombe, N.; Green, S.; Growcott, J.; Barker, A.; Wilkinson, R. W. AZD5438, a potent oral inhibitor of cyclin-dependent kinases 1, 2, and 9, leads to pharmacodynamic changes and potent antitumor effects in human tumor xenografts. *Molecular Cancer Therapeutics* **2009**, 8, 1856-1866.

140. Jones, C. D.; Andrews, D. M.; Barker, A. J.; Blades, K.; Daunt, P.; East, S.; Geh, C.; Graham, M. A.; Johnson, K. M.; Loddick, S. A.; McFarland, H. M.; McGregor, A.;

Moss, L.; Rudge, D. A.; Simpson, P. B.; Swain, M. L.; Tam, K. Y.; Tucker, J. A.; Walker, M. The discovery of AZD5597, a potent imidazole pyrimidine amide CDK inhibitor suitable for intravenous dosing. *Bioorganic & medicinal chemistry letters* **2008**, 18, 6369-6373.

141. Boss, D. S.; Schwartz, G. K.; Middleton, M. R.; Amakye, D. D.; Swaisland, H.; Midgley, R. S.; Ranson, M.; Danson, S.; Calvert, H.; Plummer, R.; Morris, C.; Carvajal, R. D.; Chirieac, L. R.; Schellens, J. H. M.; Shapiro, G. I. Safety, tolerability, pharmacokinetics and pharmacodynamics of the oral cyclin-dependent kinase inhibitor AZD5438 when administered at intermittent and continuous dosing schedules in patients with advanced solid tumours. *Annals of Oncology* **2010**, 21, 884-894.

142. Raghavan, P.; Tumati, V.; Yu, L.; Chan, N.; Tomimatsu, N.; Burma, S.; Bristow, R. G.; Saha, D. AZD5438, an Inhibitor of Cdk1, 2, and 9, Enhances the Radiosensitivity of Non-Small Cell Lung Carcinoma Cells. *International Journal of Radiation Oncology • Biology • Physics* 84, e507-e514.

143. Hole, A. J.; Baumli, S.; Shao, H.; Shi, S.; Huang, S.; Pepper, C.; Fischer, P. M.; Wang, S.; Endicott, J. A.; Noble, M. E. Comparative structural and functional studies of 4-(thiazol-5-yl)-2-(phenylamino)pyrimidine-5-carbonitrile CDK9 inhibitors suggest the basis for isotype selectivity. *Journal of medicinal chemistry* **2013**, 56, 660-70.

144. Shao, H.; Shi, S.; Huang, S.; Hole, A. J.; Abbas, A. Y.; Baumli, S.; Liu, X.; Lam, F.; Foley, D. W.; Fischer, P. M.; Noble, M.; Endicott, J. A.; Pepper, C.; Wang, S. Substituted 4-(thiazol-5-yl)-2-(phenylamino)pyrimidines are highly active CDK9

inhibitors: synthesis, X-ray crystal structures, structure-activity relationship, and anticancer activities. *Journal of medicinal chemistry* **2013**, 56, 640-59.

145. Shao, H.; Shi, S.; Foley, D. W.; Lam, F.; Abbas, A. Y.; Liu, X.; Huang, S.; Jiang, X.; Baharin, N.; Fischer, P. M.; Wang, S. Synthesis, structure–activity relationship and biological evaluation of 2,4,5-trisubstituted pyrimidine CDK inhibitors as potential anti-tumour agents. *European journal of medicinal chemistry* **2013**, 70, 447-455.

146. Kryštof, V.; Chamrád, I.; Jorda, R.; Kohoutek, J. Pharmacological targeting of CDK9 in cardiac hypertrophy. *Medicinal Research Reviews* **2010**, 30, 646-666.

147. Fabbro, D.; Ruetz, S.; Buchdunger, E.; Cowan-Jacob, S. W.; Fendrich, G.; Liebetanz, J.; Mestan, J.; O'Reilly, T.; Traxler, P.; Chaudhuri, B.; Fretz, H.; Zimmermann, J.; Meyer, T.; Caravatti, G.; Furet, P.; Manley, P. W. Protein kinases as targets for anticancer agents: from inhibitors to useful drugs. *Pharmacology & Therapeutics* **2002**, 93, 79-98.

148. Traxler, P.; Furet, P. Strategies toward the Design of Novel and Selective Protein Tyrosine Kinase Inhibitors. *Pharmacology & Therapeutics* **1999**, 82, 195-206.

149. Schulze-Gahmen, U.; De Bondt, H. L.; Kim, S.-H. High-Resolution Crystal Structures of Human Cyclin-Dependent Kinase 2 with and without ATP: Bound Waters and Natural Ligand as Guides for Inhibitor Design. *Journal of medicinal chemistry* **1996**, 39, 4540-4546.

150. Alaimo, P. J.; Knight, Z. A.; Shokat, K. M. Targeting the gatekeeper residue in phosphoinositide 3-kinases. *Bioorganic & medicinal chemistry* **2005**, 13, 2825-2836.

151. Brasca, M. G.; Albanese, C.; Amici, R.; Ballinari, D.; Corti, L.; Croci, V.; Fancelli, D.; Fiorentini, F.; Nesi, M.; Orsini, P.; Orzi, F.; Pastori, W.; Perrone, E.; Pesenti, E.; Pevarello, P.; Riccardi-Sirtori, F.; Roletto, F.; Roussel, P.; Varasi, M.; Vulpetti, A.; Mercurio, C. 6-Substituted Pyrrolo[3,4-c]pyrazoles: An Improved Class of CDK2 Inhibitors. *ChemMedChem* **2007**, 2, 841-852.

152. D'Alessio, R.; Bargiotti, A.; Metz, S.; Brasca, M. G.; Cameron, A.; Ermoli, A.; Marsiglio, A.; Polucci, P.; Roletto, F.; Tibolla, M.; Vazquez, M. L.; Vulpetti, A.; Pevarello, P. Benzodipyrazoles: a new class of potent CDK2 inhibitors. *Bioorganic & medicinal chemistry letters* **2005**, 15, 1315-1319.

153. Brasca, M. G.; Amboldi, N.; Ballinari, D.; Cameron, A.; Casale, E.; Cervi, G.; Colombo, M.; Colotta, F.; Croci, V.; D'Alessio, R.; Fiorentini, F.; Isacchi, A.; Mercurio, C.; Moretti, W.; Panzeri, A.; Pastori, W.; Pevarello, P.; Quartieri, F.; Roletto, F.; Traquandi, G.; Vianello, P.; Vulpetti, A.; Ciomei, M. Identification of N,1,4,4-Tetramethyl-8-{[4-(4-methylpiperazin-1-yl)phenyl]amino}-4,5-dihydro-1H-pyrazolo[4,3-h]quinazoline-3-carboxamide (PHA-848125), a Potent, Orally Available Cyclin Dependent Kinase Inhibitor. *Journal of medicinal chemistry* **2009**, 52, 5152-5163.

154. McInnes, C.; Wang, S.; Anderson, S.; O'Boyle, J.; Jackson, W.; Kontopidis, G.; Meades, C.; Mezna, M.; Thomas, M.; Wood, G.; Lane, D. P.; Fischer, P. M. Structural Determinants of CDK4 Inhibition and Design of Selective ATP Competitive Inhibitors. *Chemistry & biology* **2004**, 11, 525-534.

155. Traxler, P. M.; Furet, P.; Mett, H.; Buchdunger, E.; Meyer, T.; Lydon, N. 4-(Phenylamino)pyrrolopyrimidines: Potent and Selective, ATP Site Directed Inhibitors of the EGF-Receptor Protein Tyrosine Kinase. *Journal of medicinal chemistry* **1996**, 39, 2285-2292.

156. Baumli, S.; Lolli, G.; Lowe, E. D.; Troiani, S.; Rusconi, L.; Bullock, A. N.; Debreczeni, J. É.; Knapp, S.; Johnson, L. N. The structure of P-TEFb (CDK9/cyclin T1), its complex with flavopiridol and regulation by phosphorylation. *The EMBO Journal* **2008**, 27, 1907-1918.

157. Fernanda, C.; Walter Filgueira de, A., Jr. Structural Basis for Interaction of Inhibitors with Cyclin-Dependent Kinase 2. *Current Computer-Aided Drug Design* **2005**, 1, 53-64.

158. Kim, S.-H.; Schulze-Gahmen, U.; Brandsen, J.; de Azevedo, W. F. Structural basis for chemical inhibition of CDK2. In *Progress in Cell Cycle Research*, Meijer, L.; Guidet, S.; Vogel, L., Eds. Springer US: Boston, MA, 1996; pp 137-145.

159. Liu, H.; Herrmann, C. H. Differential localization and expression of the Cdk9 42k and 55k isoforms. *Journal of Cellular Physiology* **2005**, 203, 251-260.

160. Baumli, S.; Endicott, J. A.; Johnson, L. N. Halogen Bonds Form the Basis for Selective P-TEFb Inhibition by DRB. *Chemistry & biology* **2010**, 17, 931-936.

161. Krystof, V.; Baumli, S.; Furst, R. Perspective of Cyclin-dependent kinase 9 (CDK9) as a Drug Target. *Current Pharmaceutical Design* **2012**, 18, 2883-2890.

162. De Azevedo, W. F.; Mueller-Dieckmann, H. J.; Schulze-Gahmen, U.; Worland,

P. J.; Sausville, E.; Kim, S. H. Structural basis for specificity and potency of a flavonoid inhibitor of human CDK2, a cell cycle kinase. *Proceedings of the National Academy of Sciences of the United States of America* **1996**, 93, 2735-2740.

163. Sun, H.; Zhu, J.; Chen, Y.; Sun, Y.; Zhi, H.; Li, H.; You, Y.; Xiao, Q. Docking Study and Three-Dimensional Quantitative Structure-Activity Relationship (3D-QSAR) Analyses and Novel Molecular Design of a Series of 4-Aminoquinazolines as Inhibitors of Aurora B Kinase. *Chinese Journal of Chemistry* **2011**, 29, 1785-1799.

164. Sessa, F.; Mapelli, M.; Ciferri, C.; Tarricone, C.; Areces, L. B.; Schneider, T. R.; Stukenberg, P. T.; Musacchio, A. Mechanism of Aurora B activation by INCENP and inhibition by hesperadin. *Molecular cell* **2005**, 18, 379-91.

165. Keen, N.; Taylor, S. Aurora-kinase inhibitors as anticancer agents. *Nature reviews. Cancer* **2004**, 4, 927-36.

166. Sen, S.; Zhou, H.; White, R. A. A putative serine/threonine kinase encoding gene BTAK on chromosome 20q13 is amplified and overexpressed in human breast cancer cell lines. *Oncogene* **1997**, 14, 2195-2200.

167. Bischoff, J. R.; Anderson, L.; Zhu, Y.; Mossie, K.; Ng, L.; Souza, B.; Schryver, B.; Flanagan, P.; Clairvoyant, F.; Ginther, C.; Chan, C. S. M.; Novotny, M.; Slamon, D. J.; Plowman, G. D. A homologue of Drosophila aurora kinase is oncogenic and amplified in human colorectal cancers. *The EMBO Journal* **1998**, 17, 3052-3065.

168. Shao, H. Design, synthesis and biological evaluation of highly selective CDK9 inhibitors for cancer treatment. *Thesis from University of Nottingham* **2014**.

169. Elkins, J. M.; Santaguida, S.; Musacchio, A.; Knapp, S. Crystal structure of human aurora B in complex with INCENP and VX-680. *Journal of medicinal chemistry* **2012**, 55, 7841-8.

170. Girdler, F.; Sessa, F.; Patercoli, S.; Villa, F.; Musacchio, A.; Taylor, S. Molecular basis of drug resistance in aurora kinases. *Chemistry & biology* **2008**, 15, 552-62.

171. Fairley, G.; Hall, C.; Greenwood, R. Selective Methylation of NH-Containing Heterocycles and Sulfonamides Using N,N-Dimethylformamide Dimethylacetal Based on Calculated pKa Measurements. *Synlett* **2013**, 24, 570-574.

172. Brown, G. R.; Foubister, A. J.; Ratcliffe, P. D. High yields of meta-substituted amination products in the SNAr substitution of benzenes. *Tetrahedron Letters* **1999**, 40, 1219-1222.

173. Bandgar, B. P.; Pandit, S. S. Highly rapid and direct synthesis of monoacylated piperazine derivatives from carboxylic acids under mild conditions. *Tetrahedron Letters* **2003**, 44, 3855-3858.

174. Montalbetti, C. A. G. N.; Falque, V. Amide bond formation and peptide coupling. *Tetrahedron* **2005**, 61, 10827-10852.

175. Valeur, E.; Bradley, M. Amide bond formation: beyond the myth of coupling reagents. *Chemical Society reviews* **2009**, 38, 606-31.

176. van der Eide, E. F.; Piers, W. E. Mechanistic insights into the ruthenium-catalysed diene ring-closing metathesis reaction. *Nature chemistry* **2010**, 2, 571-6.

177. Hoveyda, A. H.; Zhugralin, A. R. The remarkable metal-catalysed olefin metathesis reaction. *Nature* **2007**, 450, 243-51.

178. Phillips, A. J.; Abell, A. D. Ring-Closing Metathesis of Nitrogen-Containing Compounds: Applications to Heterocycles, Alkaloids, and Peptidomimetics. *Aldrichimica Acta* **1999**, 32, 75-90.

179. Vougioukalakis, G. C.; Grubbs, R. H. Ruthenium-Based Heterocyclic Carbene-Coordinated Olefin Metathesis Catalysts. *Chemical Review* **2010**, 110, 1746-1787.

180. Deiters, A.; Martin, S. F. Synthesis of Oxygen- and Nitrogen-Containing Heterocycles by Ring-Closing Metathesis. *Chemical Review* **2004**, 104, 2199-2238.

181. Scholl, M.; Ding, S.; Lee, C. W.; Grubbs, R. H. Synthesis and Activity of a New Generation of Ruthenium-Based Olefin Metathesis Catalysts Coordinated with 1,3-Dimesityl-4,5-dihydroimidazol-2-ylidene Ligands. *Organic Letters* **1999**, 1, 953-956.

182. Grela, K.; Olszewski, T.; Bieniek, M.; Skowerski, K. A New Tool in the Toolbox: Electron-Withdrawing Group Activated -Ruthenium Catalysts for Olefin Metathesis. *Synlett* **2013**, 24, 903-919.

183. Rutjes, F. P. J. T.; Schoemaker, H. E. Ruthenium-Catalyzed Ring Closing Olefin Metathesis of Non-Natural α-Amino Acids. *Tetrahedron Letters* **1997**, 38, 677-680.

184. William, A. D.; Lee, A. C.; Goh, K. C.; Blanchard, S.; Poulsen, A.; Teo, E. L.; Nagaraj, H.; Lee, C. P.; Wang, H.; Williams, M.; Sun, E. T.; Hu, C.; Jayaraman, R.; Pasha, M. K.; Ethirajulu, K.; Wood, J. M.; Dymock, B. W. Discovery of kinase spectrum

selective macrocycle (16E)-14-methyl-20-oxa-5,7,14,26-tetraazatetracyclo[19.3.1.1(2,6).1(8,12)]heptaco sa-1(25),2(26),3,5,8(27),9,11,16,21,23-decaene (SB1317/TG02), a potent inhibitor of cyclin dependent kinases (CDKs), Janus kinase 2 (JAK2), and fms-like tyrosine kinase-3 (FLT3) for the treatment of cancer. *Journal of medicinal chemistry* **2012**, 55, 169-96.

185. Goh, K. C.; Novotny-Diermayr, V.; Hart, S.; Ong, L. C.; Loh, Y. K.; Cheong, A.; Tan, Y. C.; Hu, C.; Jayaraman, R.; William, A. D.; Sun, E. T.; Dymock, B. W.; Ong, K. H.; Ethirajulu, K.; Burrows, F.; Wood, J. M. TG02, a novel oral multi-kinase inhibitor of CDKs, JAK2 and FLT3 with potent anti-leukemic properties. *Leukemia* **2012**, 26, 236-43.

186. Matsuya, Y.; Kobayashi, Y.; Kawaguchi, T.; Hori, A.; Watanabe, Y.; Ishihara, K.; Ahmed, K.; Wei, Z. L.; Yu, D. Y.; Zhao, Q. L.; Kondo, T.; Nemoto, H. Design, synthesis, and biological evaluation of artificial macrosphelides in the search for new apoptosis-inducing agents. *Chemistry* **2009**, 15, 5799-813.

187. Matsuya, Y.; Kawaguchi, T.; Ishihara, K.; Ahmed, K.; Zhao, Q.-L.; Kondo, T.; Nemoto, H. Synthesis of Macrosphelides with a Thiazole Side Chain: New Antitumor Candidates Having Apoptosis-Inducing Property. *Organic Letters* **2006**, 8, 4609-4612.

188. Cohrt, A. E.; Nielsen, T. E. Solid-phase synthesis of peptide thioureas and thiazole-containing macrocycles through Ru-catalyzed ring-closing metathesis. *ACS combinatorial science* **2014**, 16, 71-7.

189. Kim, S.; Hwang, W.; Lim, I. S.; Kim, S. H.; Lee, S.-g.; Kim, B. M. Acid-

mediated activation of modified ring-closing metathesis catalysts. *Tetrahedron Letters* **2010**, 51, 709-713.

190. Tsipis, A. C.; Orpen, A. G.; Harvey, J. N. Substituent effects and the mechanism of alkene metathesis catalyzed by ruthenium dichloride catalysts. *Dalton transactions* **2005**, 2849-2858.

191. Richter, D. T.; Kath, J. C.; Luzzio, M. J.; Keene, N.; Berliner, M. A.; Wessel, M. D. Selective addition of amines to 5-trifluoromethyl-2,4-dichloropyrimidine induced by Lewis acids. *Tetrahedron Letters* **2013**, 54, 4610-4612.

192. Walker, D. P.; Bi, F. C.; Kalgutkar, A. S.; Bauman, J. N.; Zhao, S. X.; Soglia, J. R.; Aspnes, G. E.; Kung, D. W.; Klug-McLeod, J.; Zawistoski, M. P.; McGlynn, M. A.; Oliver, R.; Dunn, M.; Li, J. C.; Richter, D. T.; Cooper, B. A.; Kath, J. C.; Hulford, C. A.; Autry, C. L.; Luzzio, M. J.; Ung, E. J.; Roberts, W. G.; Bonnette, P. C.; Buckbinder, L.; Mistry, A.; Griffor, M. C.; Han, S.; Guzman-Perez, A. Trifluoromethylpyrimidine-based inhibitors of proline-rich tyrosine kinase 2 (PYK2): structure-activity relationships and strategies for the elimination of reactive metabolite formation. *Bioorganic & medicinal chemistry letters* **2008**, 18, 6071-7.

193. Rogers, J. F.; Green, D. M. Mild conversion of electron deficient aryl fluorides to phenols using 2-(methylsulfonyl)ethanol. *Tetrahedron Letters* **2002**, 43, 3585-3587.

194. Billingsley, K. L.; Buchwald, S. L. A general and efficient method for the Suzuki-Miyaura coupling of 2-pyridyl nucleophiles. *Angewandte Chemie* **2008**, 47, 4695-8.

195. Hughes, J. D.; Blagg, J.; Price, D. A.; Bailey, S.; DeCrescenzo, G. A.; Devraj, R. V.; Ellsworth, E.; Fobian, Y. M.; Gibbs, M. E.; Gilles, R. W.; Greene, N.; Huang, E.; Krieger-Burke, T.; Loesel, J.; Wager, T.; Whiteley, L.; Zhang, Y. Physiochemical drug properties associated with in vivo toxicological outcomes. *Bioorganic & medicinal chemistry letters* **2008**, 18, 4872-4875.

196. Davis, T. A.; Hyster, T. K.; Rovis, T. Rhodium(III)-Catalyzed Intramolecular Hydroarylation, Amidoarylation, and Heck-type Reaction: Three Distinct Pathways Determined by an Amide Directing Group. *Angewandte Chemie International Edition* **2013**, 52, 14181-14185.

197. National Center for Biotechnology Information. PubChem Compound Database; CID=107276969, https://pubchem.ncbi.nlm.nih.gov/compound/107276969. **2018**.

198. National Center for Biotechnology Information. PubChem Compound Database; CID=28800153, https://pubchem.ncbi.nlm.nih.gov/compound/28800153. **2018**.

199. William, A. D.; Lee, A. C.; Blanchard, S.; Poulsen, A.; Teo, E. L.; Nagaraj, H.; Tan, E.; Chen, D.; Williams, M.; Sun, E. T.; Goh, K. C.; Ong, W. C.; Goh, S. K.; Hart, S.; Jayaraman, R.; Pasha, M. K.; Ethirajulu, K.; Wood, J. M.; Dymock, B. W. Discovery of the macrocycle 11-(2-pyrrolidin-1-yl-ethoxy)-14,19-dioxa-5,7,26-triaza-tetracyclo[19.3.1.1(2,6). 1(8,12)]heptacosa-1(25),2(26),3,5,8,10,12(27),16,21,23-decaene (SB1518), a potent Janus kinase 2/fms-like tyrosine kinase-3 (JAK2/FLT3)

inhibitor for the treatment of myelofibrosis and lymphoma. *Journal of medicinal chemistry* **2011**, 54, 4638-58.

200. Takrouri, K.; Cooper, H. D.; Spaulding, A.; Zucchi, P.; Koleva, B.; Cleary, D. C.; Tear, W.; Beuning, P. J.; Hirsch, E. B.; Aggen, J. B. Progress against Escherichia coli with the Oxazolidinone Class of Antibacterials: Test Case for a General Approach To Improving Whole-Cell Gram-Negative Activity. *ACS Infectious Diseases* **2016**, 2, 405-426.

201. National Center for Biotechnology Information. PubChem Compound Database; CID=113367070, https://pubchem.ncbi.nlm.nih.gov/compound/113367070. **2018**.

202. Friesner, R. A.; Banks, J. L.; Murphy, R. B.; Halgren, T. A.; Klicic, J. J.; Mainz, D. T.; Repasky, M. P.; Knoll, E. H.; Shelley, M.; Perry, J. K.; Shaw, D. E.; Francis, P.; Shenkin, P. S. Glide: A New Approach for Rapid, Accurate Docking and Scoring. 1. Method and Assessment of Docking Accuracy. *Journal of medicinal chemistry* **2004**, 47, 1739-1749.

203. KinaseProfile Service Assay Protocols. http://www.komabiotech.co.kr/pdf/kinaseprofiler_assay_protocol_guide_eurofins_v64.pdf.

204. Kinase Assay Protocal for CDK9. http://www.eurofinsdiscovery.com/14-685-K-Cdk9/Cyclin-T1-active/.